CHAPTER V
RESULTS AND DISCUSSION

In this chapter, the experimental results and discussion are divided into 3 sections. The concept of cooperative effect, which is important in the study of the deactivation mechanism, will be firstly discussed in Section 5.1. Section 5.2 will be devoted to the effective parameters on the coke formation over the physically mixed catalysts, i.e., time, temperature, H_2/HC ratio and catalyst types. Finally, the mode of coke formation of coke will be proposed in Section 5.3.

5.1 The cooperative effect study

Carbonaceous deposits cause deactivation of naphtha reforming which decrease the activity, selectivity and lifetime of the catalysts [4, 7, 24]. Catalysts which contain Pt or Pt and a second metal supported on and acidic carrier such as Al_2O_3 are widely used in the catalytic reforming [50, 68]. Coke formation occurs both on metals and on the acidic carriers by different mechanism. Thus, it is essential to understand the relationship between the two functions, metal and acidic carrier, on deactivation behavior of the reforming catalysts. Recently, there have been a number of papers reporting the cooperative effect of catalytic species on the catalytic reaction with hydrocarbons [69, 70]. The cooperative effect is observed with a combination of solid acidity and metal species, which are mixed together mechanically or physically.

In this section, the cooperation of two catalytic species for catalyst deactivation of dehydrogenation reaction was studied in order to give further insights into the reaction mechanism and to obtain new concepts for the future catalyst design and development. In order to explore the cooperative effect in details, the performance of the physical mixtures of Pt-based/SiO_2 represented the metal site and Al_2O_3 represented the acid site in equal amounts was examined.

5.1.1 The cooperative effect test

The physical mixtures were prepared by mixing Pt/SiO_2 and Al_2O_3, which had been crushed separately and sieved to desired grain size. The size of alumina support used for the reaction test was 60-80 mesh, where the sizes of Pt/SiO_2 were varied as 20-30, 40-60, 80-100 and 100-120 mesh, the minimum size, which can be used to avoid pressure drop. The simplicity of the reactions has led to their use as illustrative examples of the application of different theoretical concepts and there is more general agreement that geometric effects are important in this system. Metal catalyzed reactions can be dependent on particle size, on crystal face and on the number of sites available on the surface [2, 3, 142]. To measure the active sites of the catalysts, CO adsorption technique was used. The numbers of active sites of Pt/Al_2O_3 and Pt/SiO_2-Al_2O_3 system with various sizes are summarized in Table 5.1. It is clear that the difference of active site between Pt-based catalysts supported on alumina and silica is observed. Interestingly, the amount of active sites of the physical mixtures were close to Pt-based catalysts supported directly on acidic function when the grain size of mixture was smaller, especially the mixtures of 100-120 mesh Pt/SiO_2 and Al_2O_3.

An alternative approach is to select a catalyst which favors both the desired reaction and the gasification of coke. The coking reaction of dehydrogenation was carried out in an ordinary flow microreactor with 1-hexene dehydrogenation reaction (10% hexene in N_2). The reaction conditions were undertaken at the temperature of 400°C, H_2/HC ratio of 0 and time on stream of 120 min and the total pressure of 1 atm.

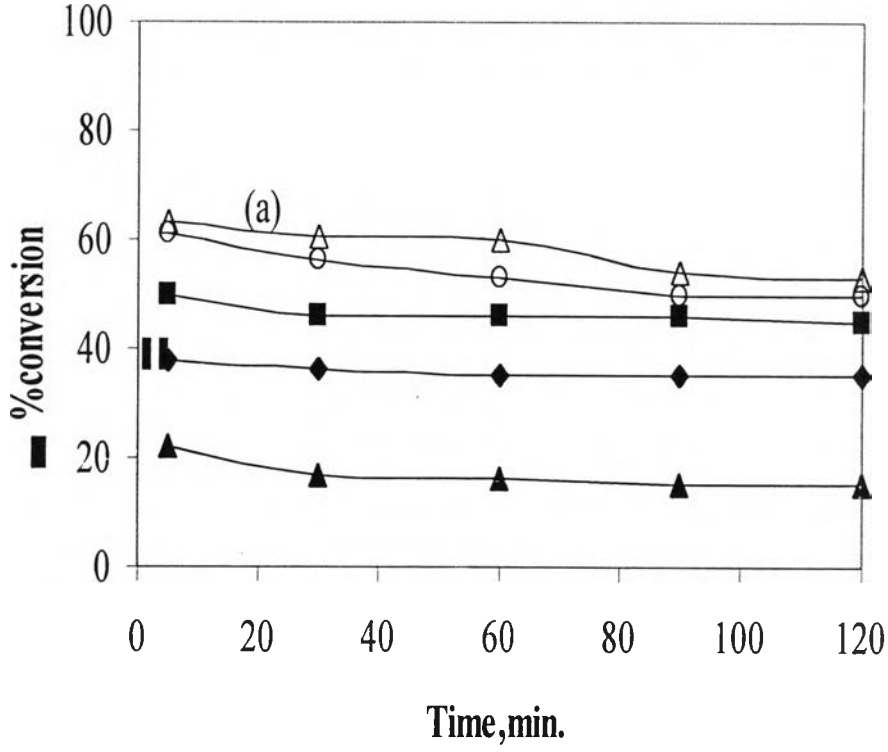

Figure 5.1 %Conversion of Pt/Al_2O_3 and Physical mixtures for hexene dehydrogenation

(a) Pt/Al_2O_3
(b) Pt/SiO_2 (100-120) + Al_2O_3
(c) Pt/SiO_2 (80-100) + Al_2O_3
(d) Pt/SiO_2 (40-60) + Al_2O_3
(e) Pt/SiO_2 (20-30) + Al_2O_3

Table 5.1 The number of active sites on the catalysts

Catalysts	active sites (molecules of CO/g.catalyst)
Pt/Al_2O_3	6.14×10^{18}
Physical mixtures	
Pt/SiO_2 (20-30) $+Al_2O_3$	4.15×10^{18}
Pt/SiO_2 (40-60) $+Al_2O_3$	4.85×10^{18}
Pt/SiO_2 (80-100) $+Al_2O_3$	5.07×10^{18}
Pt/SiO_2 (100-120)$+Al_2O_3$	5.32×10^{18}

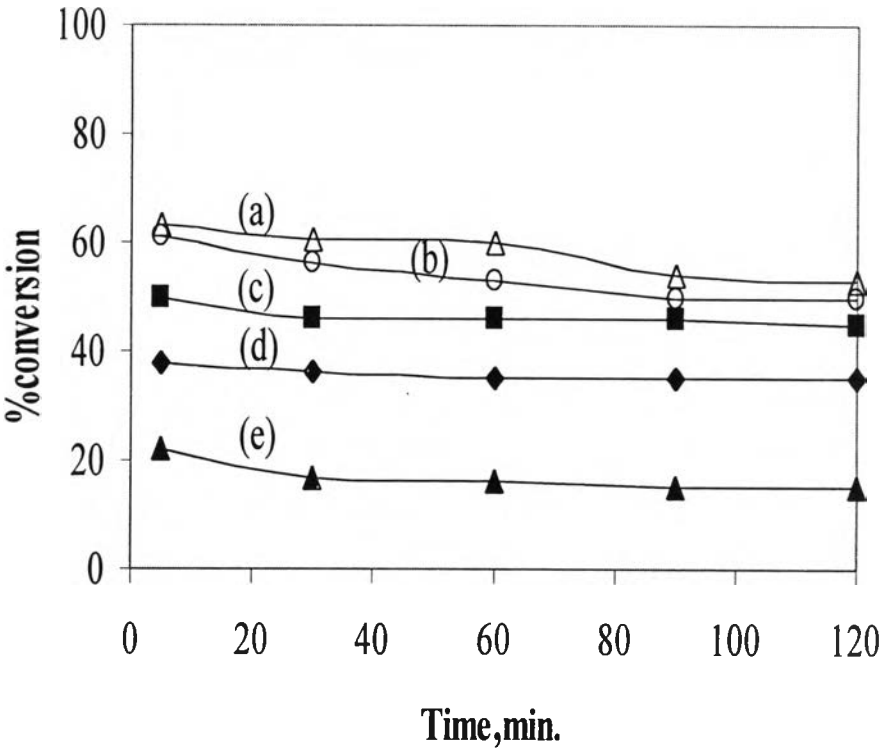

Figure 5.1 %Conversion of Pt/Al_2O_3 and Physical mixtures for hexene dehydrogenation

(a) Pt/Al_2O_3
(b) Pt/SiO_2 (100-120) + Al_2O_3
(c) Pt/SiO_2 (80-100) + Al_2O_3
(d) Pt/SiO_2 (40-60) + Al_2O_3
(e) Pt/SiO_2 (20-30) + Al_2O_3

Table 5.1 The number of active sites on the catalysts

Catalysts	active sites (molecules of CO/g.catalyst)
Pt/Al_2O_3	6.14×10^{18}
Physical mixtures	
Pt/SiO_2 (20-30) $+Al_2O_3$	4.15×10^{18}
Pt/SiO_2 (40-60) $+Al_2O_3$	4.85×10^{18}
Pt/SiO_2 (80-100) $+Al_2O_3$	5.07×10^{18}
Pt/SiO_2 (100-120)$+Al_2O_3$	5.32×10^{18}

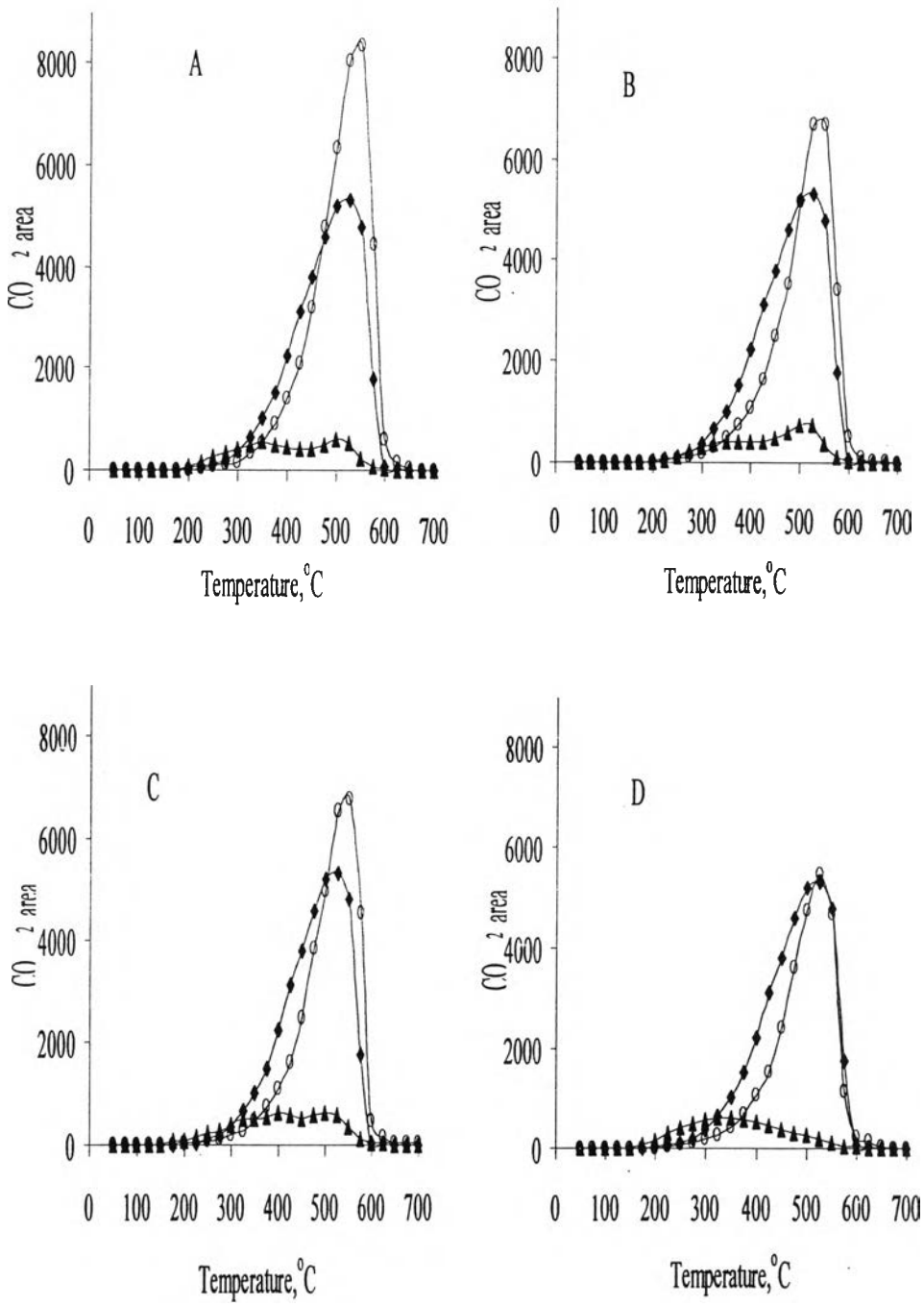

Figure 5.2 Temperature programmed oxidation of carbonaceous deposits with various mesh size of Pt/SiO_2 for hexane dehydrogenation;(A) ◆ Pt/Al_2O_3,❍ Al_2O_3, ▲ Pt/SiO_2(20-30) ; (B) ◆ Pt/Al_2O_3, ❍ Al_2O_3, ▲ Pt/SiO_2(40-60); (C) ◆ Pt/Al_2O_3, ❍ Al_2O_3, ▲ Pt/SiO_2(80-100); (D) ◆ Pt/Al_2O_3, ❍ Al_2O_3, ▲ Pt/SiO_2(100-120)

The catalytic activities and selectivities of these mixture systems were investigated considering the conversion of hexene. In this way, the dehydrogenated products such as C_1-C_4, cyclopentane, methyl cyclopentane and other aromatic products were detected, while benzene occurred was the main product. Furthermore, hexane, a hydrogenated product, was also obtained. Figure 5.1 shows the hexene conversions observed over Pt/Al_2O_3 and physical mixtures of Al_2O_3 and various sizes of Pt/SiO_2. Conversions are declined as a function of time due to the catalyst deactivation. Initial conversion of real system (3 min-TOS) is about 60% while the conversions of mixed catalyst system are approximating 20% for 20-30 mesh Pt/SiO_2, 40% for 40-60 mesh Pt/SiO_2, 55% for 80-100 mesh Pt/SiO_2 and 60% for 100-120 mesh Pt/SiO_2. Surprisingly, the physical mixtures behave like Pt/Al_2O_3 when the grain sizes decrease owing to the closely contact interaction. This is corresponded with literature [69]. For Pt/SiO_2 with 100-120 mesh, conversion observed was very close to that found when platinum was supported directly on acidic alumina. This is associated with the selectivity of product obtained as reported in Table 5.2.

Table 5.2 % Product selectivity of Pt/Al_2O_3 and Physical mixtures for hexene dehydrogenation

Catalysts	% Selectivity						H/D
	C_1-C_4	CP	Hexane	MCP	Benzene	Others	ratio
Pt/Al_2O_3	6.10	3.53	61.90	23.60	4.48	0.39	1.63
Physical mixtures							
Pt/SiO_2 (100-120)+Al_2O_3	6.25	2.40	62.09	25.53	3.57	0.15	1.64
Pt/SiO_2 (80-100) +Al_2O_3	21.09	6.67	43.86	20.17	6.59	1.62	0.78
Pt/SiO_2 (40-60) +Al_2O_3	24.87	7.64	33.29	21.35	7.80	5.02	0.50
Pt/SiO_2 (20-30) +Al_2O_3	28.57	12.36	29.32	19.32	6.90	3.40	0.42

H/D ratio = ratio of hydrogenated/dehydrogenated product
CP = cyclopentane
MCP = methylcyclopentane

The amount and nature of coke deposited on the spent catalysts were characterized employing the TPO technique. After the reaction test, the catalyst was separated to the original Pt-based/SiO_2 and Al_2O_3 grains by sieving. Figure 5.2 A-D

exhibits the comparison of the nature of coke between real system and physical mixture system. The difference types of coke on the metal and support function of Pt/Al_2O_3 can not been observed. Thus, it is reasonable to use the physical mixture of catalysts because it can be well separated between the two types of coke deposits as coke on the metal site occurred on the Pt/SiO_2 and coke on the support site obtained were observed. It is also found that when the grain size of Pt/SiO_2 mixed was smaller, coke profile is similar to that directly supported on alumina. From Table 5.2, the hydrogenated product of smaller size of Pt/SiO_2 was also more than that of bigger Pt/SiO_2, resulting in the lower amount coke. Additionally, it is implied the transport of coke precursor from one site to another site. This is corresponded with the earlier report [4, 30]. It is clear that coke covered on the support sites of the physically mixed catalyst and on the alumina supported platinum show the identical profile, especially the Pt/SiO_2 (100-120 mesh) physically mixed with Al_2O_3. Additionally, the combination area of two zones on physical mixture is also close to that of Pt/Al_2O_3. These results are attributed to the amount of carbonaceous deposits which is calculated from the area underneath as listed in Table 5.3. Consequently, Pt/SiO_2 with 100-120 mesh size combined with Al_2O_3 with 60-80 mesh size was chosen for the subsequent investigation.

Table 5.3 Comparison of the amount of carbonaceous deposits between Pt/A_2O_3 and Physical mixture with various sizes

Catalysts	%C on the metal site	%C on the support site	Total %C
Pt/Al_2O_3	-	-	3.17
Physical mixtures			
Pt/SiO_2 (20-30) $+Al_2O_3$	0.35	3.75	4.10
Pt/SiO_2 (40-60) $+Al_2O_3$	0.38	2.97	3.35
Pt/SiO_2 (80-100) $+Al_2O_3$	0.31	3.12	3.42
Pt/SiO_2 (100-120)$+Al_2O_3$	0.28	2.43	2.71

According to statistical observation, the interaction between metal and support is well established as well as the H_2 spillover. H_2-TPD method was used to measure H_2 uptake, which demonstrates H_2 spillover behavior [2, 172, 173]. Figure 5.3 exhibits H_2 uptake of the Pt/Al_2O_3 and the combination of Pt/SiO_2 and Al_2O_3. It appears that no desorption peak was detected over Al_2O_3. It can be speculated that hydrogen was originally generated on the metal sites and spilled over to the support sites as reported in elsewhere [2, 174-176]. However, the possibility of spill over of surface species of physical mixture is not as high as the Pt/Al_2O_3 catalysts because of many contact points between the two catalytic species in the case of the Pt/SiO_2-Al_2O_3 system.

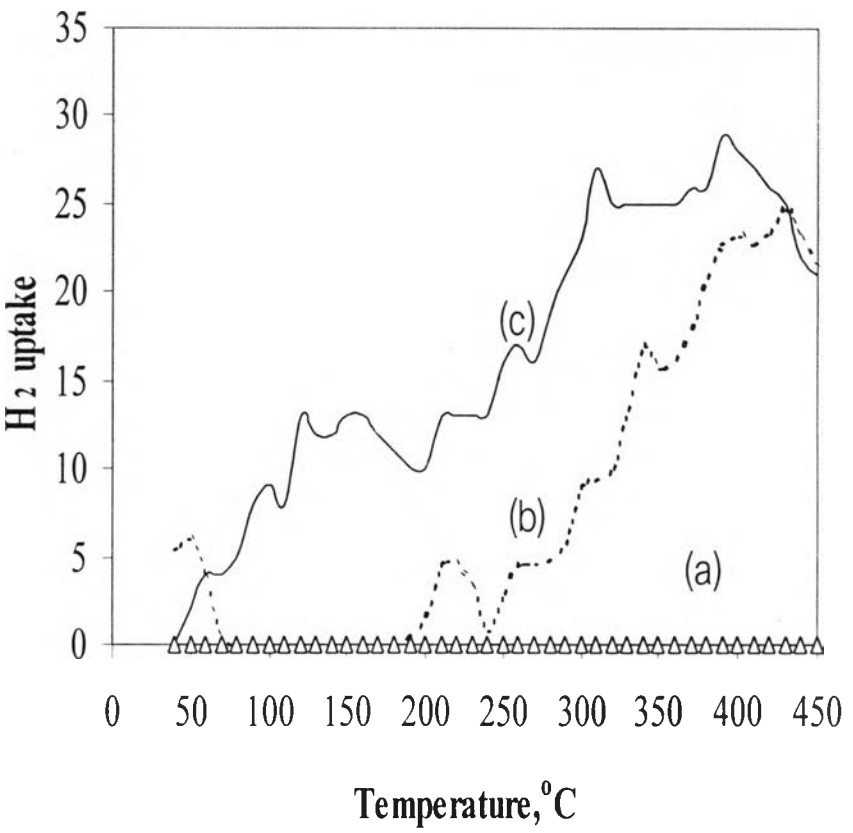

Figure 5.3. TPD of hydrogen after reduction at 30 °C: (a) Al_2O_3 (b) Pt/SiO_2 (100-120 mesh) mixed with Al_2O_3 and (c) Pt/Al_2O_3

In order to support the cooperative effect, the catalyst deactivation for hexane dehydrogenation over the combination of acidic and metal species was studied at 475°C and 2 h-TOS as shown in Figures 5.4 and 5.5. Figure 5.4 illustrates the comparative activity of real system, whereas the cooperative effect for the hexane dehydrogenation and the amount of coke for these systems are exhibited in Figure 5.5. For this case, the catalyst activity and deactivation behaviors were observed over both catalysts (Pt/Al_2O_3 and physically mixed Pt/SiO_2 with Al_2O_3). The amount of coke computed from the area underneath the TPO curve is illustrated in Table 5.4. Interestingly, it is seen that coke on the support sites of physical mixture system was coincident with coke on the support site of the real system. It is emphatically supported that the transfer of coke precursor was generated by gas phase instead of the drain off effect. This is confirmed by the fact that if the drain effect is the reason for the coke transfer mechanism, the disagreement of the coke profiles between the acidic sites and Pt/Al_2O_3 must be expressed because of the restriction of contact between particles.

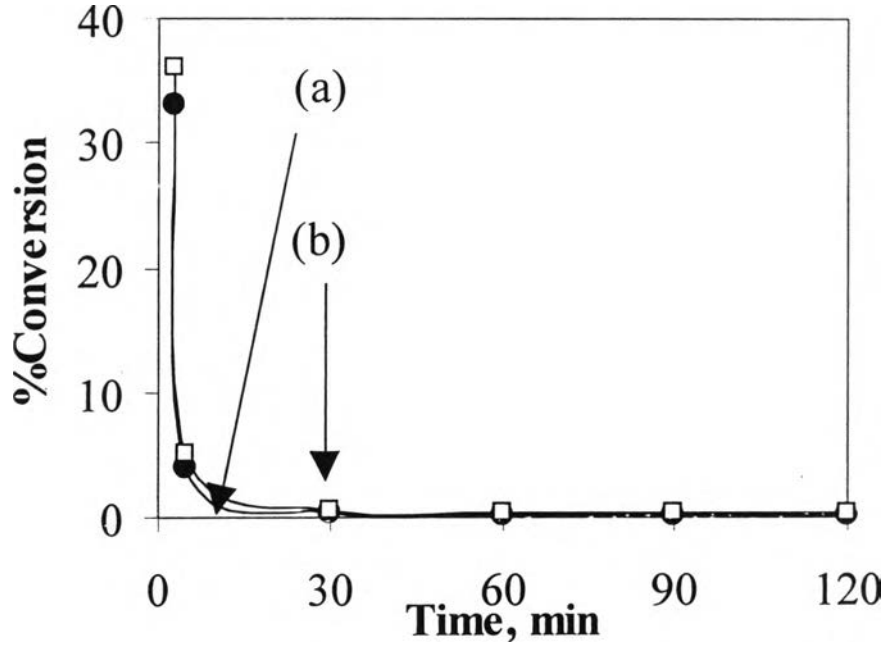

Figure 5.4. % Conversion of Pt/Al_2O_3 and Physical mixtures for hexane dehydrogenation: (a) Pt/Al_2O and, (b) Pt/SiO_2 (100-120) + Al_2O_3

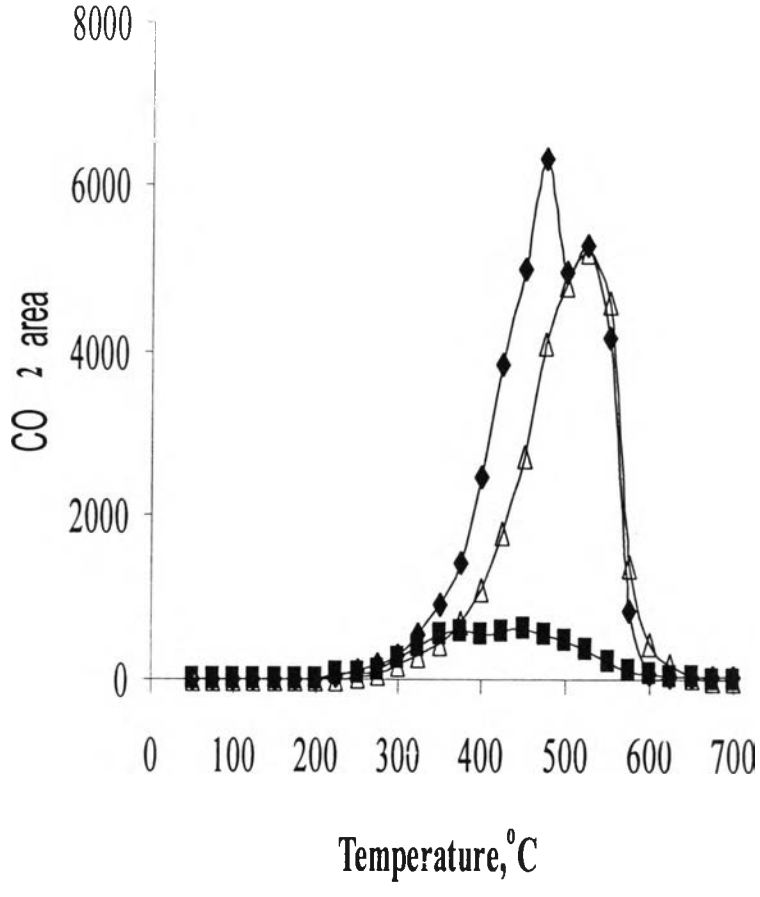

Figure 5.5. Temperature programmed oxidation of carbonaceous deposits with various mesh sizes of Pt/SiO_2 for hexane dehydrogenation;
◆ Pt/Al_2O_3, Δ Al_2O_3, ■ Pt/SiO_2(100-120)

Table 5.4 The amount of coke on Pt/Al_2O_3 and Pt/SiO_2 mixed with Al_2O_3 from hexane dehydrogenation

Catalyst	%C on the metal site	%C on the support site	Total %C
Pt/Al_2O_3	-	-	3.27
Physical mixture Pt/SiO_2 (100-120)+Al_2O_3	0.36	2.50	2.86

As mentioned above, it can be concluded that this cooperative effect is generated even if the two species exist as separate catalyst particle. Although the physical mixture is not real, it is only virtual. It can be applied a combination of acidic and metal species for study catalyst deactivation for dehydrogenation reaction. The small grain size of Pt/SiO_2 with 100-120 mesh size and Al_2O_3 with 60-80 mesh size is close to the behavior of Pt/Al_2O_3. The transformation of intermediates from one site to other sites by gas phase seem to be responsible for coking on support.

5.2 Coking study using the physical mixture of Pt/SiO_2 and Al_2O_3

The coke deposited on the metal and the support at different hexane dehydrogenation conditions was studied with many techniques as follows:

5.2.1 The effect of time

1. Carbon deposition and catalytic activity

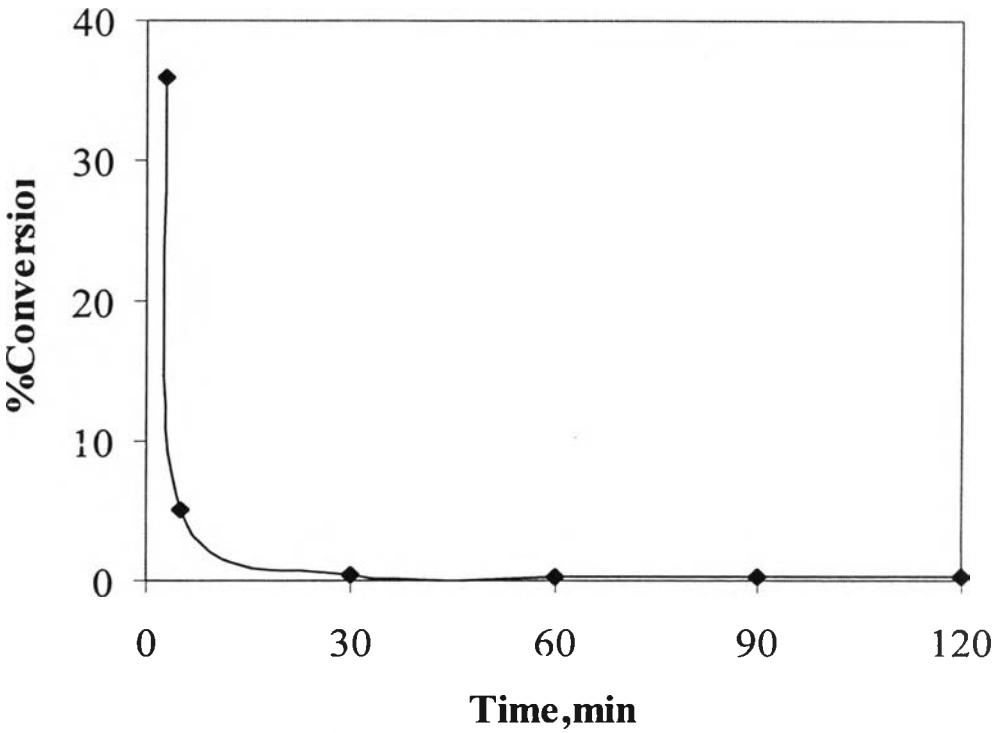

Figure 5.6 % Conversion of Physical mixture for hexane dehydrogenation with various times

As pointed out by many authors, the most convenient way to throw light on the mechanism is to follow the coke formation rate by measuring in some way the growing amount of coke deposited with time. This study was carried out on a physical mixture of Pt/SiO_2 and Al_2O_3 at 475°C under normal pressure with the hexane dehydrogenation. Usually, the analytical samples were taken after 10, 30, 60 and 120 min time on-stream. Figure 5.6 exhibits the conversion of the hexane

dehydrogenation at various times. After sharp initial increase, this manifested itself decreasing the conversion per unit time as the reaction proceeded. The conversion measured at 3 min was already 35 % and after that the conversion obtain was close to zero. The accumulation of carbonaceous deposits results in a gradual deactivation of Pt catalysts [3, 40, 73, 79, 86].

The TPO profiles observed over the coked catalysts are illustrated in Figures 5.7 and 5.8. Figure 5.7 shows that the two peaks around 300°C and 425°C corresponding to coke oxidized at the metal phase as reported elsewhere [3]. Furthermore, it is shown the increasing amount of carbonaceous deposited over the metallic sites (second peak) with the increasing time. However, coke accumulated over support sites was also generated as depicted in Figure 5.8. In this case, it shows only a peak around 525°C in the TPO profile. Additionally, the amount of carbon deposited on the metal surface atom and on the support site is shown as a function of coking time in Table 5.5. The coke accumulation on support function occurred rapidly at the initial period and became gradually generated later. In the earlier work [44, 120], deposition of coke on the catalysts was also measured as a function of time on stream, under the standard reforming conditions. Results were fitted to the Voorhies correlation for coking. Voorhies empirically described coke formation as a function of time-on-stream via the following simple equation,

$$\% C = at^b$$

where % C is the percentage carbon formed in time t, and a and b are constants.

Concerning the area and the amount of coke, there was a greater value on the support function compared with that on the metal phase. The amount of coke on the catalyst increased with the increase in the time on stream. This is in associated with the other researcher [14]. Most researchers have studied the rate of carbon deposition over long operation periods, but less attention has been paid to the dynamic process of carbon deposition. These results can be implied that coke deposits on metal site is less dehydrogenated than that on the support in accordance with the literature reviews [184, 185]. The metal function regulates the amount of coke deposited on itself and

amount formed on the support since it is primarily responsible for the production of the coke precursor species [11].

Table 5.5. The amount of carbon deposited on the catalysts with various times

time, min	Coke on the metal sites % C	Coke on the support sites % C
10	0.28	1.47
30	0.31	1.64
60	0.31	2.10
120	0.36	2.50

2. Characterization of C_xH_y species

IR spectra of coke collected from 10, 30, 60 and 120 min time on stream are illustrated in Figure 5.9. On the metal site shown in Figure 5.9A, the individual spectra in each time were coincident. One intense band was detected at approximately 1610 cm-^{1}. Normally, this band in this region is specific to stretching mode of aromatic system [23]. This evidence indicates that there was so little modification in the structure of coked catalyst for the reaction time in period of 10-120 min. As shown in Figure 5.9B, there was also the presence of band around 1610 cm^{-1}. However, the higher intensity over the coke on metal sites was shown, suggesting that coke began to condense into aromatic ring. It is interesting to note that, as the reaction time proceeded to 30 min, there was a presence of the characteristic group of C=C stretching in aromatic ring at 1540 cm^{-1}. This indicates that the longer the reaction time the more complicated the spectrum [41]. Compared with these spectra, the spectrum of coked catalyst on the metal sites showed a slightly increase in aromatic band. Coke band at higher wave number (1610 cm^{-1}) indicates the formation of graphite-like coke [61, 186]. No IR adsorption bands of aliphatic hydrocarbons at 2960 and 2800 cm^{-1} for CH_3 and 2930 cm^{-1} for CH_2 were observed for both sites of the coked catalysts. Thus, only aromatic ring structure can be identified.

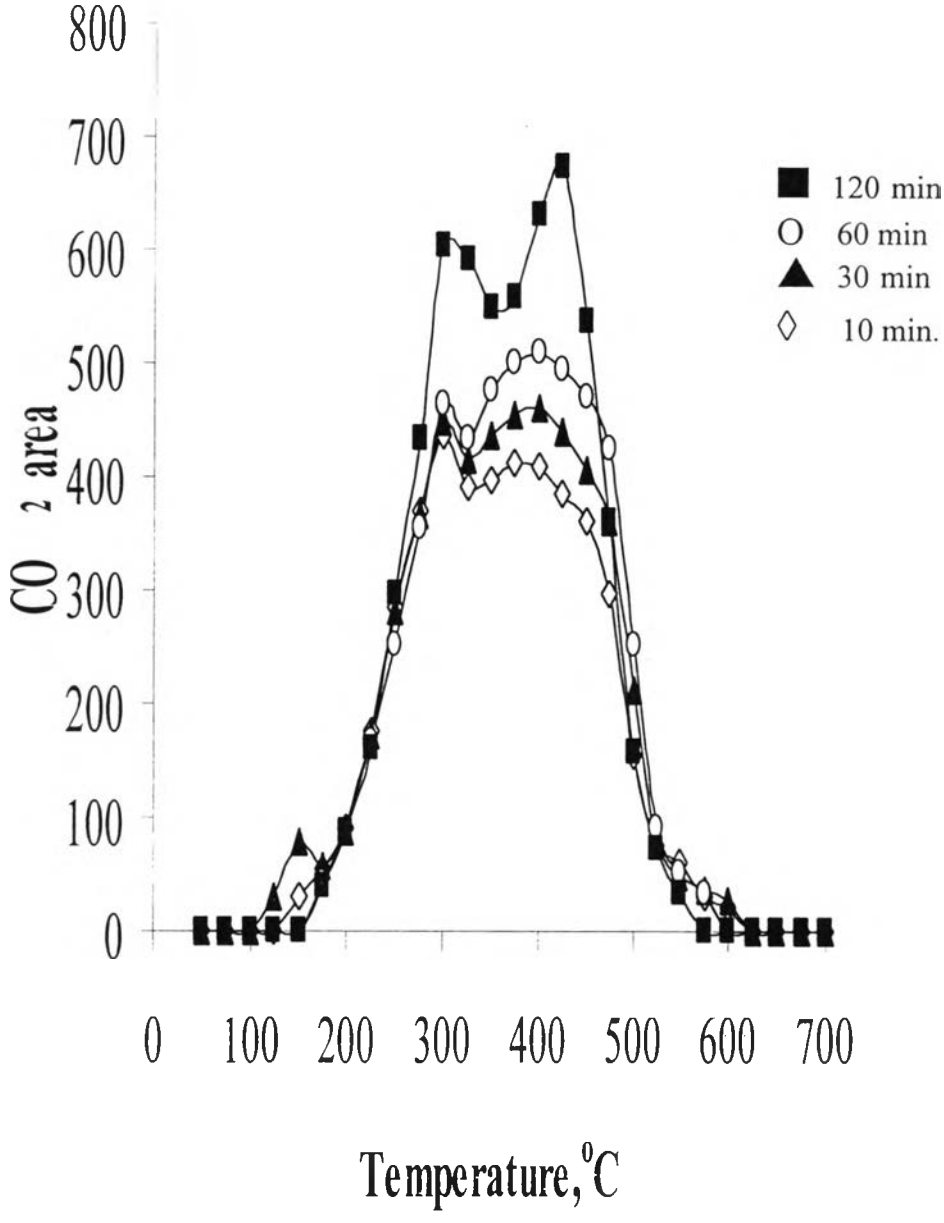

Figure 5.7 TPO of carbonaceous deposits produced on the metal at 475°C and H_2/HC = 0 with various times on stream

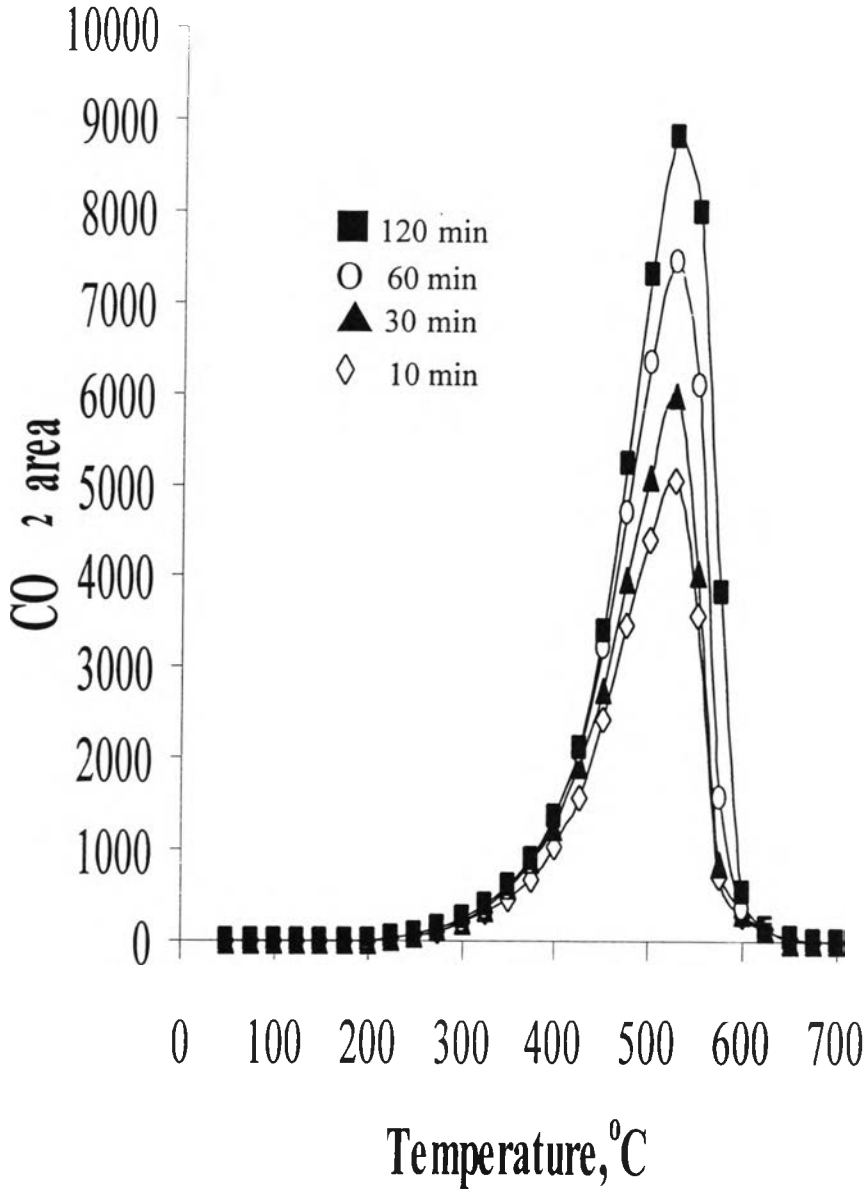

Figure 5.8 TPO of carbonaceous deposits produced on the support at 475°C and H_2/HC=0 with various times on stream

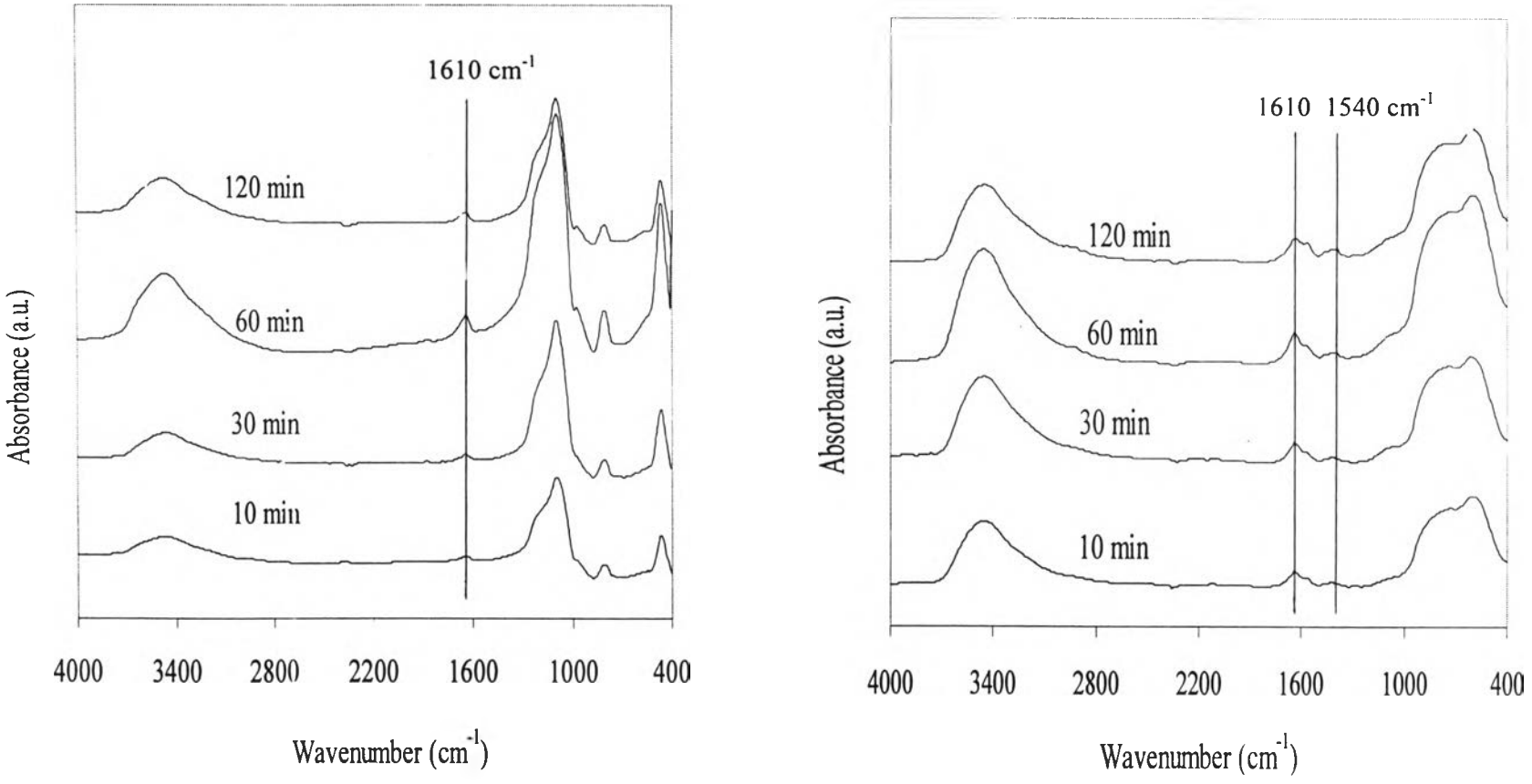

Figure 5.9 IR spectra obtained after coking at various times over (A) the metal and (B) support

Electron Spin Resonance (ESR) has long been an effective technique to estimate the radical density of coke. ESR spectra are obtained by measuring the intensity vs wavelength (or frequency) of a beam of electromagnetic radiation as it passes through a sample of matter, which is presented in a derivative trace of absorption curve. Then, the radical density can be computed from the integrated area of the spectra obtained [160]. Further coke radicals are representative of the overall coke, for both its nature and its amount because the amount of olefin or allylic radicals are characteristic of carbonaceous matter as introduced elsewhere [137, 125, 178-181]. In earlier studies [178, 179], they investigated low temperature coke (below about 500 K) and high temperature coke radicals (above about 500 K). They found that olefinic or allylic oligomeric species were low-temperature coke radicals while highly unsaturated species were high-temperature coke radicals. Consequently, the formation of radicals enables us to discriminate between individual coke of various catalysts including coke on the metal sites and the support surface.

Figure 5.10 shows the ESR spectra of the metal phase with increasing in the time on stream. It is obvious that the line of ESR signal of coke continued to grow. This is parallel to the amount of radicals of coke as presented in Table 5.6. In case of acidic function, the ESR spectra are presented in Figure 5.11. These signal intensities are not seemed to be different. Thus, the amount of carbonaceous radicals integrated from ESR spectra, listed in Table 5.6, was considered instead. It is reported that the increase in ESR signal resulted from increasing time. The comparison of carbon radicals in the both sites shows the obvious difference of intensity and amount. Therefore, most of carbon radicals generated on the support sites. Approximately, the carbon radicals presented on the support were twofold of that on the metal sites after 10 min-TOS. This indicates that the rapid growth of carbon radicals was in the initial time and gradually produced with the longer time. This is in agreement with the previous results. However, the absorbed g values for the coked catalyst at different reaction time are similar to each other (g value 2.003) with both sites. The corresponding radicals are referred to intermediate radicals, i.e., olefinic or allylic radicals [144, 178, 181, 182].

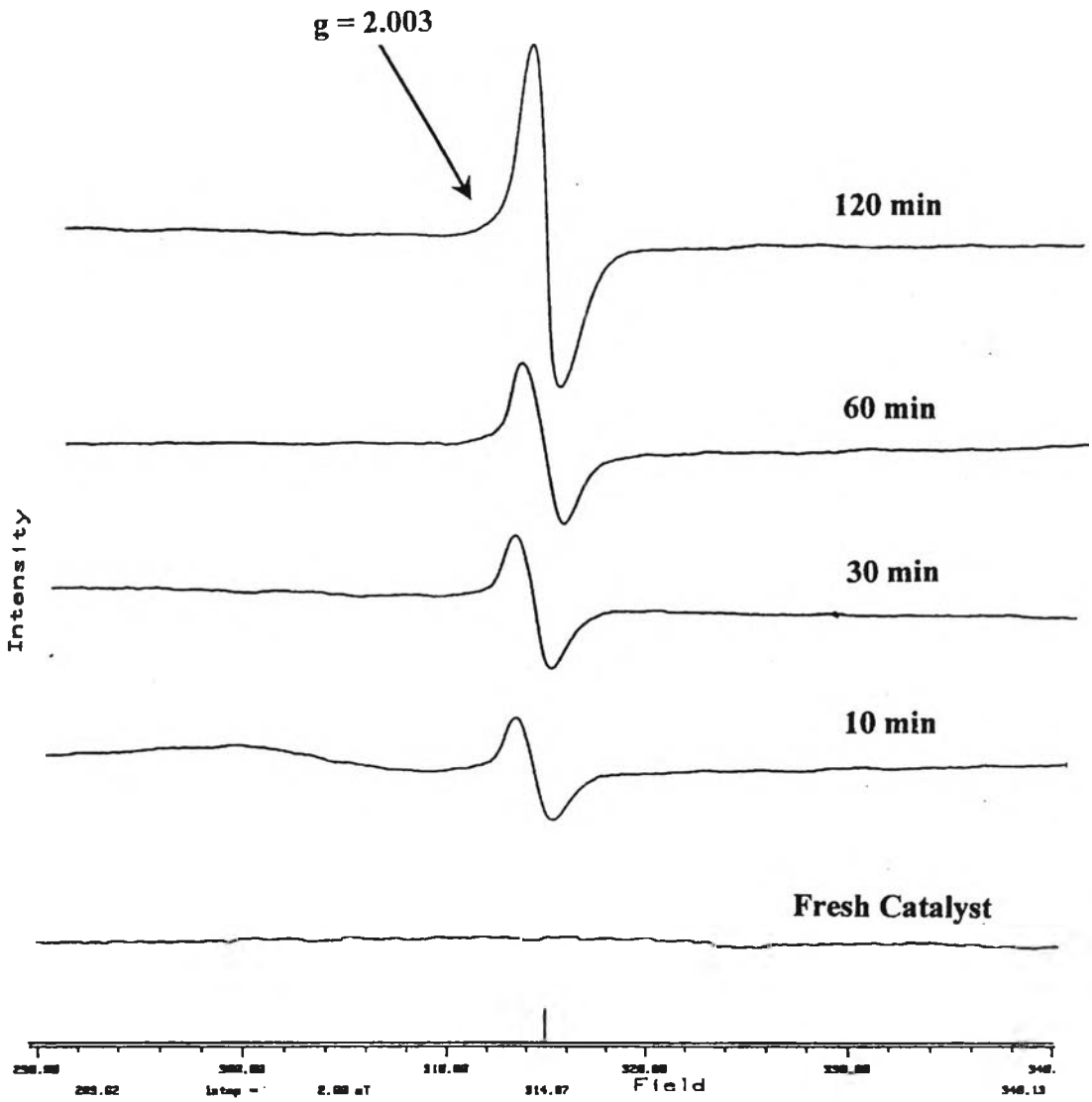

Figure 5.10 ESR spectra of coke on the metal at 475°C and H_2/HC = 0 with various times on stream

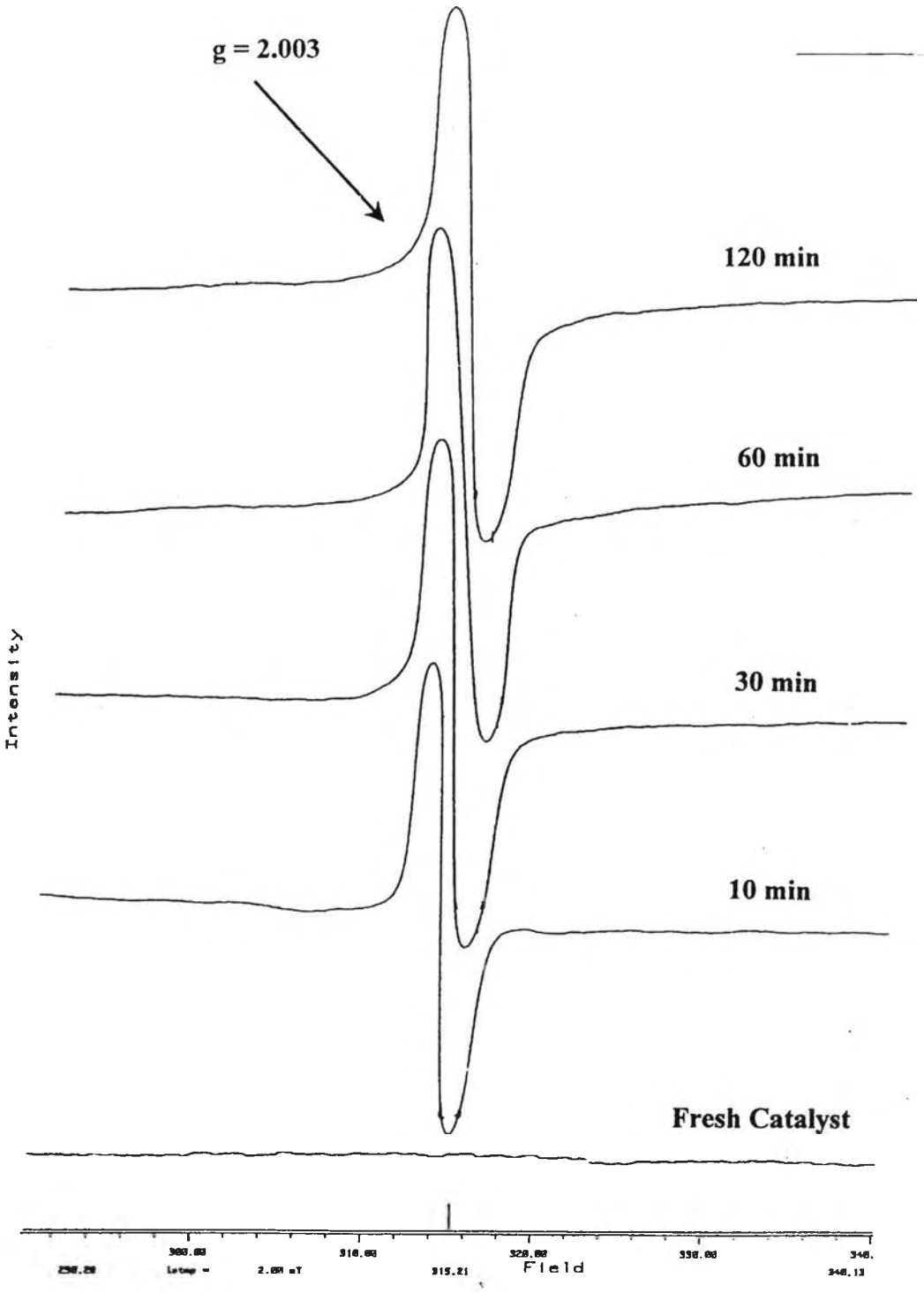

Figure 5.11 ESR spectra of coke on the support at 475°C and H_2/HC = 0 with various times on stream

Table 5.6. The density of carbon radicals of coke per gram catalyst with various times on stream

time, min	The metal sites	The support sites
10	2.27×10^{5}	1.45×10^{6}
30	3.73×10^{5}	2.28×10^{6}
60	4.70×10^{5}	2.33×10^{6}
120	8.55×10^{5}	3.02×10^{6}

3. Carbonaceous morphology

The morphology of carbon deposited at various periods of time on stream was checked by taking successive photographs. Figures 5.12 and 5.13 show TEM photographs of fresh and coked catalysts taken at two different magnifications. The particles were well separated from each other with narrow size distribution. Coke coverage on the metal sites was found to be a function of time on stream. In case of the support sites, the growth of carbon chain with time was strongly pronounced as seen from Figure 5.13. This aspect could be linked to the formation of an encapsulating layer of carbonaceous that was responsible for deactivation [12, 38, 183]. In the present study, it is confirmed that coke built up both on the metal phase and on the support function. In addition, the progression of coke is sometimes limited by the edges of the alumina sheets on which the metal particle sticks, but coke spilling onto neighboring sheets occurs frequently [18, 34]. Hence, more coverage occurring on the support site was noticed. Considering the graphitic coke followed the literatures [151, 184, 185], neither regular graphite spacing nor fingerprint like arrangements characteristic of graphitic structures were observed. Therefore, it can be concluded that the coke deposited on the metal and support functions probably had an amorphous structure.

ต้นฉบับ หน้าขาดหาย

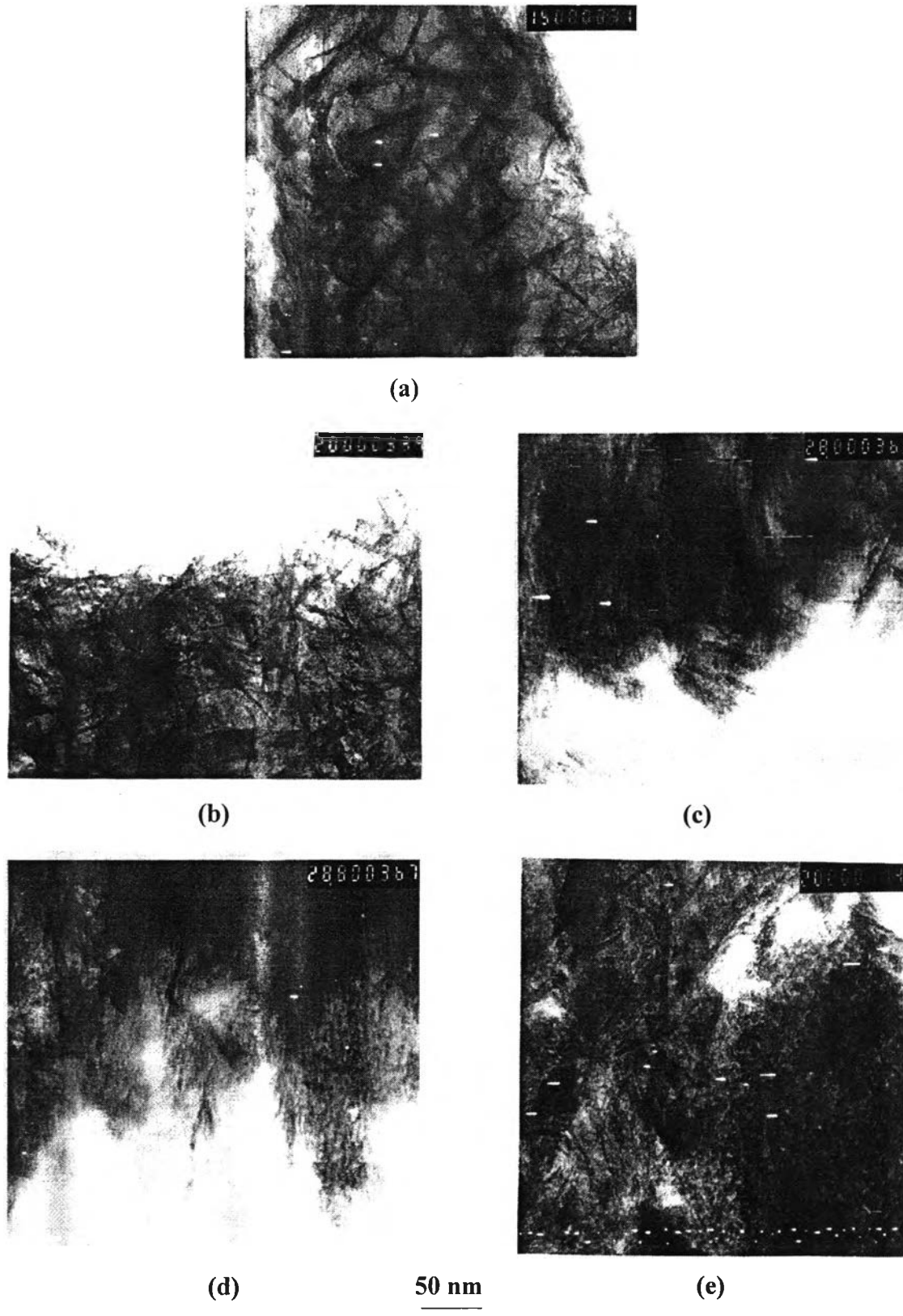

Figure 5.13 TEM photograph of coke on the support at various times on stream: (a) fresh catalyst, (b) 10 min, (c) 30 min, (d) 60 min and (e) 120 min

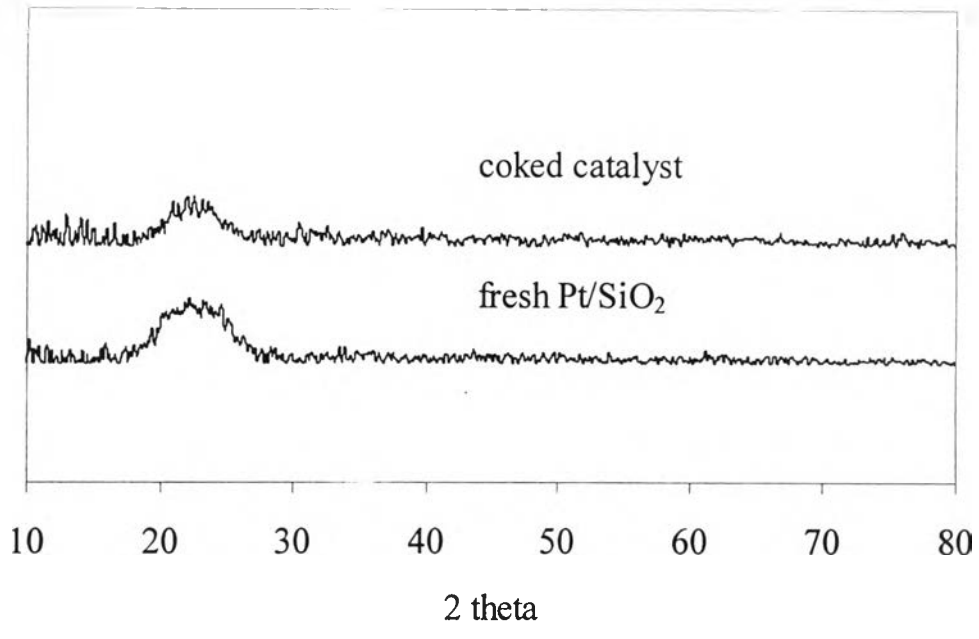

Figure 5.14 XRD spectra of coked sample on the metal at 120 min

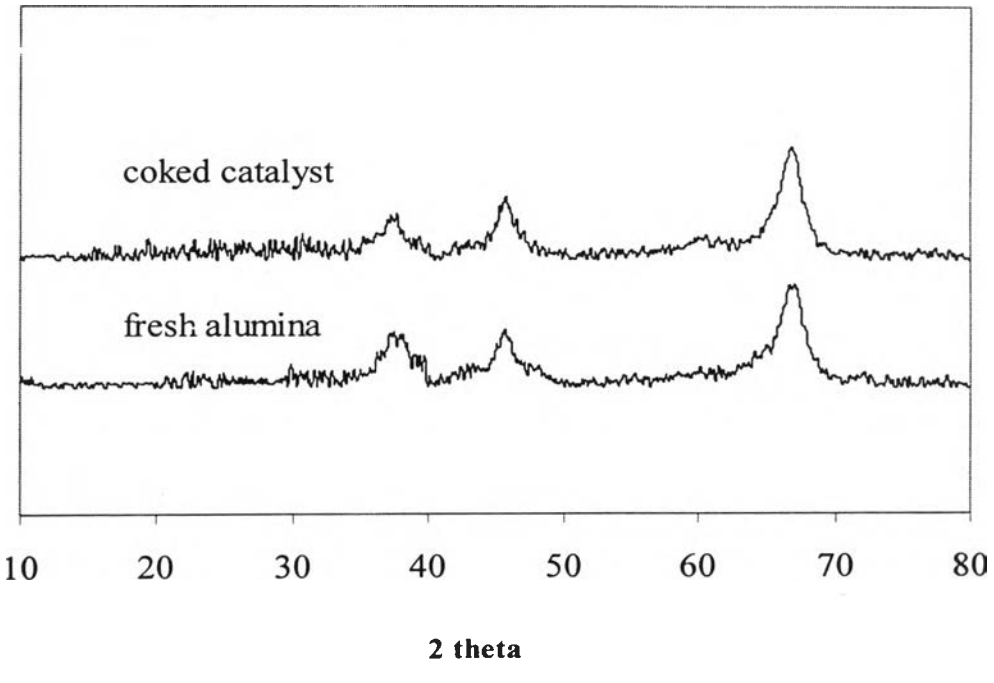

Figure 5.15 XRD spectra of coked sample on the support at 120 min

The XRD patterns of fresh Pt sample and that used for 2 h are reported in Figure 5.14 and Figure 5.15. For the metal site, both fresh Pt/SiO_2 and used Pt/SiO_2 exhibited the same position as a broad peak around $2\theta = 22^{\circ}$ owing to the silica gel. Comparing with XRD pattern on the support site (Figure 5.15), it is seen that fresh and spent Al_2O_3 catalysts gave the same peak, which is the characteristic peak of amorphous Al_2O_3. The presence of graphite or pregraphitic carbon can be especially ruled out from the absence of XRD peak [38, 105]. Hence, the coke deposition occurred in the amorphous phase on the both sites that can not be detected by XRD. Consequently, XRD was not employed for the characterization in the next section.

4. The changes of textural properties and the dispersion factors of coke on the metal and the acid with various times

Table 5.7. The textural properties of catalysts samples before and after testing and dispersion factor with various times

Time,min	The metal sites			The support sites		
	SA (m^2/g)		dispersion	SA (m^2/g)		dispersion
	Fresh	Used	factor	Fresh	Used	factor
10	447	336	396	390	330	41
30	447	352	309	390	333	35
60	447	363	270	390	336	25
120	447	386	171	390	343	19

In order to investigate the degree of filling of coke into the pore of catalyst [6, 38, 147, 180, 186, 187], the pore structure of coked catalyst was examined with N_2 adsorption isotherms of fresh and used catalysts formed at different times. The BET surface area is tabulated in Table 5.7. It is seen that with the coke coverage, the BET surface area was decreased. However, the decrease in surface area was less significant in case of the acidic site coverage. The presence of large concentrations of carbon in pore of coked catalysts implies that much of porosity has been filled [131]. The degree of pore filling can be calculated from the chemical composition of coked

catalysts as previously reported in Table 5.7. The dispersion factor is the ratio of change of surface area to the quantity of carbon deposits. Higher values of dispersion factor proved that carbon deposited on this catalyst is better dispersed with the fine small grain structure. It is seen that the dispersion factors obtained gave the same trend on both sites. These values increase when it was more severe temperature conditions. Interestingly, these dispersion factors of metal site were greater than those of support function.

5. Characterization of coke extracted from coked catalyst with different times

In order to determine the chemical composition of coke, the coke on the support and metal sites was extracted by toluene for 24 h. The soluble coke components were analyzed by GC-14B with capillary column (DB1) for the study of coke distribution. Figures 5.16 and 5.17 show the extracted coke profile of a typical chromatogram on the metal sites and the acidic sites as a function of time-on-stream, respectively. On the metal site, the soluble coke was mainly composed of C_8-C_{12}. The extracted coke became more aromatic in nature with the increase in the reaction time. Extracted coke from acidic sites also displayed dominantly components of C_8-C_{12}. However, it is found that in the initial time the soluble coke was constituted of lower carbon atom. Regarding the amount of soluble coke, the extracted coke on the metal site was more qualitative and more easily removed than that on the support site. This was expected since highly polyaromatic coke molecules are insoluble in toluene. This was furthermore confirmed through the above results of TPO, ESR and IR. It can be reasonably assumed that the soluble coke molecules are intermediates in the formation of the insoluble coke, which is composed of higher polynuclear aromatics [75, 87]. It has been shown previously that part of the insoluble coke molecules resulted from the growth of soluble coke molecules. The desorption of coke precursors and the increase of contact time facilitated the formation of insoluble coke molecules. This change in the coke composition can be attributed to dehydrogenative couple of polyaromatic species. The dehydrogenative coupling of polyaromatic molecules could explain the particular behavior regarding the formation of non-

soluble coke. The greater formation of non-soluble coke would be due to the longer time on stream required for the formation of coke [34, 38, 79]. Moreover, the transformation of intermediate from the metal to support sited occurred as attributed in the above analysis results. The more intermediate generated, the more carbonaceous deposits are produced. The soluble coke molecules were therefore intermediates in the formation of insoluble coke, which was what allowed us to suppose that: (i) insoluble coke is not formed at low coke content and (ii) the aromaticity of the soluble coke increases with the coke content (indeed insoluble soluble coke is composed of highly polyaromatic molecules).

The hydrocarbon compositions in coke, which were analyzed as previously described, are reported in ASF plots used to calculate α values shown in Figures 5.18 and 5.19. It is obvious for both sites that the α values grew up to a higher value with increasing time. From Figure 5.18 a-d, the α values increased from 0.29 to 0.67. In the same way, on the support site α values enhanced from 0.32 to 0.65. The higher α value, the more heavier products generated in the coke fractions. This may reflect the increase of less volatile compound or greater adsorptivity of long chains [193]. Probability of chain branching is seen to be strongly dependent on carbon number. Interestingly, in the region of 10-60 min, the probability of chain growth on the metal function was different from that on the support site. It is found that the acid sites resulted in a greater α value. This is suggested that the two alpha values correspond to different product grouping [189]. Previously, the two alpha values have been attributed to two, or more, types of sites. Significantly, two probabilities of chain growth are occurrence of different catalytic sites or the existence of different chain termination reaction. Additionally, two different alpha value are suggested that two independent chain-growth mechanisms contributed to the overall distributions. For the longer time, the probability of chain growth on both sites were closely equal. This is attributed to the transformation of coke intermediate from the metal site to the support site. Significantly, it is apparent that a break occurred in the plot at carbon number c.a. 10. This deviation is likely caused by accumulation of higher molecular weight hydrocarbon. These results are very similar to those reported in the published

ต้นฉบับ หน้าขาดหาย

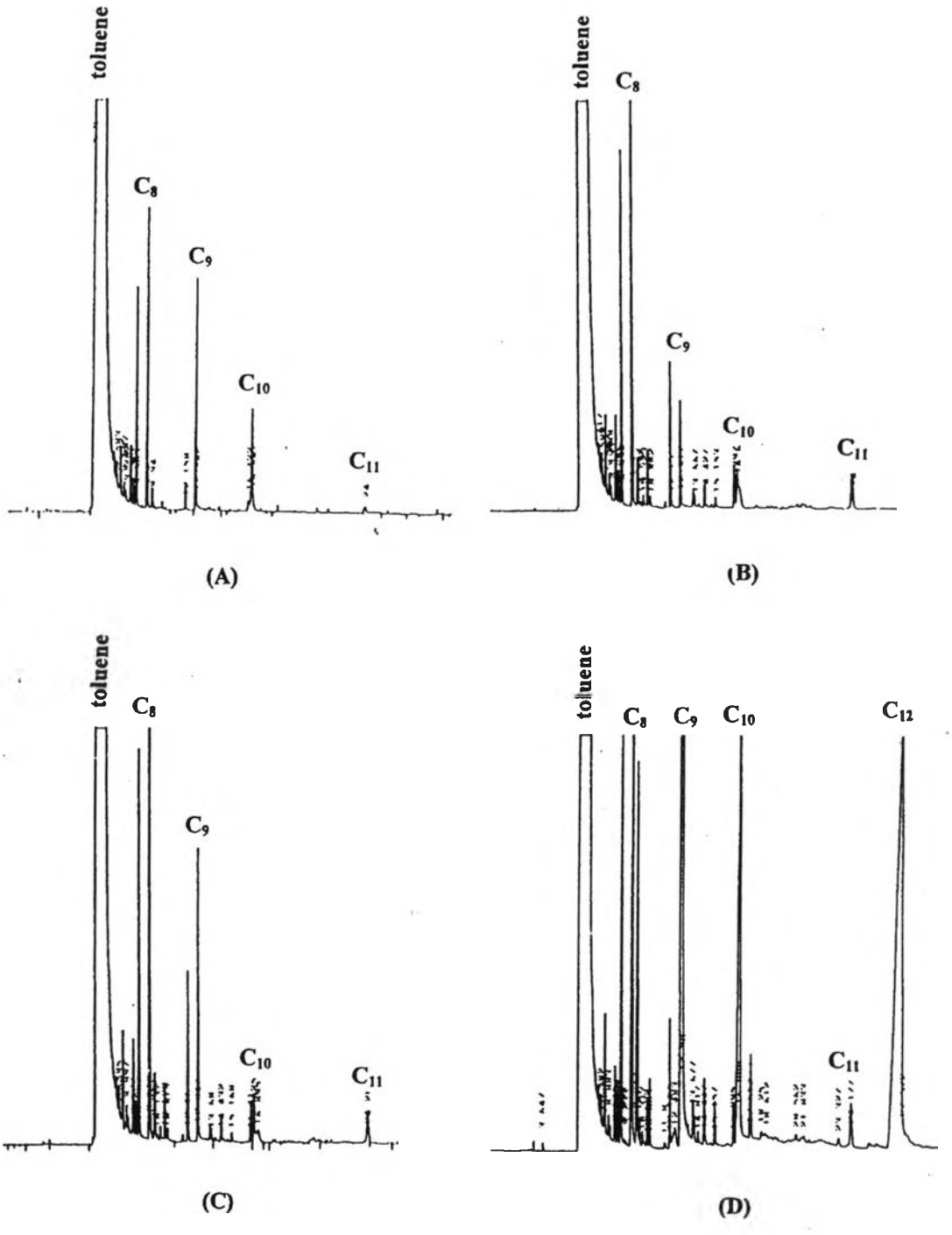

Figure 5.16 The component of the extracted coke on the metal at various times on stream: (A) 10 min, (B) 30 min, (C) 60 min and (D) 120 min.

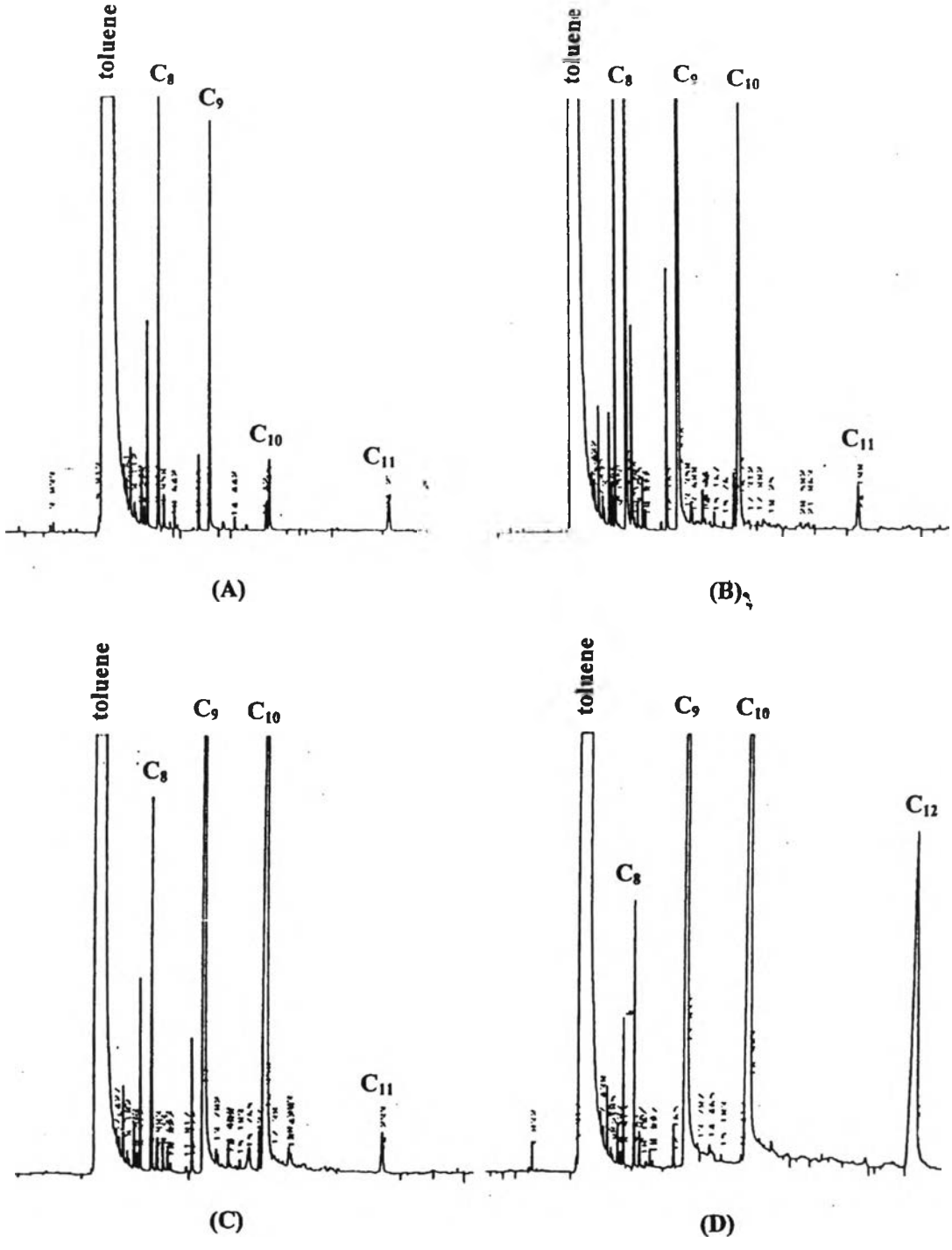

Figure 5.17 The component of the extracted coke on the support at various times on stream: (A) 10 min, (B) 30 min, (C) 60 min and (D) 120 min.

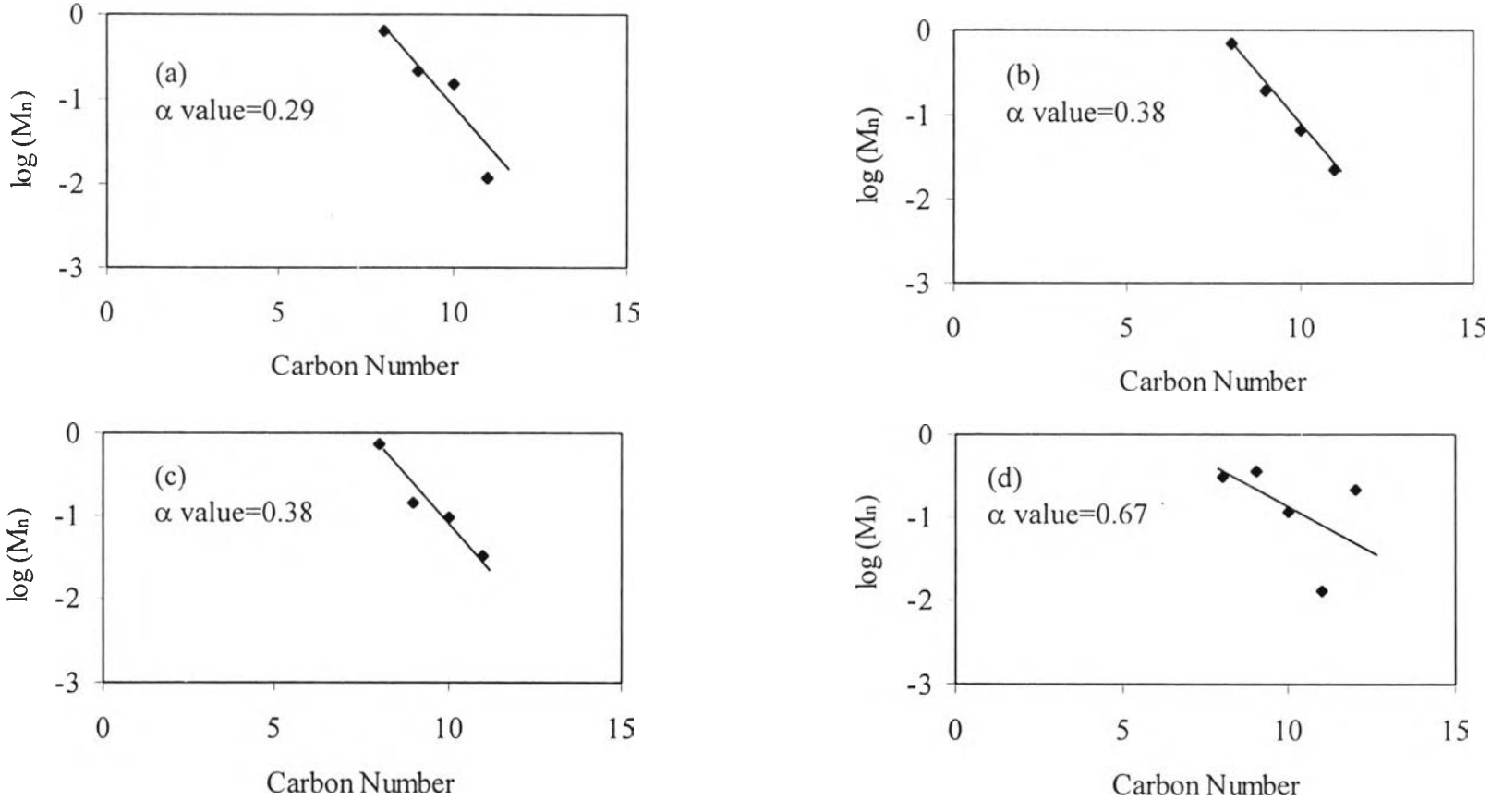

Figure 5. 18 Schulz-Flory diagram of soluble coke from the metal at various times on stream: (a) 10 min, (b) 30 min, (c) 60 min and (d) 120 min

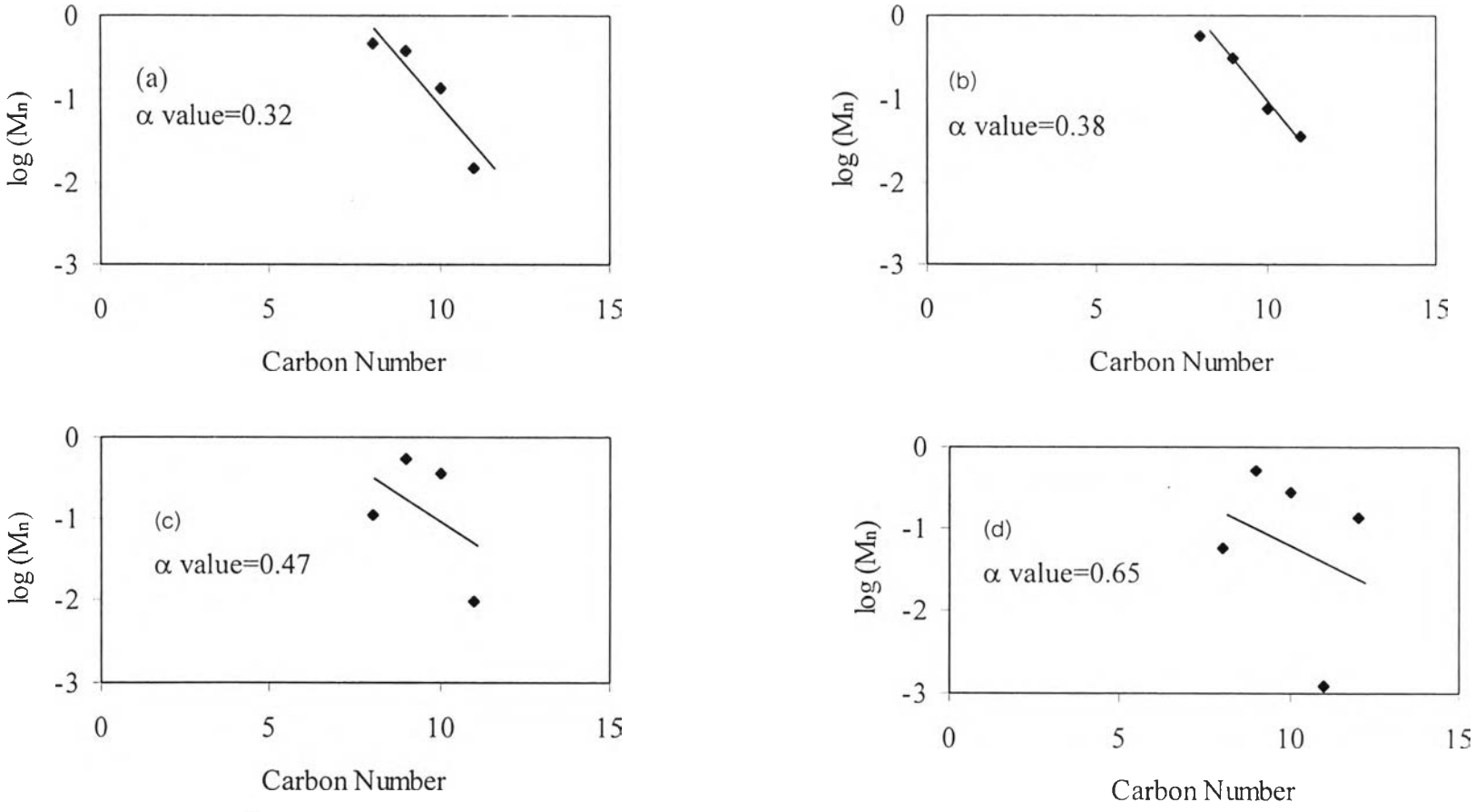

Figure 5.19 Schulz-Flory diagram of soluble coke from the support at various times on stream: (a) 10 min, (b) 30 min, (c) 60 min and (d) 120 min

5.2.2 The effect of temperature

1. Carbon deposition and catalytic activity

The coking reaction with n-hexane was carried out on a physically mixed catalyst (0.3% Pt/SiO_2 100-120 mixed with Al_2O_3) for 2 h in the temperature ranging between 300°C and 500°C. Figure 5.20 shows the TPO curves of coke deposition on the metal site. Two successive peaks, which represent two types of carbon deposits on the surface of catalyst, were displayed in all the TPO profiles around 300°C and 425°C. Except at the temperature reaction of 300°C, carbon deposited expressed in the first peak of spectrum began to react with oxygen at lower temperature than any other temperatures. The TPO peak maximum was shifted towards higher temperatures with the increase in coking temperature. It is indicated that coke removal becomes increasingly difficult with increase in the coking temperature [4, 10]. An overall decrease of the TPO areas was observed as the temperature of coking reaction decreased. This effect was more obvious for the second peak on the metallic function around 425°C. Determination of the amount of carbon deposited on metal surface under area was summarized in Table 5.8. The amount of carbon deposition increased with the increasing temperature.

Table 5.8 The amount of carbon deposited on the catalysts with different temperatures

Temperature,°C	Coke on the metal sites % C	Coke on the support sites % C
300	0.28	1.61
400	0.30	1.64
475	0.36	2.50

For the peak at ca. 525°C, it corresponded to the coke on the support (see Figure 5.21). It is also found that at higher coking temperature this peak became very large. However, it is found that the much higher levels of coke deposited on the Al_2O_3 as compared to the Pt sites associated with the amount of carbon deposits listed

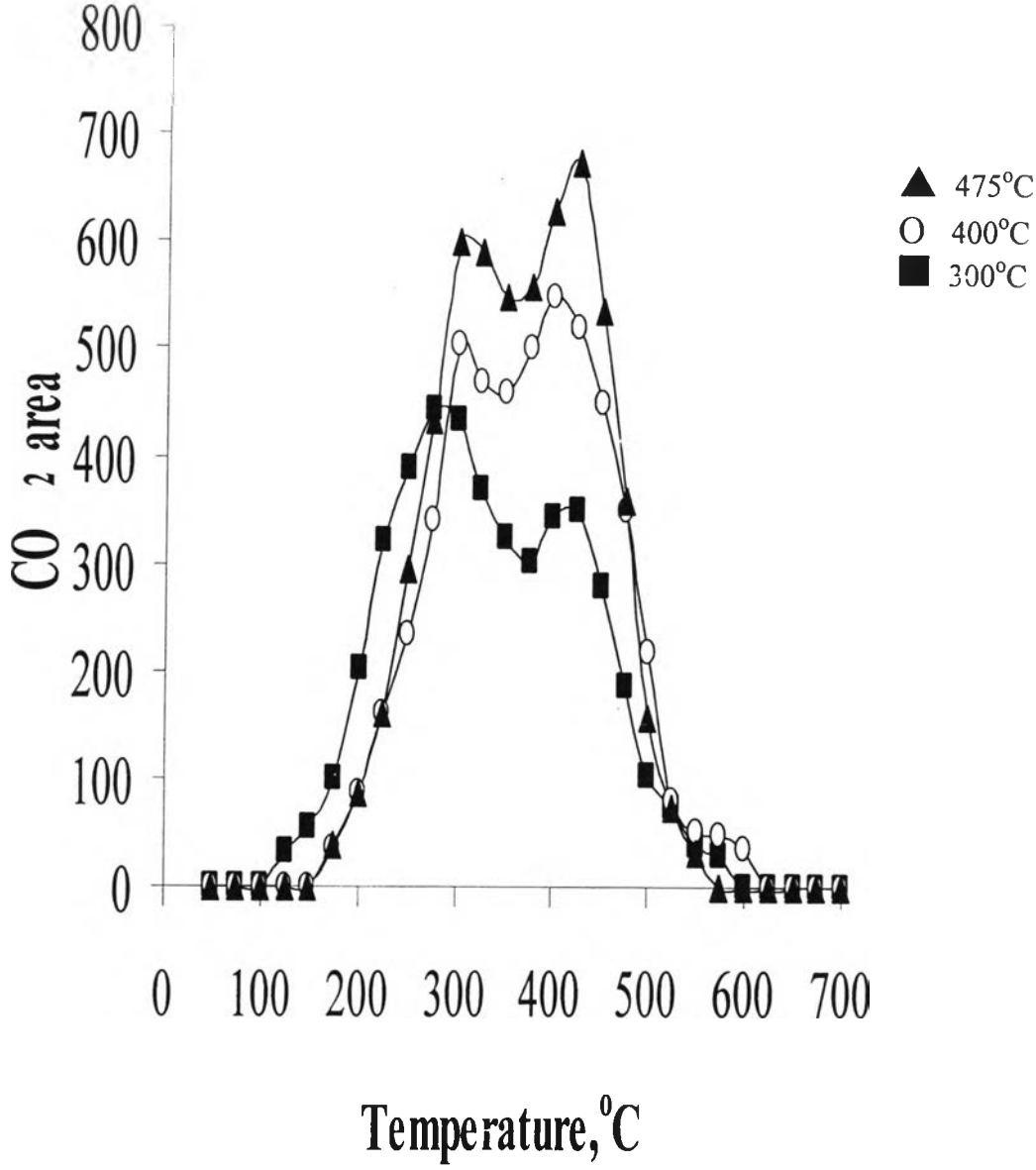

Figure 5.20. TPO of carbonaceous deposits produced on the metal at 120 min and H_2/HC=0 with various temperatures

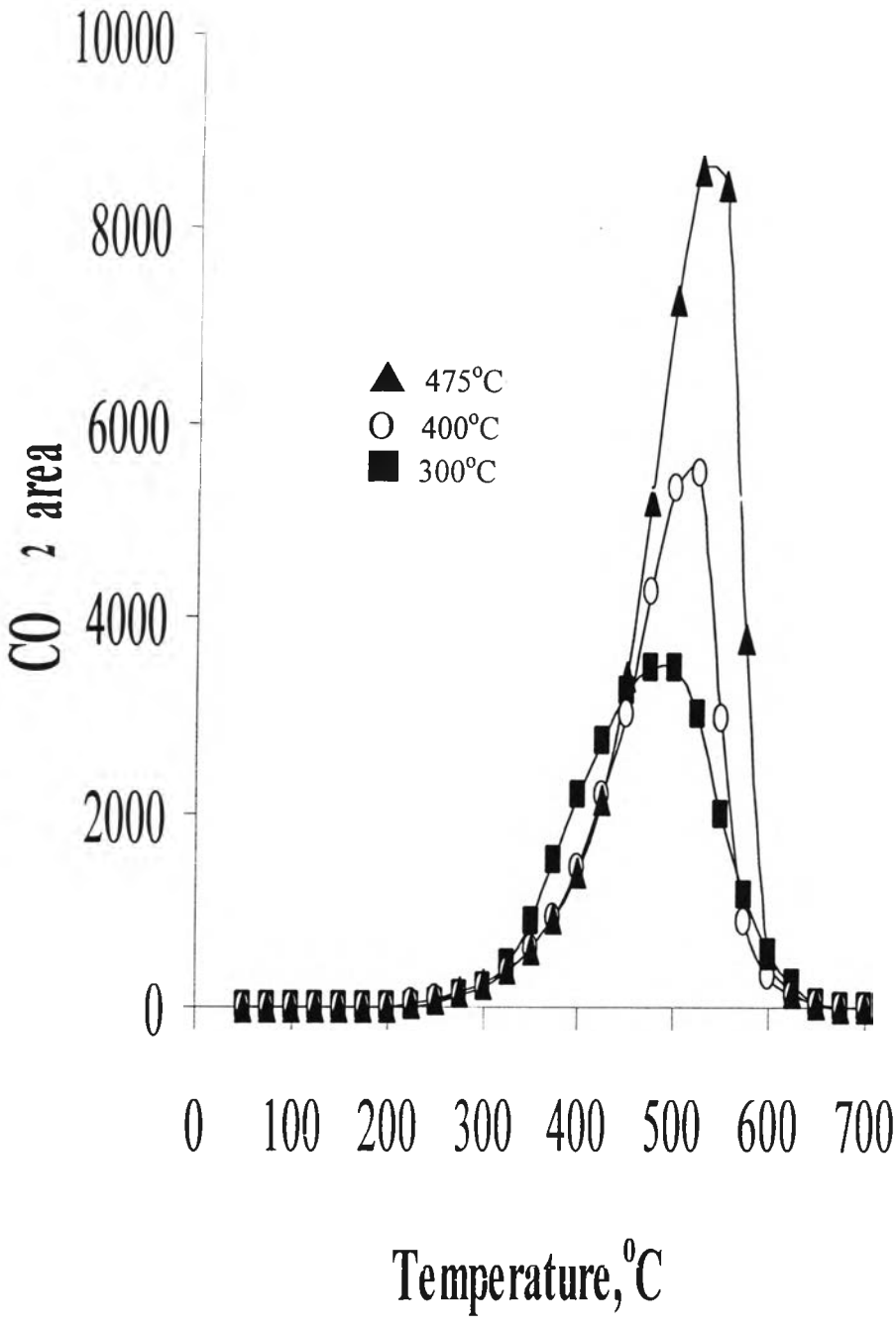

Figure 5.21 TPO of carbonaceous deposits produced on the support at 120 min and H_2/HC=0 with various temperatures

in Table 5.8. These results indicated that the coke on the metal site formed weakly bound carbonaceous species on the surface, which can be removed by oxygen. It is implied that the overall H/C ratio of coke decreased with increasing coking temperature [1, 13, 48, 73, 121, 129].

Measurable catalytic activity for the n-hexane conversion is maintained by all catalysts for reaction times of 2 h as illustrated in Figure 5.22. At these reaction conditions, it exhibits the initial n-hexane conversions of 300°C, 400°C and 475°C, respectively. In each condition, conversion decreases closely to essentially zero within 10 min on stream. The decrease of activity may be caused by the formation of coke, which decreases the size of the Pt ensembles [4]. Also carbon occurred within the pores and this pore blocking may account for the rapid decline with time on catalyst activity.

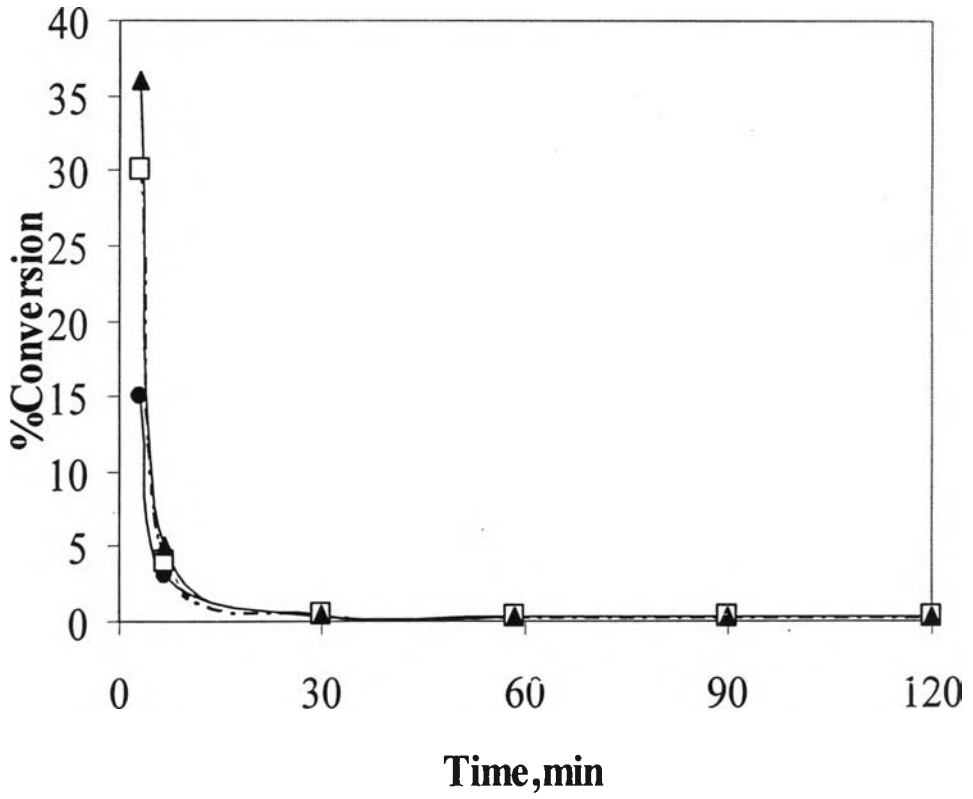

Figure 5.22 % Conversion of hexane dehydrogenation at different temperatures as a function of time: ▲ 475°C, □ 400°C and ● 300°C

These results can be explained by assuming that coke accumulation is the resultant of the formation and elimination of coke on the surface [4]. Not only an increase in production of the precursors of coke was occurred, but also an increase in the rate of destruction of this coke was observed. However, activation energy of destruction of coke was higher than that production of coke precursors. Consequently, at high temperature the production of coke will be increased.

2. Characterization of C_xH_y species

The identities of sets of ESR spectra as a function of temperature obtained at room temperature are shown in Figures 5.23 and 5.24. Exactly, the temperature affects dependently on the both sites as seen in the ESR signal and the amount of carbon radicals ascribed in Table 5.9. For the ESR spectra on the metal site (Figure 5.23), the catalyst without coke depositions showed no ESR signal, indicating the absence of any paramagnetic species on them. The ESR spectra of coke for the Pt/SiO_2 showed a strong ESR signal at higher temperature, whereas it showed a weak ESR signal at lower temperature. It is indicated that the observed weak ESR signal for the low temperature presented a low concentration of paramagnetic carbon species. In case of high temperature, the strong ESR signal indicates the presence of the paramagnetic carbon species at high concentration [74, 144, 178, 181, 182]. This is accounting for the observed decrease in the number of radicals as a function of decreasing temperature as demonstrated in Table 5.9. However, the observed g-values for the coked catalyst at different reaction temperatures were quite close to each other (average g-value $\approx$ 2.003) that observed for sp^2 hybridized aromatic carbon.

Table 5.9 The density of carbon radicals of coke per gram catalyst at different temperatures

Temperature,°C	The metal sites	The support sites
300	8.00×10^4	6.47×10^5
400	3.27×10^5	1.82×10^6
475	8.55×10^5	3.02×10^6

Likewise carbon radicals of coke on the acidic site had the same position and behavior. Considering between carbon radicals on both sites, however, the graduate difference in the intensity was found. This can be confirmed with the number of intermediate radicals of coke on spent catalyst as exhibited in Table 5.9. It is found that on the support function, the number of radicals for 300°C, 400°C and 475°C were greater about 8, 6 and 3.5 times, respectively.

A set of IR spectra on the metal site and the support site obtained after runs is subsequently displayed in Figure 5.25A and Figure 5.25B. The prominent bands of all coke bands showed at 1610 cm^{-1} and 1540 cm^{-1}. The both bands might be indicative of polyalkences and/or aromatics. However, the difference of coke between the metal and support site became obviously in the IR spectra of the coked samples. They were the same position at 1610 cm^{-1}, the so called- coke band, while another band at 1540 cm^{-1} was found only on the support sites. The band at 1540 cm^{-1} is ascribed to alkylnaphthalenes or polyphenylene structures. Increasing coking temperature, these bands of both sites were slightly increased as shown in the growth of the absorbance of typical coke bands. As pointed out the intensity, these bands on the support site were produced more than those ones on the metal site. It can be said that coke on both sites can clearly be distinguished due to their different H/C ratios. The findings are in full agreement with earlier results obtained in TPO and ESR.

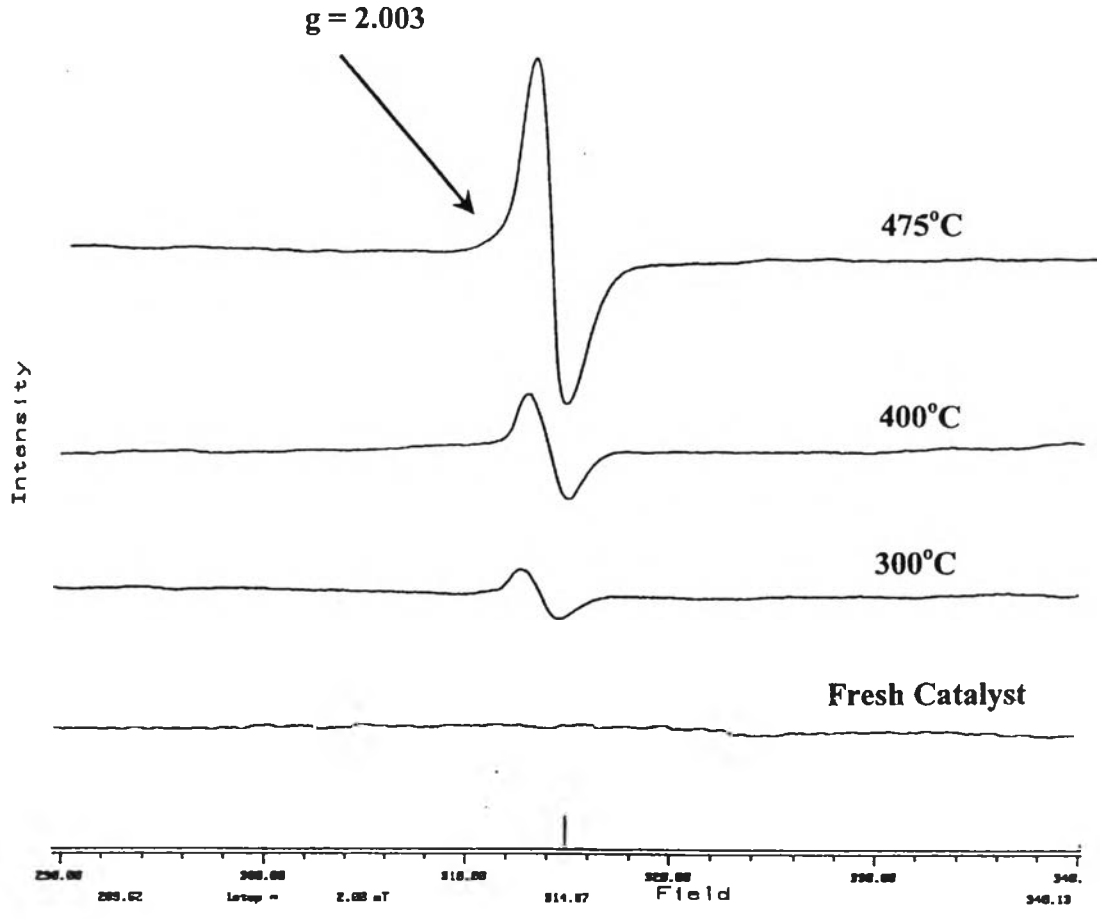

Figure 5.23 ESR spectra of coke on the metal at 120 min and H_2/HC=0 with various temperatures

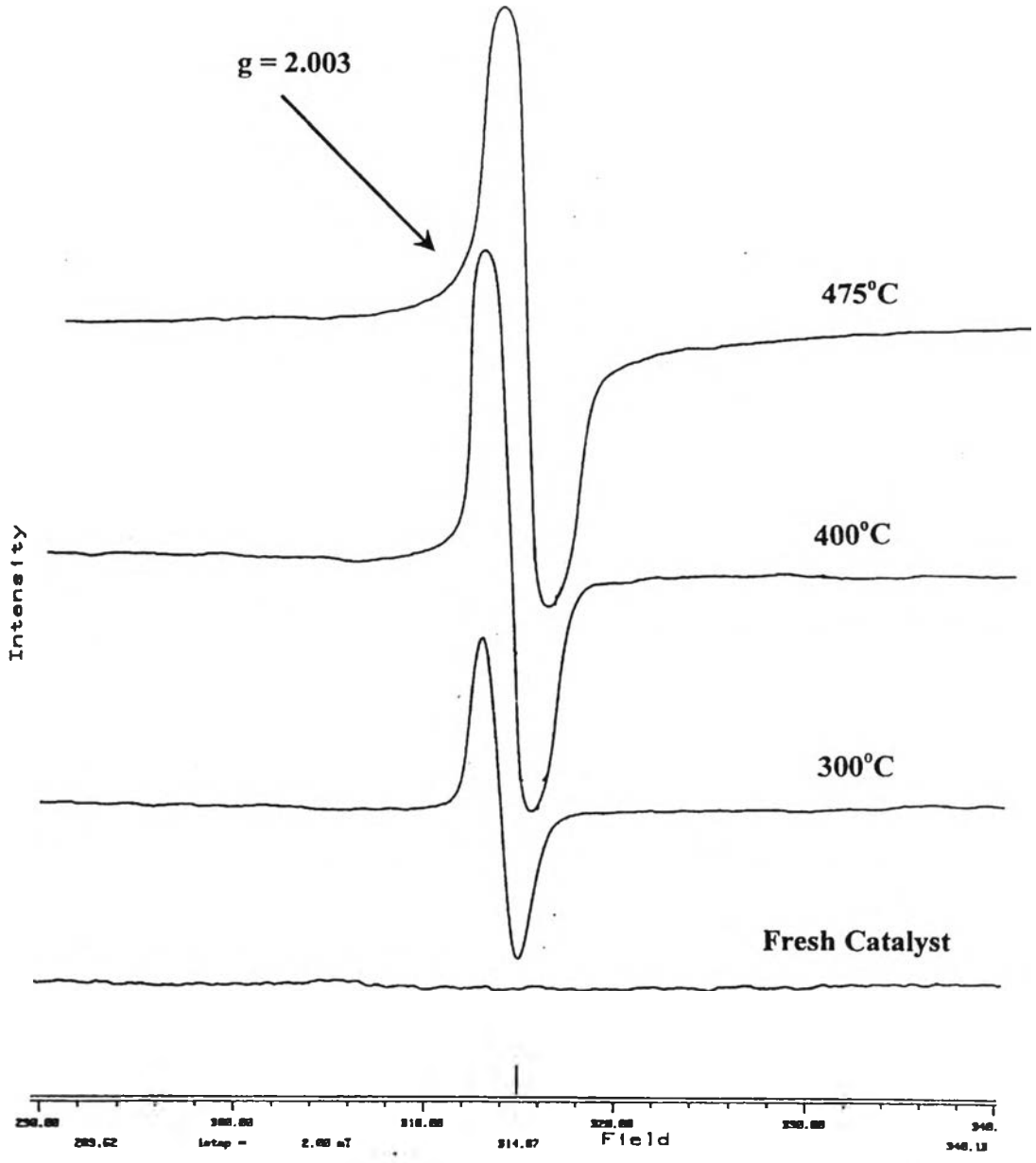

Figure 5.24 ESR spectra of coke on the support at 120 min and H_2/HC=0 with various temperatures

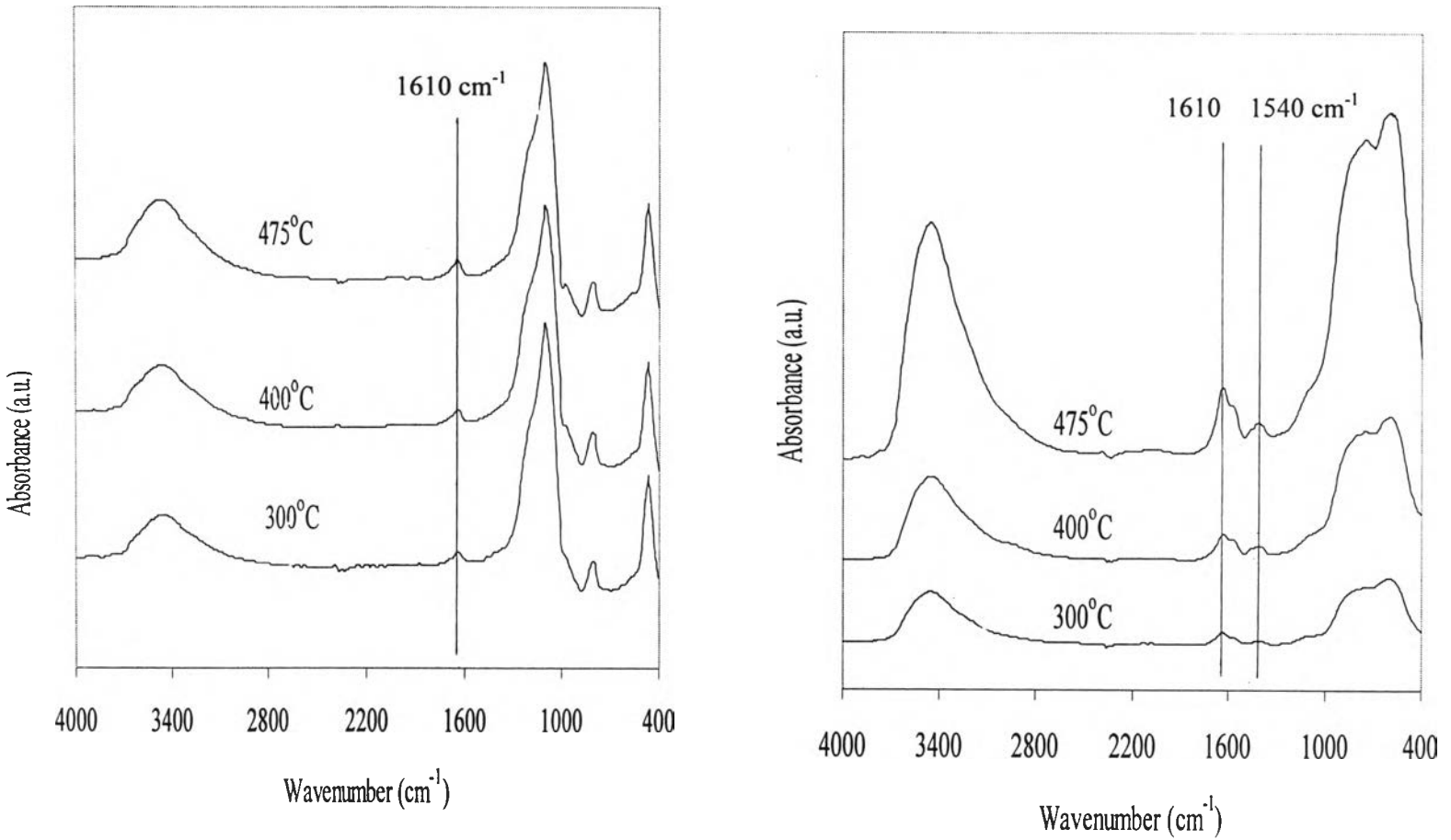

Figure 5.25 IR spectra obtained after coking with various temperatures over (A) the metal and (B) the support

3. **Carbonaceous morphology**

In order to check the morphological change due to the effect of coking temperature, microscopic features of the liberated cokes were observed with TEM. TEM images of the liberated cokes are subsequently presented in Figures 5.26 and 5.27 for on the metal phase and the support function. As reported in Figure 5.26 (called coke on the metal site), the appearance of coked catalyst at 300°C was similar to that of the fresh catalyst. Otherwise, more particles covered at the higher temperature. From Figure 5.27, the coke on the Al_2O_3 dramatically covered small particles. More organized coke structure and higher surface coverage could well exist under more severe coking conditions such as a higher temperature in accordance with the literature [34, 139, 151, 183]. Coke deposited on both sites had spherical shape, which may be amorphous structure [184].

Compared with Figure 5.26 and Figure 5.27, it is obvious that the support was much higher density coverage. According to the earlier study [9, 12, 141], they concluded that the various morphological features was related to the rate of carbon deposition. The more complex structures were produced form the faster decomposition prevailing with unsaturated hydrocarbons. It is supported that the onset of a small amount of the sample occurred at temperature 300°C, whereas the major fraction started to undergo reaction at about 400 and 475°C. Consequently, it is speculated that structures of coke were consisted of two components, a less ordered carbon, which was removed at low temperature, and a more highly ordered component that started to combust at higher temperatures [119].

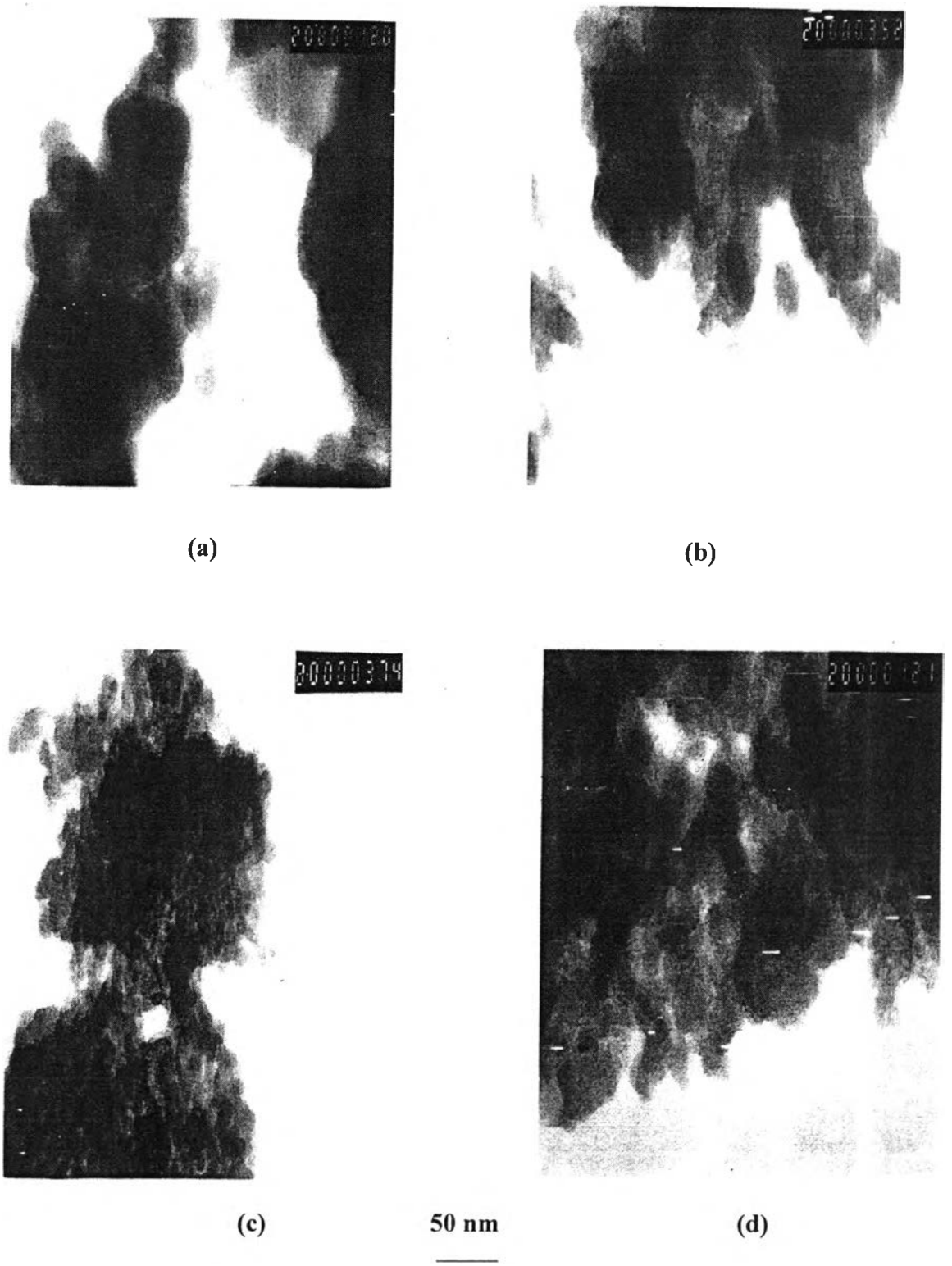

Figure 5.26 TEM photograph of coke on the metal at different temperatures: (a) fresh catalyst, (b) 300°C, (d) 400°C and (d) 475°C

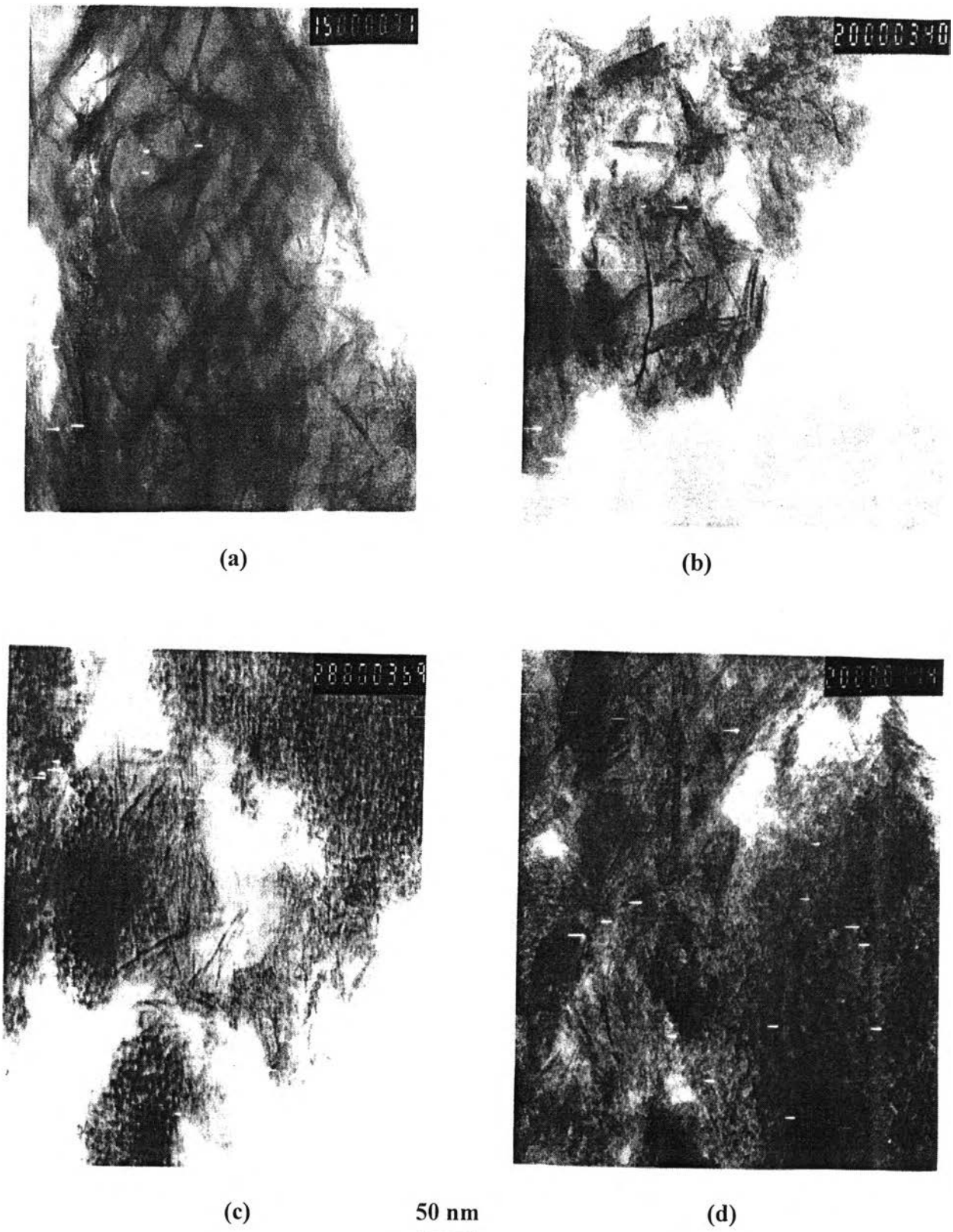

Figure 5.27 TEM photograph of coke on the support at different temperatures: (a) fresh catalyst, (b) 300°C, (d) 400°C and (d) 475°C

4. The changes of textural properties and the dispersion factors of coke on the metal and the acid at different temperatures

By taking the results from N_2 adsorption into consideration, the data are listed in Table 5.10. The temperature at which the carbon filaments were produced was found to have a significant impact on the N_2 BET surface areas of the coked material. At higher temperatures, more coke precursors and coke in the form of strongly adsorbed polyaromatic species were formed along with hydrocarbons [4]. Thus, the surface areas of spent catalysts were found to be lower values than the fresh catalysts on both sites. This is responsible for the degree of filling in the pore as well as the dispersion factor as illustrated in Table 5.10. As for carbon on metal, the higher dispersion factor of coke appeared owing to increasing temperature. The dispersion factor on the support function had the similar trend. Considering the amount of dispersion factors on both sites, carbon deposition was more dispersed on the metal site than on the support site. The individual formation rate and nature of coke were deduced.

Table 5.10 The textural properties of catalysts samples before and after testing and dispersion factor with different temperatures

Temperature,°C	The metal sites			The support sites		
	SA (m^2/g)		dispersion	SA (m^2/g)		dispersion
	Fresh	Used	factor	Fresh	Used	factor
300	447	416	108	390	363	17
400	447	399	162	390	344	18
475	447	386	171	390	343	19

5. Characterization of coke extracted from coked catalyst

For further characterization of coke deposited on catalyst, coke was extracted from the coked catalyst by Soxhlet extraction using toluene as a solvent. The morphology of these filaments, however, was found to vary as a function of the temperature. Then, the soluble coke was subjected to elemental analysis with GC (capillary column DB1). The extracted coke profiles on the metal and support sites at various temperatures are subsequently reported in Figures 5.28 and 5.29. The components of soluble coke were C_8-C_{12}. It is found that the compositions of coke strongly dependent on the coking temperature. At lower temperature the extracted coke was composed of the lower C content, C_8-C_{10}, whereas at higher temperature the extracted coke was more occurred because the coke was more produced. It is implied that the transformation of soluble coke into insoluble coke was much faster with increasing temperature on both sites. Moreover, the transformation of intermediate from the metal to the support sites seems to be occurred. However, coke on the metal phase was easily removed due to a lower aromatic content when compared with the amount of coke from the TPO result. It is noticed that the missing of lower C fragment was presented on the support site, while a high C fragment of coke intermediate was predominately produced. Hence, the carbonaceous accumulation dramatically deposited on the support site as seen from the above result. As described in the literatures [74, 75, 119, 133, 190], there was marked difference in the effect of high and low-temperature coke on diffusivity and sorption capacity of intermediate. The ability of coke at high-temperature to reduce diffusivity and sorption capacity was only very slightly lower than that of coke at low-temperature and most pronounced for the diffusivity of coke intermediate and at higher coke loading.

In all cases, the Schulz-Flory distribution was required to fit the data. Figure 5.30 is a Schulz-Flory diagram of volatile carbonaceous deposition extracted from the coked catalyst for the metal. A change of chain growth parameter was observed and strongly dependent on the temperature. A shift of higher carbonaceous composition in relevance to a greater probability of chain growth was found. From these results, the higher the temperature, the greater soluble of coke was found. It is probably the

result of thermodynamic limitations in accordance with many authors [167, 188, 189, 191]. The higher temperature was favored to coke compound. Chain growth occurred by insertion of the intermediate species. Additionally, the discussion of the increase of the transport rate of olefins with variation of carbon numbers had a great impact on the rate of re-adsorption of olefins or intermediate. The intermediate re-adsorption and chain initiation was the most importance on the coke formation. Slow removal of reactive products such as olefins due to a decrease of diffusion coefficient with increasing chain length can influence the chain growth rate. However, there was a little change of α value for each temperature on both sites. It is expected that the probability of chain growth on both sites were the same value. Moreover, it is obtained that a significant deviation from the Schulz-Flory distribution was only present in the severe temperature cases due to the formation of higher coke molecules.

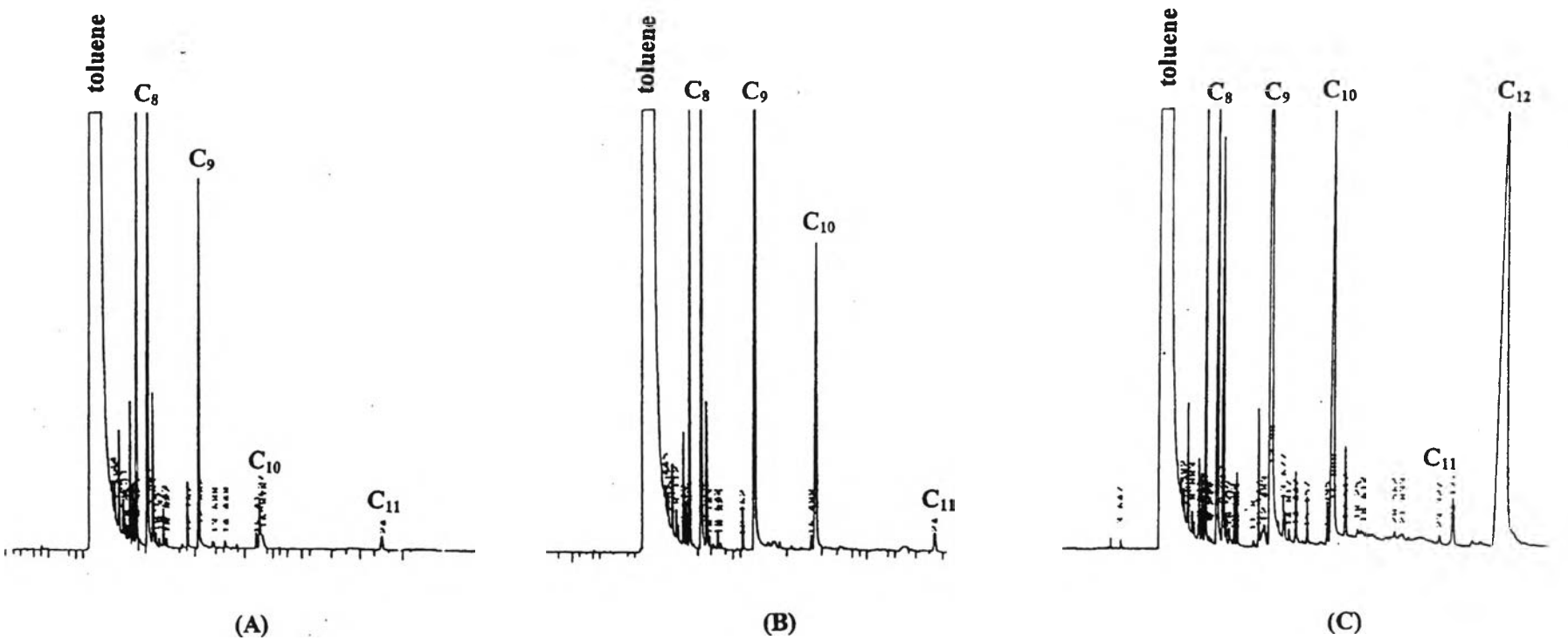

Figure 5.28 The component of the extracted coke on the metal at different Temperatures: (A) 300 °C, (B) 400°C, (C) 475°C

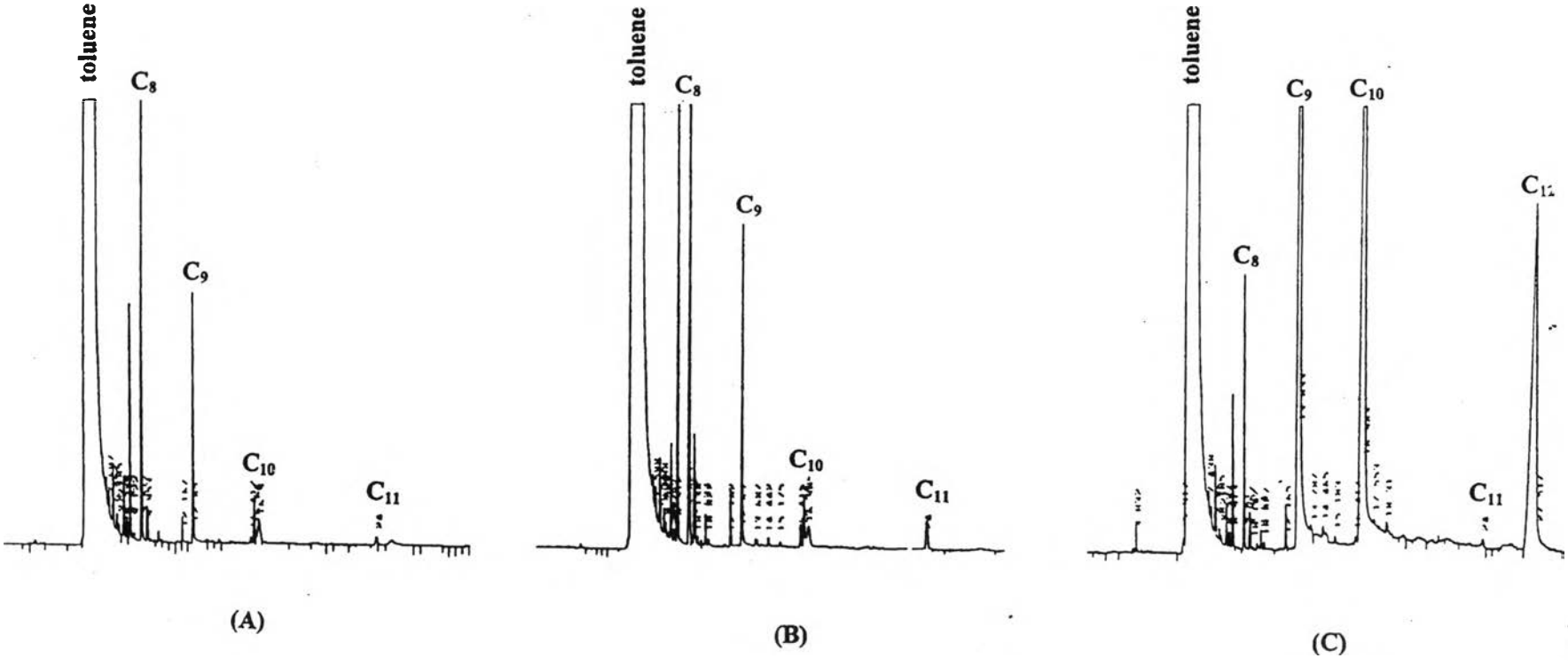

Figure 5.29 The component of the extracted coke on the support at different temperatures: (A) 300 °C, (B) 400°C, (C) 475°C

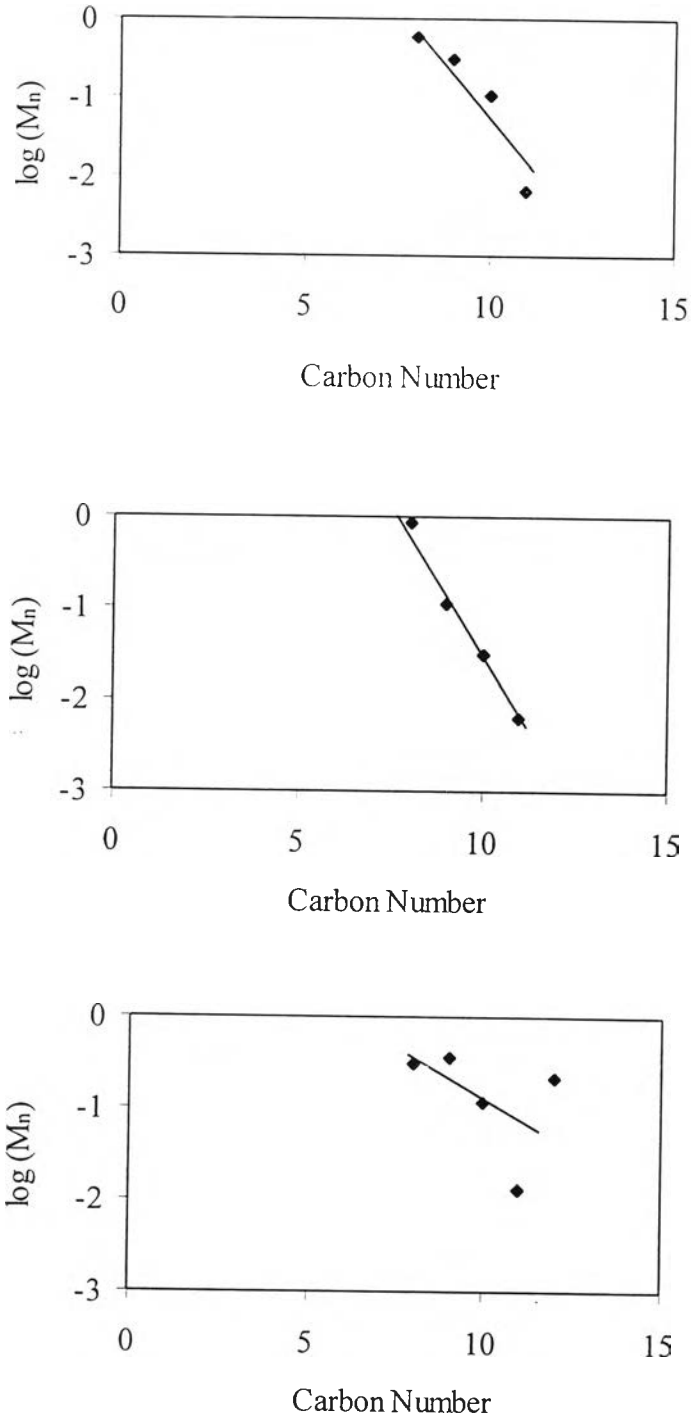

Figure 5.30 Schulz-Flory diagram of soluble coke from the metal at different temperatures: (a) 300°C, (b) 400°C and (c) 475°C

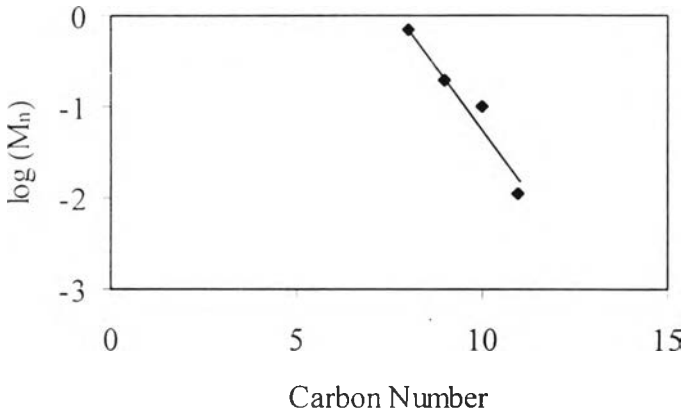

(a)
α value=0.27

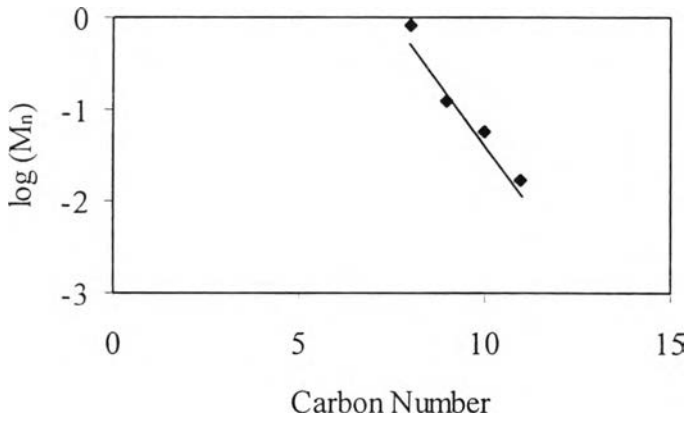

(b)
α value=0.29

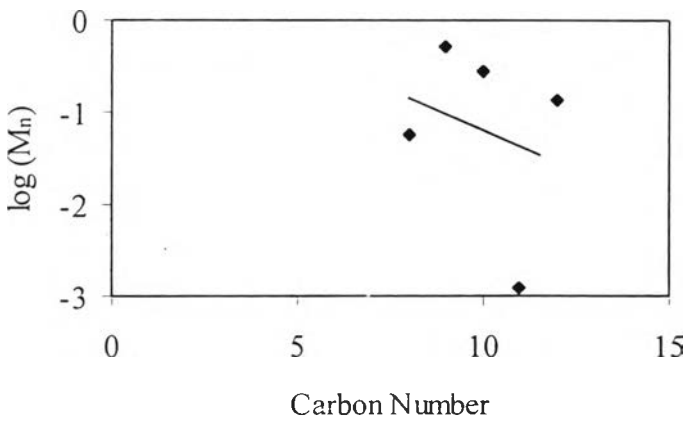

(c)
α value=0.65

Figure 5.31 Schulz-Flory diagram of soluble coke from the support at different temperatures: (a) 300°C, (b) 400°C and (c) 475°C

5.2.3 The Effect of H_2

1. Carbon deposition and catalytic activity

Reactions of n-hexane were reported in several H_2/HC ratios as follows: 0, 3, 5 and 10 at constant 475°C and 2 h. The overall conversion over Pt catalyst increased with increasing H_2/HC ratio. The conversion changes caused by varying H_2/HC ratio were attributed to the amount of carbonaceous species on the catalyst surface being controlled by the hydrogen pressure [2, 3, 9, 132]. One might accept as starting hypothesis that hydrogen introduced with the reactant assisted to produce the saturated nondegradative products (alkanes, C_5-cyclics). Since the carbonaceous intermediates on the catalyst surface were lower, the amount of coke was also decreased. For the other reason, the ensemble effect would be easily occurred on the presence of hydrogen. This effect was an important phenomenon, which suppressed the coke formation [132].

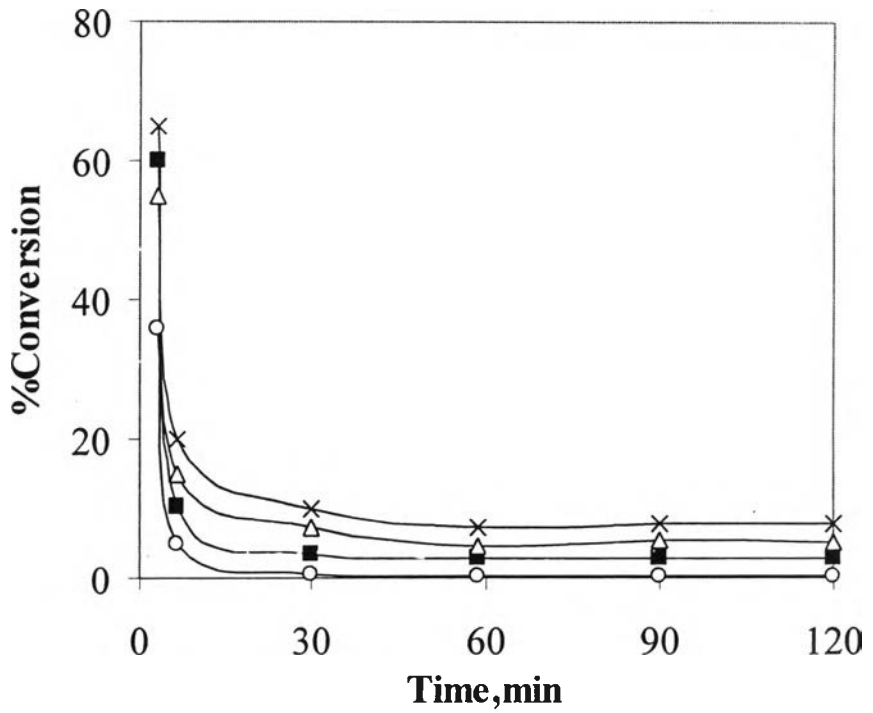

Figure 5.32 %Conversion of hexane dehydrogenation with various H_2/HC ratios as a function of time on stream: ○ H_2/HC = 0, ■ H_2/HC = 3, Δ H_2/HC = 5, × H_2/HC = 10

In order to analyze the influence of H_2 on the shape and nature of carbonaceous species, the TPO method was employed. Figure 5.33 shows the formation of coke on the metal site of catalyst. Two distinct peaks, 300°C and 425°C, were noted from coking in various H_2/HC experiments. Otherwise, the location of coke deposition on the support site of catalyst is exhibited in Figure 5.34. TPO spectra showed the single peak around 525°C. According to the other studies [3, 4], this high temperature peak corresponded to coke deposited on the support. From these figures, it is said that the degree of coverage by coke was reduced by hydrogen. However, a low addition of hydrogen in the feed stream decreased more rapidly the amount of coke on both sites than a high introduction of hydrogen did. It is possible that some parts of coke would be easily removed by hydrogen but the other one was hardly eliminated. Therefore, the presence of excess hydrogen can not reduce the latter part of carbonaceous deposits. This part may be called irreversible coke [1, 76, 77]. Consequently, the effect of hydrogen on coke removal rates was less at higher hydrogen concentration. In addition, it is found that coke was much accumulated on the acid function. This is associated with the amount of coke calculated from the TPO curves as shown in Table 5.11.

Table 5.11. The amount of carbon deposited on the catalysts with various H_2/HC ratios

H_2/HC ratio	Coke on the metal sites % C	Coke on the support sites % C
0	0.36	2.50
3	0.29	1.34
5	0.27	1.31
10	0.26	1.09

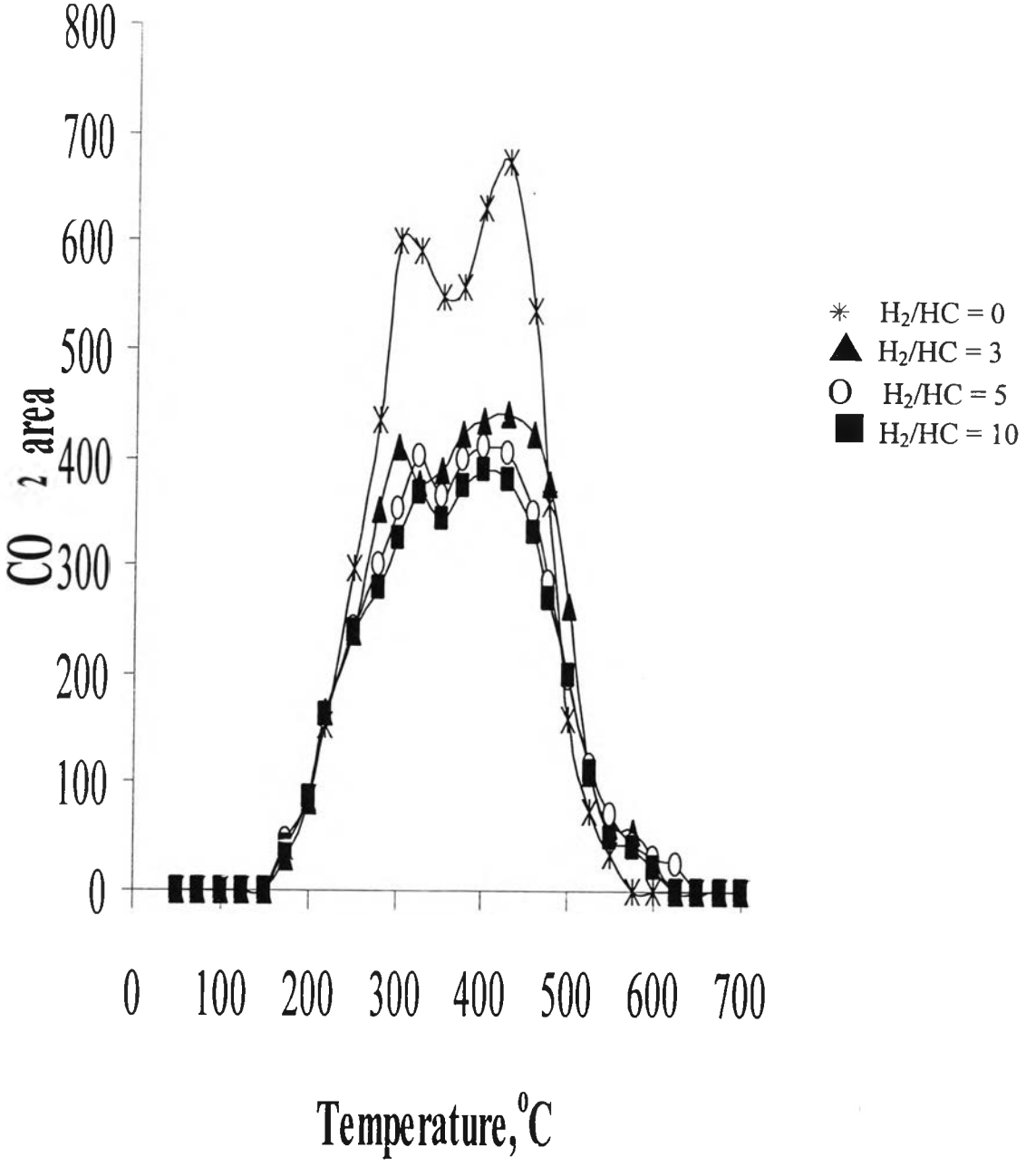

Figure 5.33 TPO of carbonaceous deposits produced on the metal at 120 min and 475°C with different H_2/HC ratios

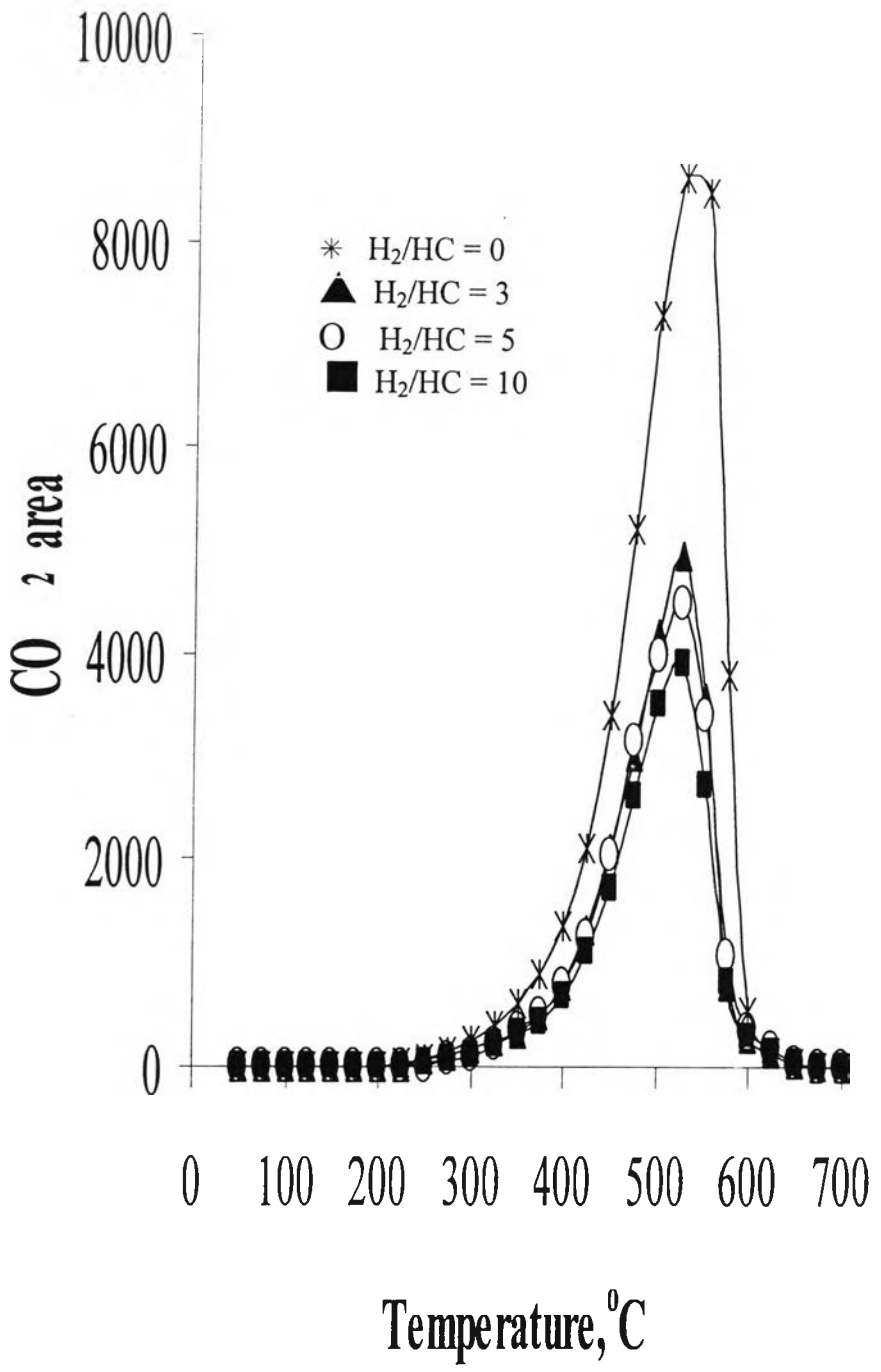

Figure 5.34 TPO of carbonaceous deposits produced on the support at 120 min and 475°C with different H_2/HC ratios

2. Characterization of C_xH_y species

Figures 5.35 and 5.36 show the ESR spectra recorded at room temperature on the metal and the support function. The intensities calculated by double integration of the spectra are exhibited in Table 5.12. The most obvious difference between the spectra of the fresh and used catalysts was revealed by a signal at $g \approx 2.003$ which appeared in the coked catalyst but not in the fresh catalyst. On support sites, there were almost no differences in the spectra of the used catalysts in each the H_2/HC ratio indicating that the local structure of the carbon radical species was not greatly influenced by addition of H_2 into feed. On the contrary, the ESR spectra show an important change after adding H_2 on the metal site. It is introduced that the intensity was quickly diminished in H_2/HC ratio from 0 to 3. However, the motion of the radicals was already restricted at a high H_2/HC ratio as well as the gradual declining of the number of carbon radical as summarized in Table 5.12.

Table 5.12. The density of carbon radicals of coke per gram catalyst with various H_2/HC ratios

H_2/HC ratio	The metal sites	The support sites
0	8.55×10^5	3.02×10^6
3	4.50×10^5	3.04×10^6
5	6.17×10^5	4.00×10^6
10	5.43×10^5	3.47×10^6

The amount of coke was additionally monitored by means of the corresponding coke bands determined *ex-situ* IR after each reaction carried out by varying H_2/HC ratio. Figure 5.37 A and B show the adsorbance of the coke band to study the effect of H_2/HC. In Figure 5.37 A, it is evident that the coke band at 1610 cm^{-1} of coke on the metal sites was a typical band associated with the aromatic bands. In the case of coke on the support, there were two main stretching bands at 1610 cm^{-1} and 1540 cm^{-1}. These bands were also the characteristics of aromatic structure. The position of 1610 cm^{-1} was more predominant. Importantly, the adding H_2 affected the

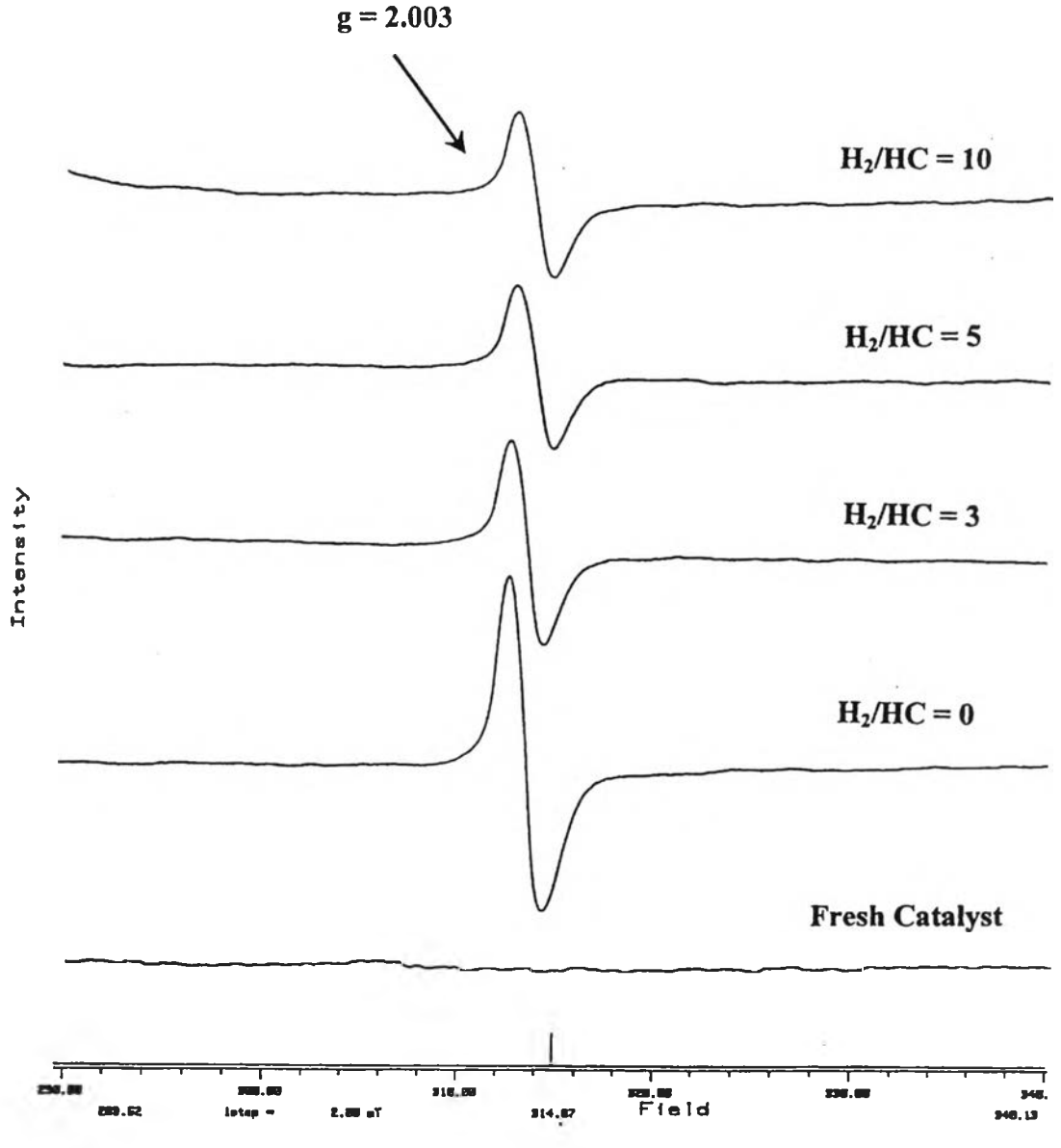

Figure 5.35 ESR spectra of coke on the metal at 120 min and 475°C with different H_2/HC ratios

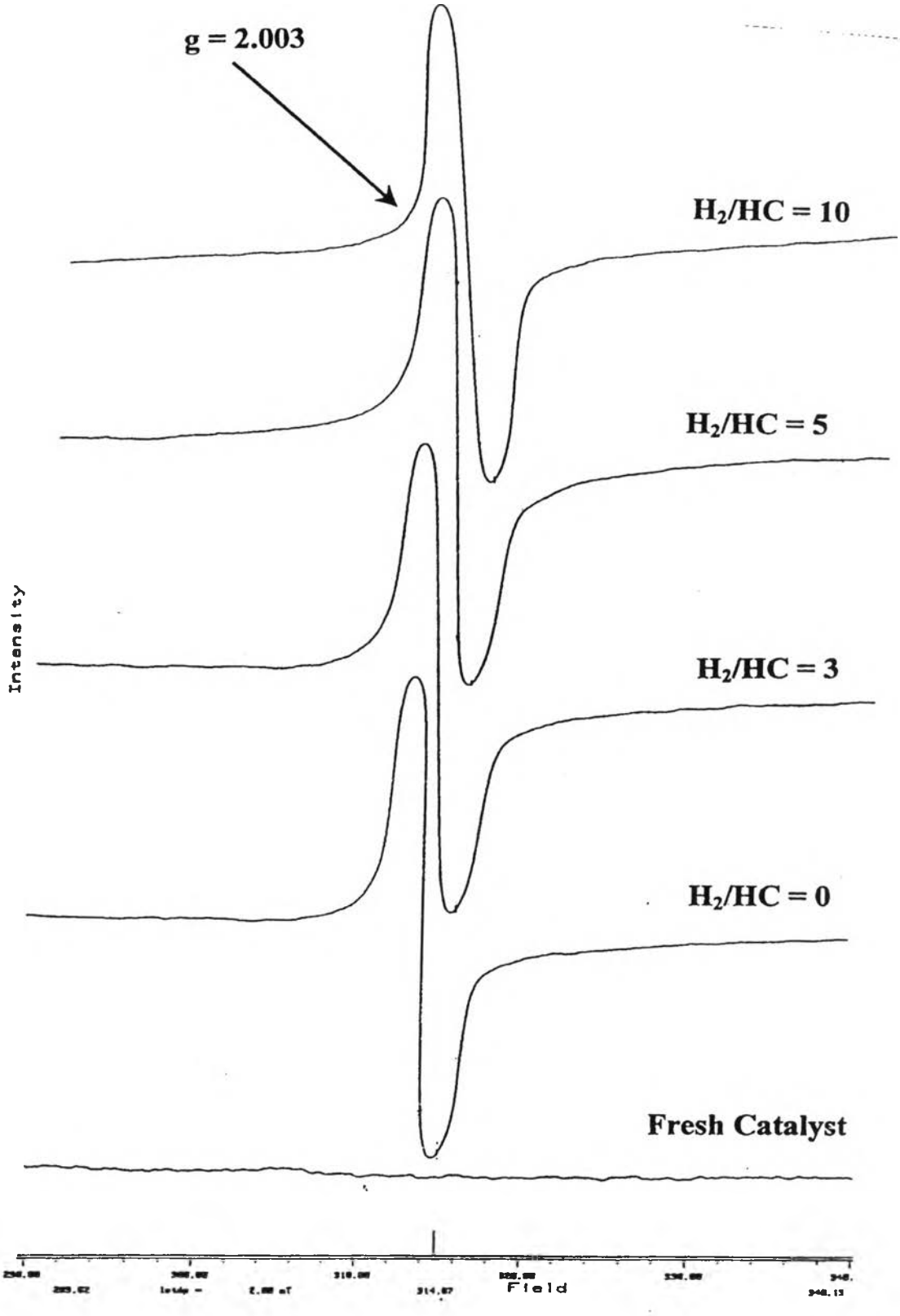

Figure 5.36 ESR spectra of coke on the support at 120 min and 475°C with different H_2/HC ratios

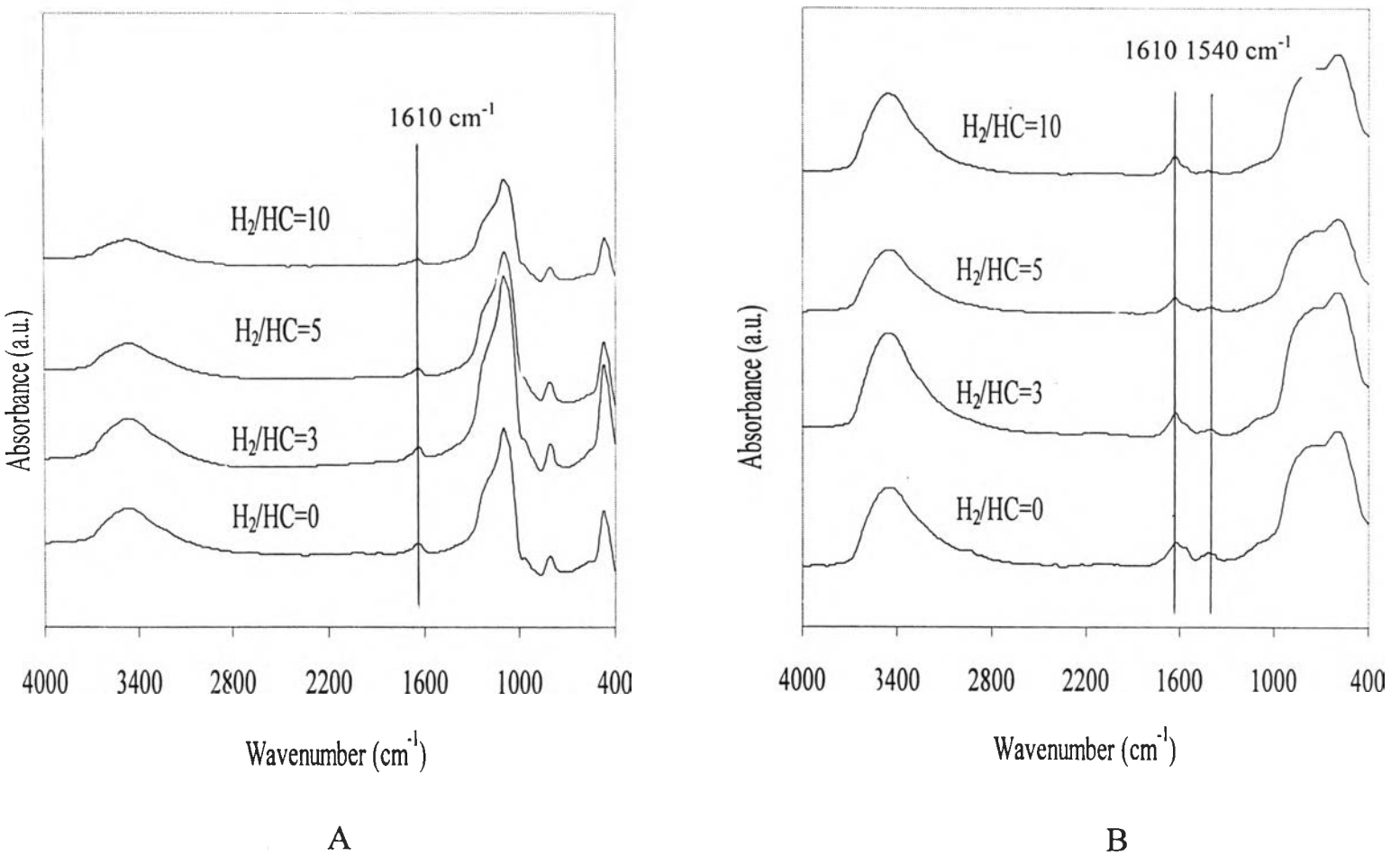

Figure 5.37 IR spectra obtained after coking with different H_2/HC ratios over (A) the metal and (B) the support

decrease of aromatic intensity, especially the 1540 cm^{-1} for coke on the support function. This result may possibly explain that the generation of coke precursor was inhibited by hydrogen. Compared with the intensity of coke between the metal and the support, it is seen that coke on the support has greater intensity and amount than coke on the metal.

3. Carbonaceous morphology

The catalysts were checked by taking successive photographs after testing on a different H_2/HC ratio. The effect of adding hydrogen to hydrocarbon on the structure of carbon filaments is presented in Figure 5.38 and Figure 5.39. On the metal phase (Figure 5.38), it is evident that there was a little difference. For the support sites (Figure 5.39), it is obvious that a little density and coverage of carbon filament were produced, that was significantly noticed at H_2/HC as 10. This is in accordance with the earlier publication [27, 137]. They said that the presence of hydrogen had been found to be an essential component of coke morphology in system. Hydrogen was not only to initiate the decomposition of carbon containing gases over certain metal systems, but also to exert an influence on the structural perfection of carbon filaments.

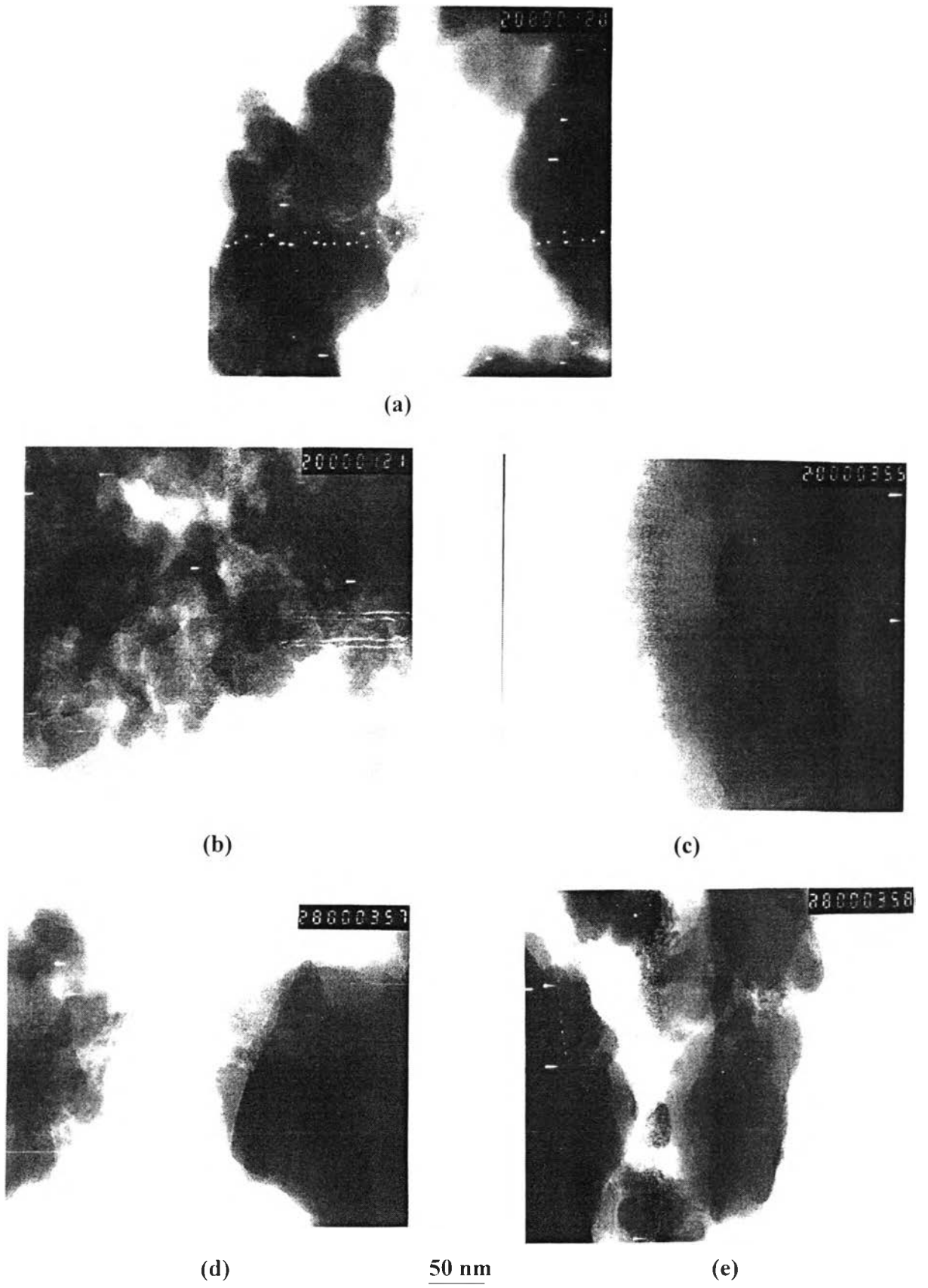

Figure 5.38 TEM photograph of coke on the metal with various H_2/HC ratios: (a) fresh catalyst, (b) H_2/HC =0, (c) H_2/HC = 3, (d) H_2/HC =5 and (e) H_2/HC = 10

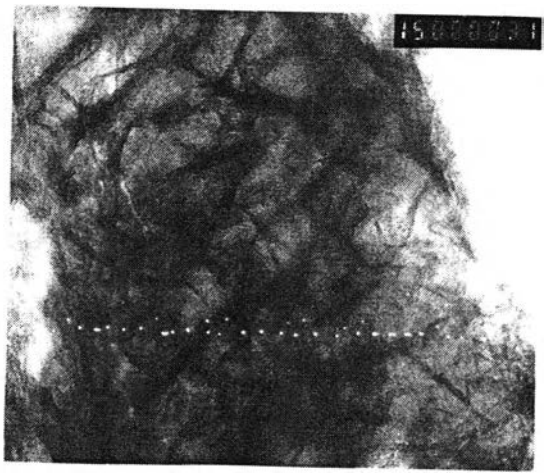

(a)

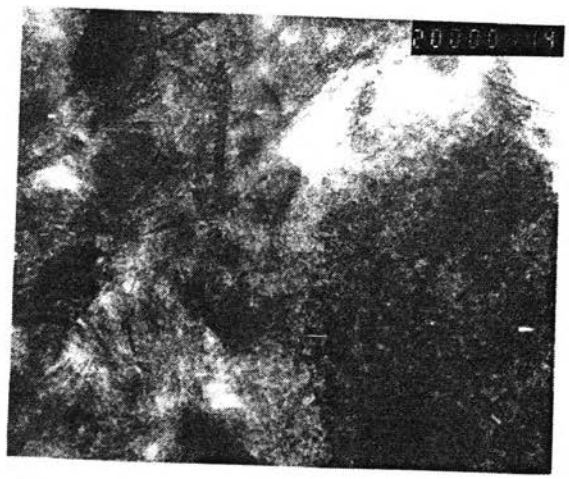

(b)

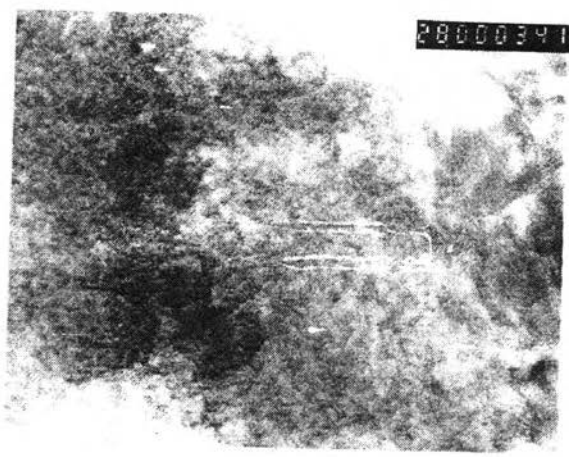

(c)

(d)

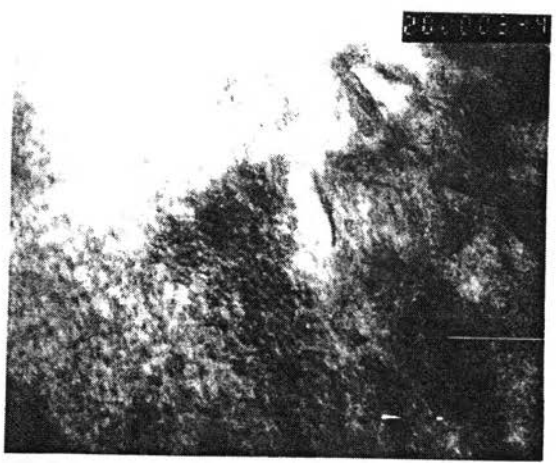

(e)

50 nm

Figure 5.39 TEM photograph of coke on the support with various H_2/HC ratios: (a) fresh catalyst, (b) H_2/HC =0, (c) H_2/HC = 3, (d) H_2/HC =5 and (e) H_2/HC = 10

4. The changes of textural properties and the dispersion factors of coke on the metal and the acid with various H_2/HC ratios

Table 5.13. The textural properties of catalysts samples before and after testing and dispersion factor with various H_2/HC ratios

H_2/HC ratio	The metal sites			The support sites		
	SA (m^2/g)		dispersion	SA (m^2/g)		dispersion
	Fresh	Used	factor	Fresh	Used	factor
0	447	386	171	390	343	19
3	447	370	266	390	324	49
5	447	363	309	390	320	54
10	447	355	354	390	320	65

The effects of H_2/HC on catalyst before and after coking leaded to physical and chemical interpretations. In general, the reported literature only affects on physical effects by means of the BET method. The BET surface area from various H_2/HC ratios is noted in Table 5.13. It is found that H_2 dramatically resulted in deducing surface area on the metal. This is taking account to the higher dispersion as presented in Table 5.13. Controversy, a limited value of the diminished surface was found at the greater ratio of 3 for the support site. The dispersion factor was higher on the metal sites than on the support sites. Nevertheless, it is introduced that the presence of hydrogen in the reactant gas was found to modify the physical characteristics of the carbonaceous deposits [37]. Basically, it can be said that the larger amount of coke deposited, the lower surface area was seen. However, the relationship between these two values is not always straightforward. For instance, the data were interestingly presented in this section. This difference in surface area between the metal and the support may be due to the difference in the location of coke in catalyst.

5. Characterization of coke extracted from coked catalyst with various H_2/HC ratios

The soxhlet extraction with toluene was used for recovering the coke. This distribution of the soluble coke components was estimated through GC-14B with a DB1 capillary column. The composition of the soluble coke on metal sites and on acid sites is illustrated in Figure 5.40 and Figure 5.41, respectively. On both sites, the increase in H_2/HC ratio resulted in the decreasing C_{10}-C_{12} products in the removed fraction. The major difference in the hydrocarbon compositions of coke removed was appeared on C_{12} fragment and its amount was maximum at H_2/HC = 0. It is suggested that the addition of H_2 hindered the formation and the transformation of intermediate, especially on the metal sites. These results were identically observed on a lower amount of coke at a higher H_2/HC in accordance with the TPO results. Surprisingly, a fairly low amount of coke intermediates was occurred on the metal with H_2 addition. However, the limit of H_2 addition was observed, i.e., less pronounced impact on the coke formation over both sites was seen when the H_2/HC ratio was higher than 3. In order to explain the slower formation of insoluble coke with H_2 addition, it can be introduced that coke molecules were more homogeneously distributed in outer surface [77, 87]. Consequently, most of soluble coke molecules were too volatile and too weak to be located on the outer surface. For explaining, a more significant effect of coke on the adsorption capacity was found with all coked samples treated with hydrogen that were directly related to the structure of surface intermediates during reaction. Concerning the study of the reaction of hexane and removal of carbonaceous residues from Pt catalyst, it was suggested that the abundance of surface hydrogen controlled coke intermediates; a less dehydrogenated one giving C_6 saturated product or a more dehydrogenated one leading to predominated benzene [77].

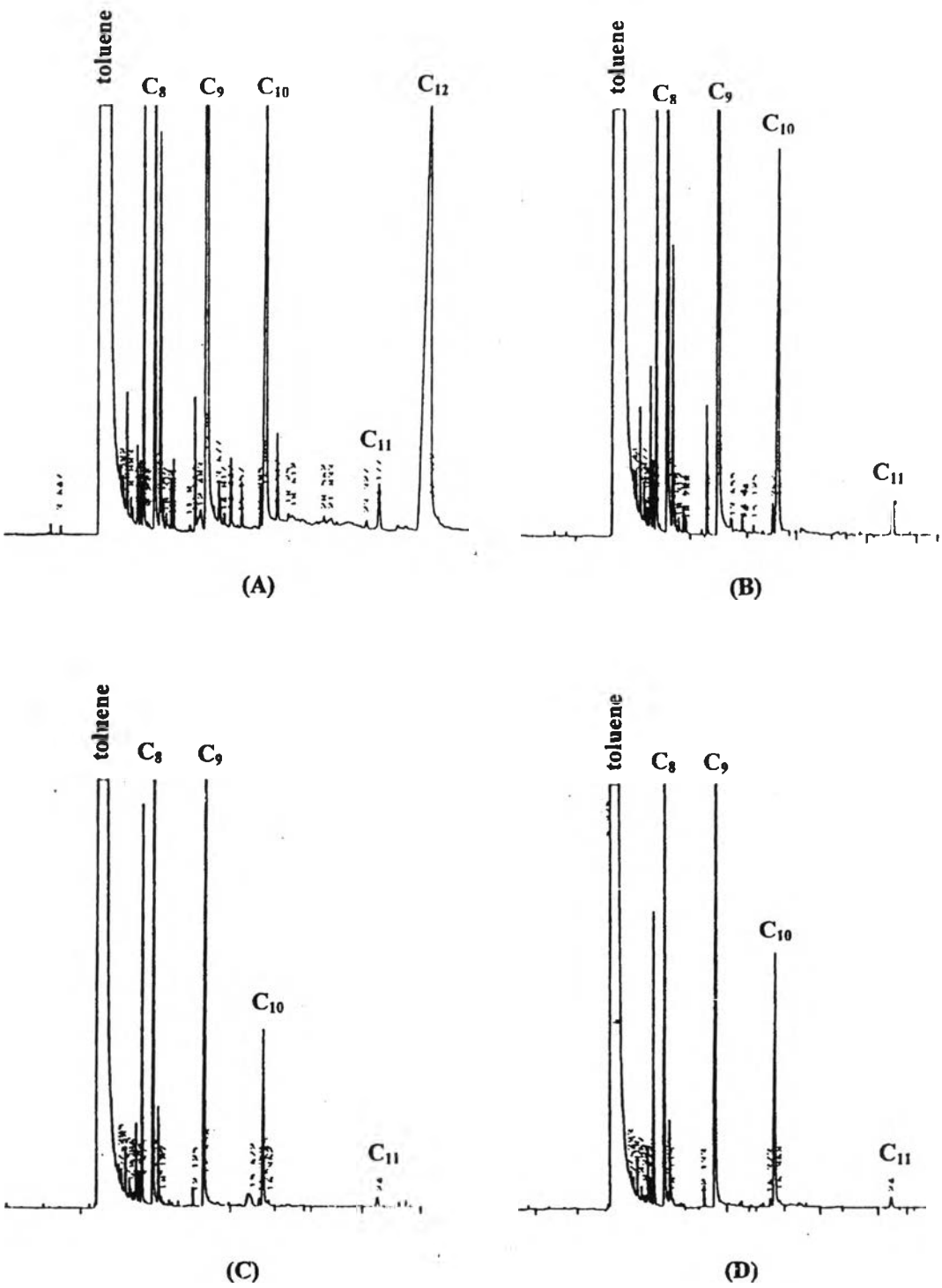

Figure 5.40 The component of the extracted coke on the metal with various H_2/HC ratios: (A) H_2/HC = 0, (B) H_2/HC = 3, (C) H_2/HC = 5 and (D) H_2/HC = 10

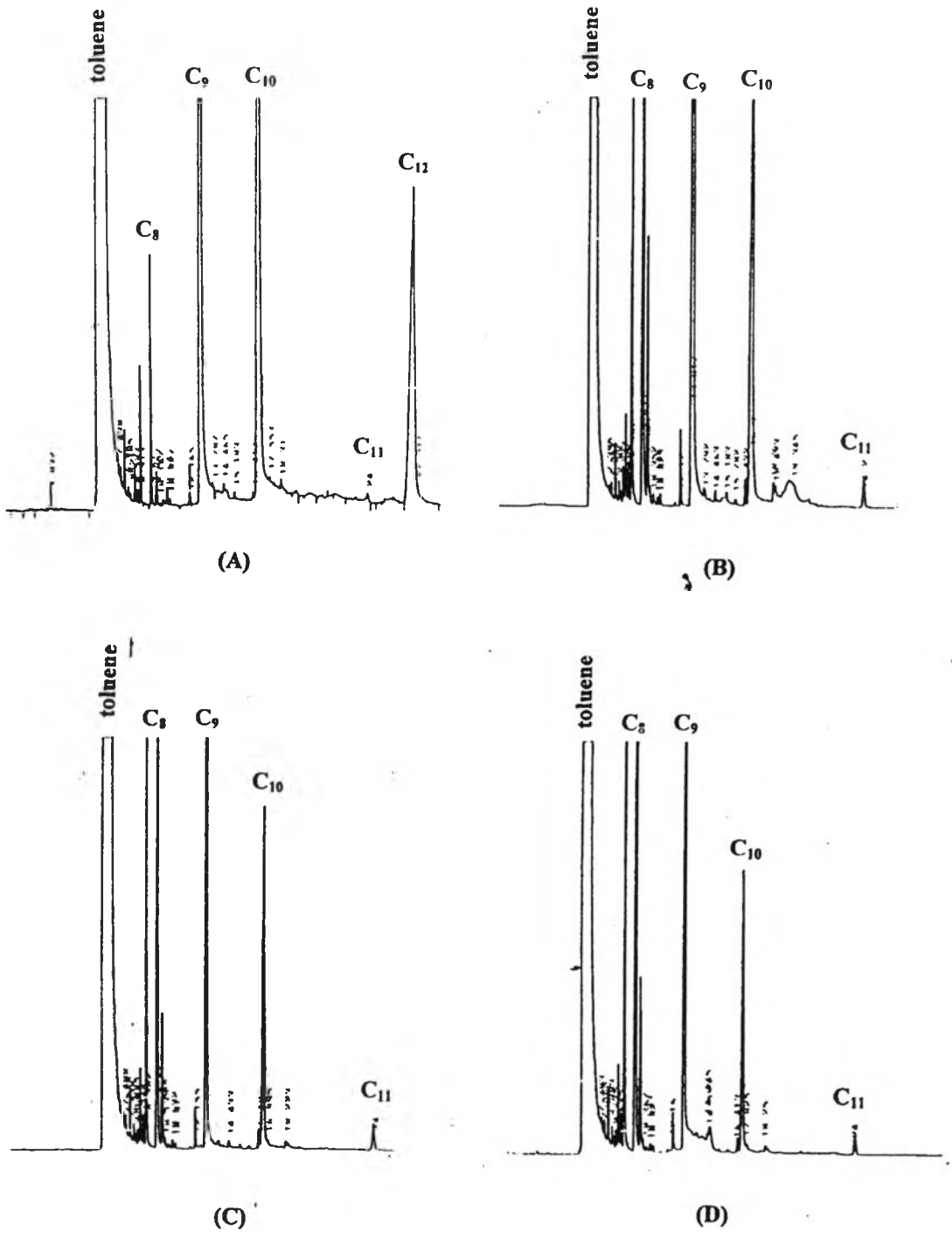

Figure 5.41 The component of the extracted coke on the metal with various H_2/HC ratios: (A) H_2/HC = 0, (B) H_2/HC = 3, (C) H_2/HC = 5 and (D) H_2/HC = 10

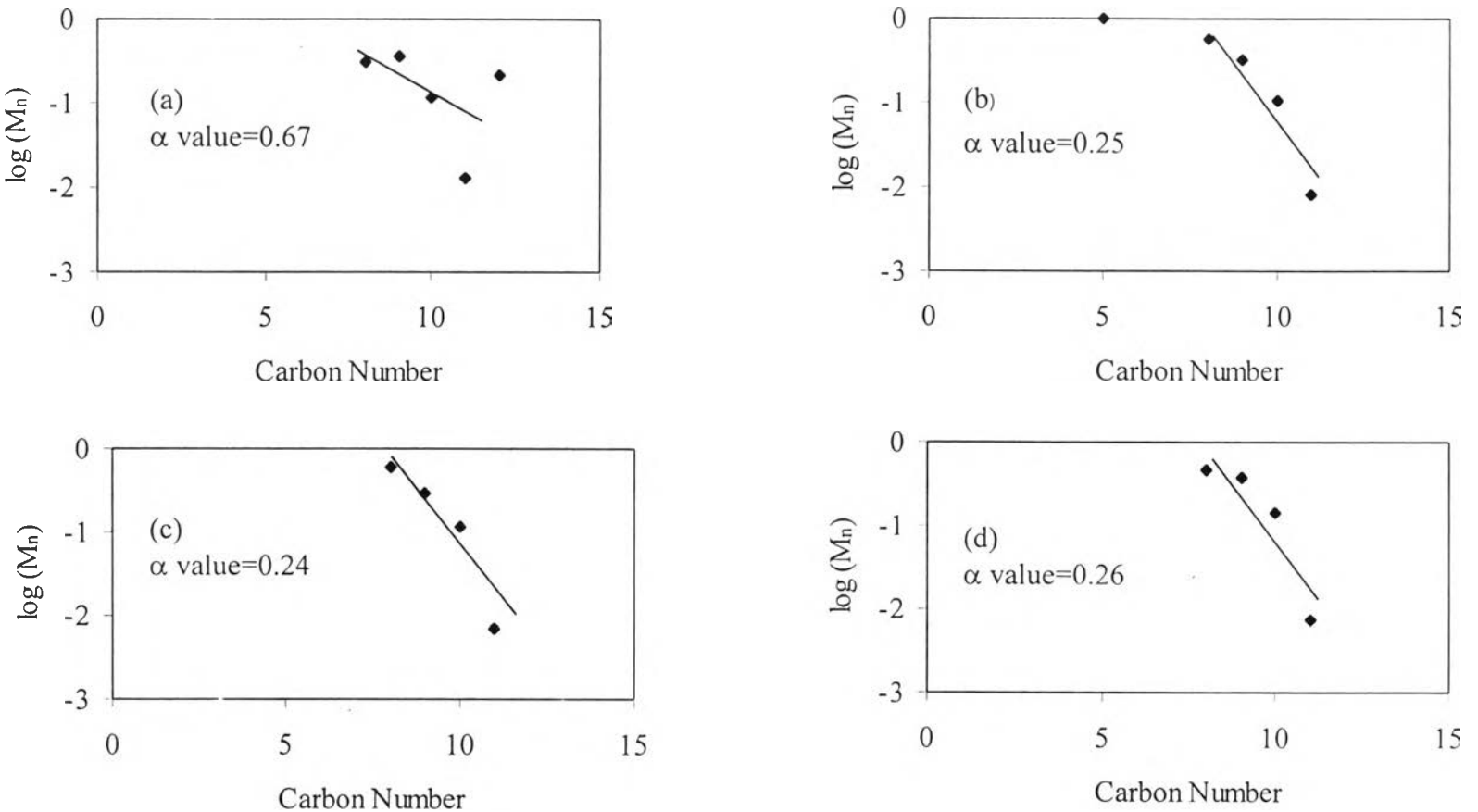

Figure 5. 42 Schulz-Flory diagram of soluble coke from the metal with different H_2/HC ratios: (a) H_2/HC = 0, (b) H_2/HC = 3, (c) H_2/HC = 5 and (d) H_2/HC = 10

ต้นฉบับ หน้าขาดหาย

Application of the Schulz-Flory equation was to adjust our data in account for the effect of carbonaceous accumulation. Figures 5.42 and 5.43 show the α value of Schulz-Flory distribution diagram on the metal sites and the support sites, respectively. An observed change in chain growth parameter in the distribution depended importantly the H_2/HC ratio. The less probability of chain growth was obtained when H_2 was added into the feed. For the higher H_2/HC ratio, α values showed a little change. Regarding the same α values of the metal and the acidic sites, the chain growing mechanism was occurred for a constant α. The introduction of hydrogen caused the absence of a break on the Schulz-Flory diagram, whereas the occurrence of the deviate was noticed in the absence hydrogen. Consequently, H_2 was a dominant role on the production of coke intermediates to generate coke precursor. At higher H_2 addition, carbonaceous intermediates were easily removed. Their nature of intermediates was less diffusitivity to extent for chain growth [191].

6. Influence of H_2 on carbonaceous deposition

Since hydrogen was such an important component of the working platinum catalysts, the following roles can be identified [3],

- the high hydrogen pressures lower in the concentration of coke precursors, keeping the coking rates low.

- the dehydrogenation reactions involved in coking are restricted by hydrogen.

-hydrogen hinders the reaction from reversible to irreversible coke by an ensemble effect.

-coke levels on the metal component are controlled by hydrogen cleaning. It is noted that the initial deposition (in hydrogen atmosphere) is reversible in nature, the attainment of a steady level of coke on the metal sites must be due to rate of reversible coking on metal = rate of cleaning of reversible coke by hydrogen.

The graphite (and also C_xH_y polymers) may have formed by polymerization of open-chain trans-polyenes. However, it reached likely the observed state dehydrogenation of 'primary carbon' upon evacuation. The increased amount of 'atomic C' indicated the subsequent splitting of a fraction of this residue into

individual C atoms [2]. Auger-electron spectroscopic studies also showed a similar phenomenon. Hydrogen splitting several C-C bonds without removing all carbonaceous over layer from Pt foil exposed to small alikeness. These C atoms or C_1 units may have some mobility between surface and subsurface layers. This would agree well with the concept of 'flexible surfaces' which could, hence, appear in the case of this, unsupported Pt consisting of the aggregates of small crystallites [9]. The presence of hydrogen promoted this mobility. This may not be so surprising, considering the extensive sintering of Pt under hydrogen exposure, indication that- likely intercalating- H atoms may 'loosen' the crystal structure of unsupported Pt. Hydrogen exposure of Pt after alkane reactions and evacuation (like in the case of XPS and UPS) may have reacted predominantly with those C_1 units producing almost entirely methane after n-hexane reaction. According to the literature review [159], hydrogen can convert coke precursors into stable products before they are converted to coke

$$Q \longrightarrow P^*$$
$$H_2 \longrightarrow 2H^*$$
$$P^* + H^* \longrightarrow P$$
$$P^* + P^* \longrightarrow P_2$$
$$P_2 \longrightarrow \text{coke}$$

In this scheme, the coke precursors generate radical P* which is either terminated by H* or converted to coke.

5.2.4 The effect of promoter

1. Carbon deposition on the metal and the acid of the Pt, Pt-Sn and Pt-Sn-K catalysts

Carbon deposits on Pt-based catalysts were investigated by the temperature programmed oxidation (TPO). On the active metal sites of various catalysts, Figure 5.44 shows the TPO profiles of Pt, Pt-Sn and Pt-Sn-K catalysts. It is observed that two peaks appeared at 300°C and 425°C in every TPO profile. This indicates that the carbon deposited on these catalysts can be divided into two types: (i) coke deposited directly on metal and (ii) coke in the vicinity of metal centers, which corresponded to the report somewhere else [15, 131]. In addition, it is obvious that coke deposited on different sites on the different catalysts and affected deactivation to defer extents. From Figure 5.44, the difference of the modified catalysts was that, for Pt and Pt-Sn catalysts, the area of the first peak at lower temperature was less than that of the second peak at higher temperature. For the Pt-Sn-K catalyst, the situation was just opposite. Interestingly, the peak of the K-doped catalyst decreased more than any other catalysts, especially in the position at 425°C. In previous studies [1, 3, 4, 15, 50, 68, 89], it is speculated that the active metal site was linked with the originally generated coke precursors. Consequently, K addition dramatically inhibited the production of coke intermediates resulting in the lower area of carbonaceous compounds. It is seen that the order of their TPO areas was as follows: Pt > Pt-Sn > Pt-Sn-K. Furthermore, the total carbon accumulated on the metal sites of different catalysts as listed in Table 5.14 was determined by the areas under the TPO profiles. The order of the decreasing amount of carbon per gram was Pt > Pt-Sn > Pt-Sn-K. It is found that the areas of the TPO peaks increased with the amount of carbon on the Pt-based catalysts.

On the other hand, Figure 5.45 exhibits TPO spectra of Pt, Pt-Sn and Pt-Sn-K catalysts on the acidic sites. It is observed that a single peak appeared on TPO spectra for the modified catalysts. This peak was coke burnt off at higher temperature, about 525°C, compared with coke on the metal. This implies that the peak was shifted to a

higher temperature because of a larger degree of polymerization of coke [111]. Moreover, the TPO area of the Pt catalyst was diminished by the addition of Sn, especially the combination with K. As presented above, it is relevant to note that the surface coverage had the different compositions, which is summarized in Table 5.14. The amount of coke on both the metal and support decreased significantly by the addition of Sn and/or K.

Table 5.14 The amount of carbon on the different catalysts

Catalyst	Coke on the metal sites % C	Coke on the support sites % C
Pt catalyst	0.36	2.50
Pt-Sn catalyst	0.32	1.73
Pt-Sn-K catalyst	0.21	1.26

Additionally, comparing the amount of coke on the metal and support as shown in Table 5.14, it is obvious that a small part of coke was located on the metal sites whereas the major fraction was accumulated on the acid. These results imply that coke deposited on the metal was less dehydrogenated and corresponded to hydrogen-rich species in accordance with the literature reviews [91, 177]. Accordingly, the H/C ratio of coke deposited on the metal sites was higher than that of the ones covered on the acidic support. It displayed the different nature of coke between the metal and alumina. Finally, the modifications of Pt catalyst by addition of Sn and K were able to reduce the amount of coke on both sites.

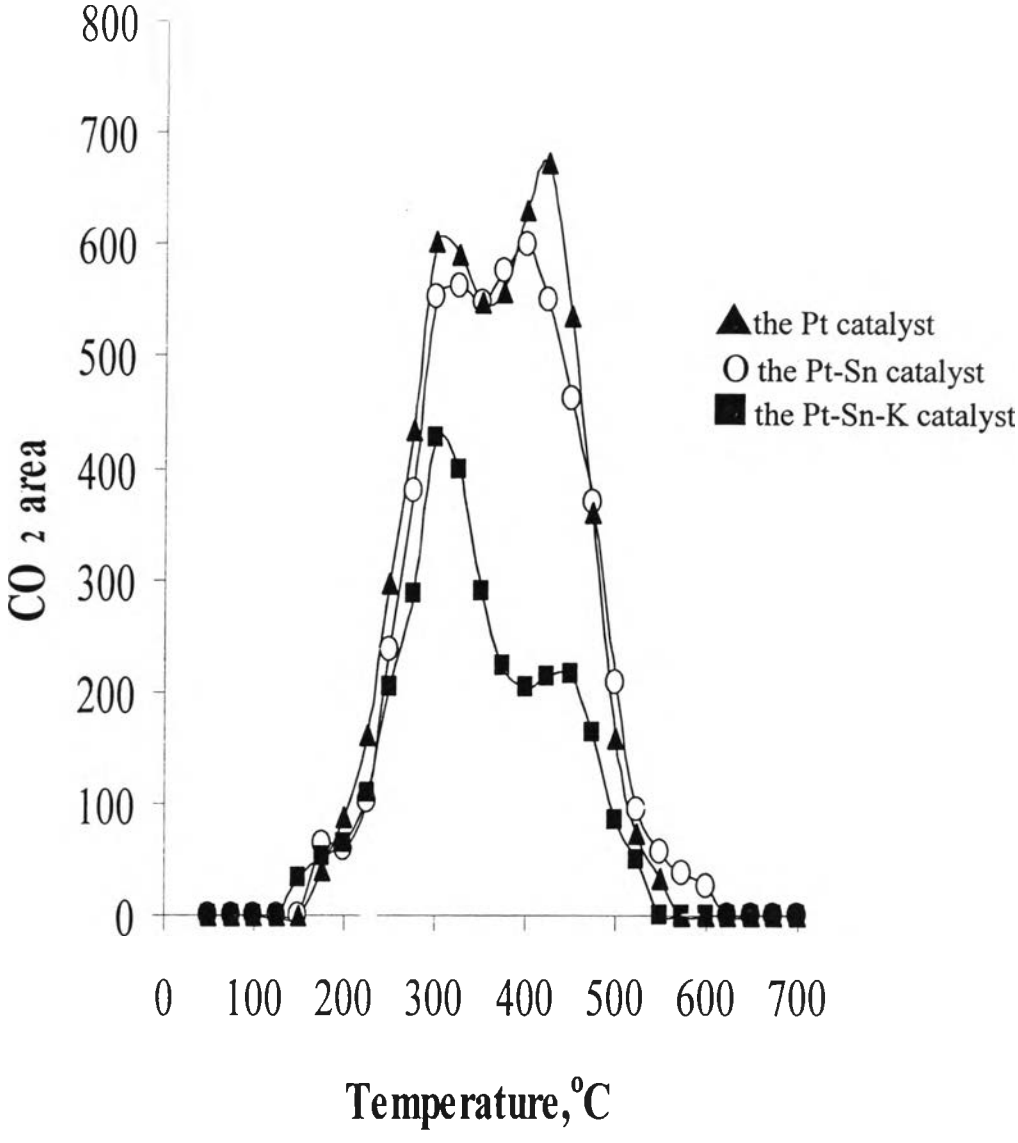

Figure 5.44 TPO of carbonaceous deposits produced on the metal at 120 min and 475°C with different catalysts

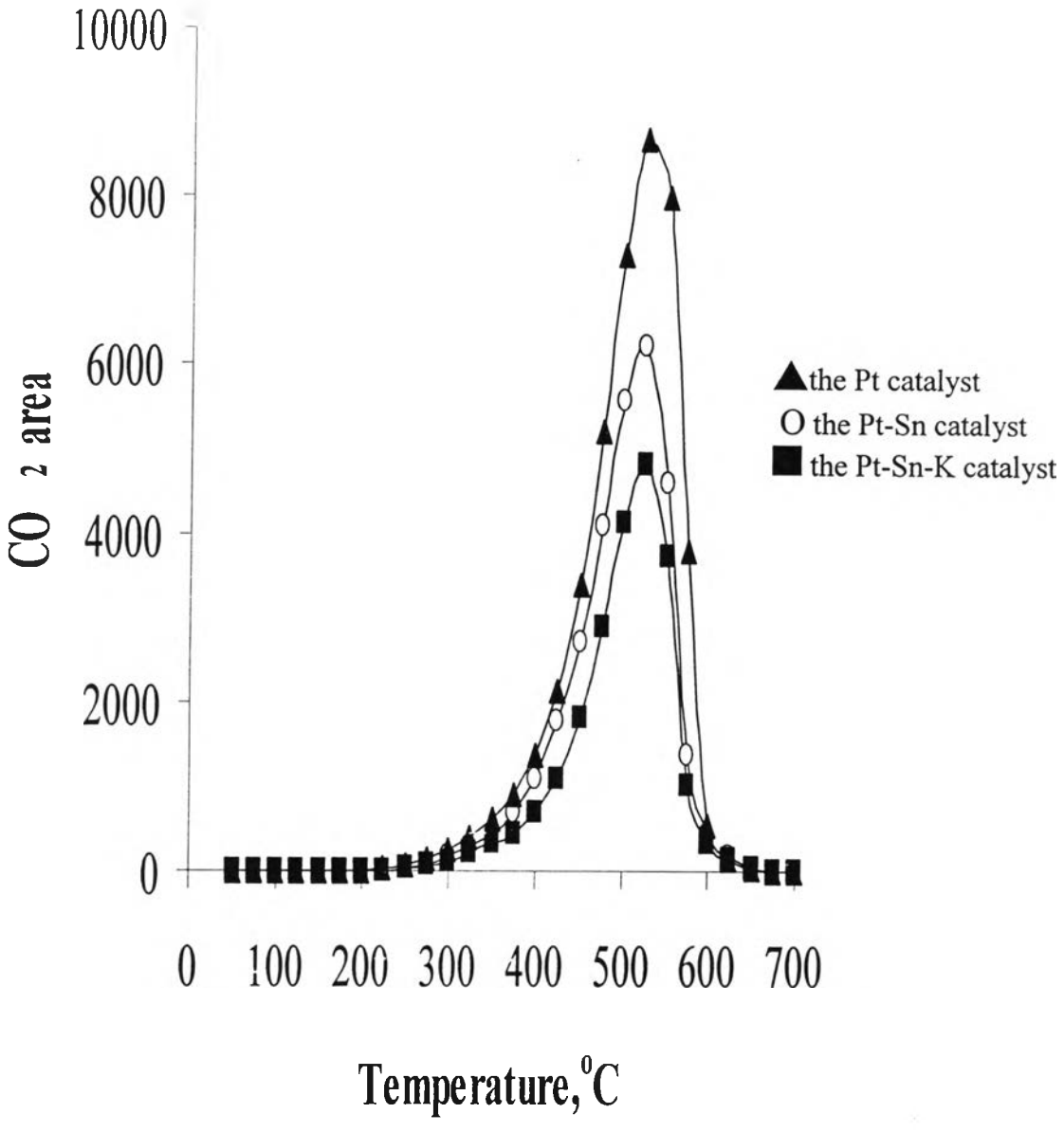

Figure 5.45 TPO of carbonaceous deposits produced on the support at 120 min and 475°C with different catalysts

2. Characterization of C_xH_y species

In order to examine the effect of Sn and K addition on coke formation with both sites in more details, the ESR experiment was studied. Figure 5.46 shows the ESR spectra of coke radicals for various catalysts on the metal. The carbon radicals density computed from the total peak area is given in Table 5.15. The g value of the coke radicals was estimated to be 2.003 in agreement with earlier literatures [181, 186]. It is found that the modification of catalysts displayed a dominant role in reducing the intensity of carbonaceous radicals as well as reducing the amount of coke precursors. Interestingly, the K-doped sample had a sharply lower amount of the coke radicals, by 27 times, compared with the Pt catalyst as shown in Table 5.15. The Sn modification of the Pt catalyst diminished carbonaceous radicals about 1.7 times. A comparison between ESR and TPO results exhibited a good correlation between the number of radicals and the amount of coke.

For the acidic sites, the ESR spectra of radicals with the Pt-based catalysts are illustrated in Figure 5.47. Table 5.15 also lists the intensity of radicals on these sites. The characteristic of carbon radicals on the acidic sites was similar to that on the metal sites as reported above. However, the density of coke radicals was greater on the alumina sites than on the metal active sites. It is clear that the amount of radicals was reduced by 1.45 times for the Sn modification and 1.65 times for the K addition compared with the carbonaceous radicals' intensity of Pt catalyst. As mentioned above, it is introduced that the metal sites was relevant to generate coke intermediates, which adsorbed to form coke on these sites and migrated to the acidic support sites. Thus, if the modification of catalysts inhibited the production of coke precursors on the metal sites, then the amount of carbonaceous compounds was accordingly decreased. From the result shown in Table 5.15, it is obvious that the K-doped sample dramatically reduced coke radicals concerned with coke species on the metal sites. Accordingly, lower amount of coke deposits was produced as shown by the TPO results.

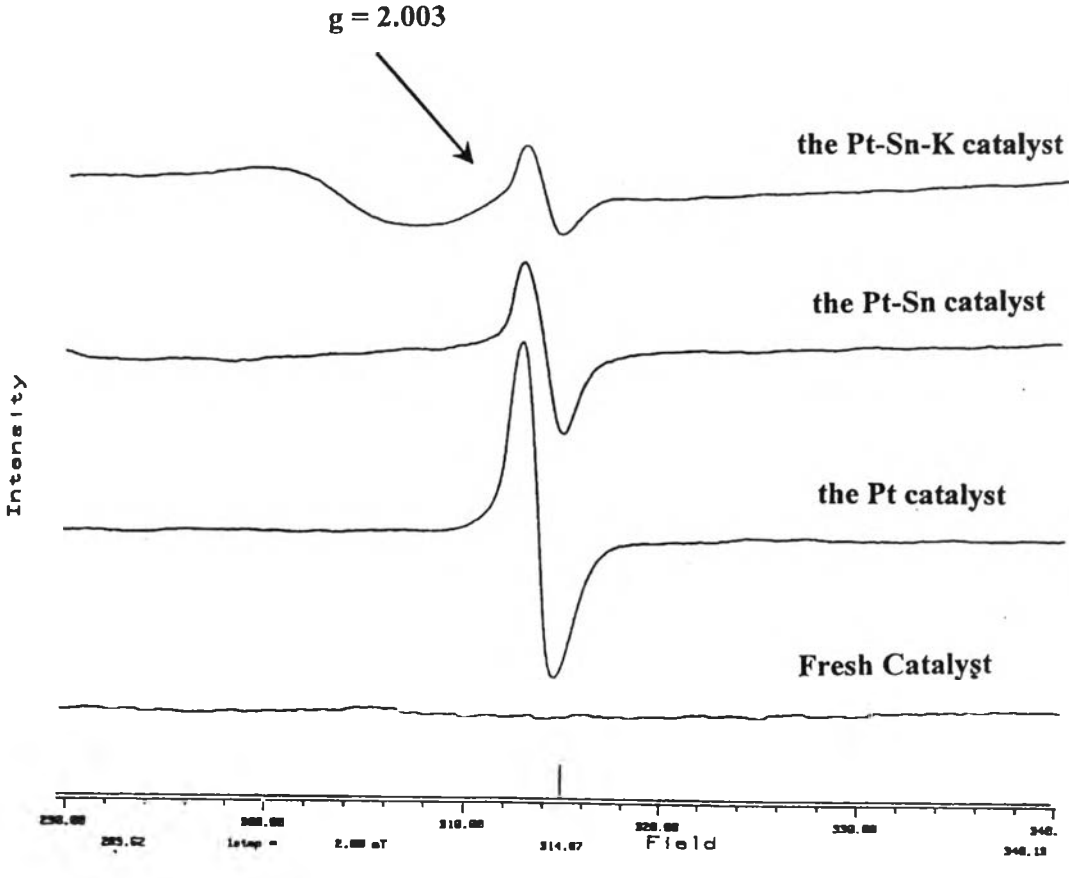

Figure 5.46 ESR spectra of coke on the metal at 120 min and 475°C with different catalysts

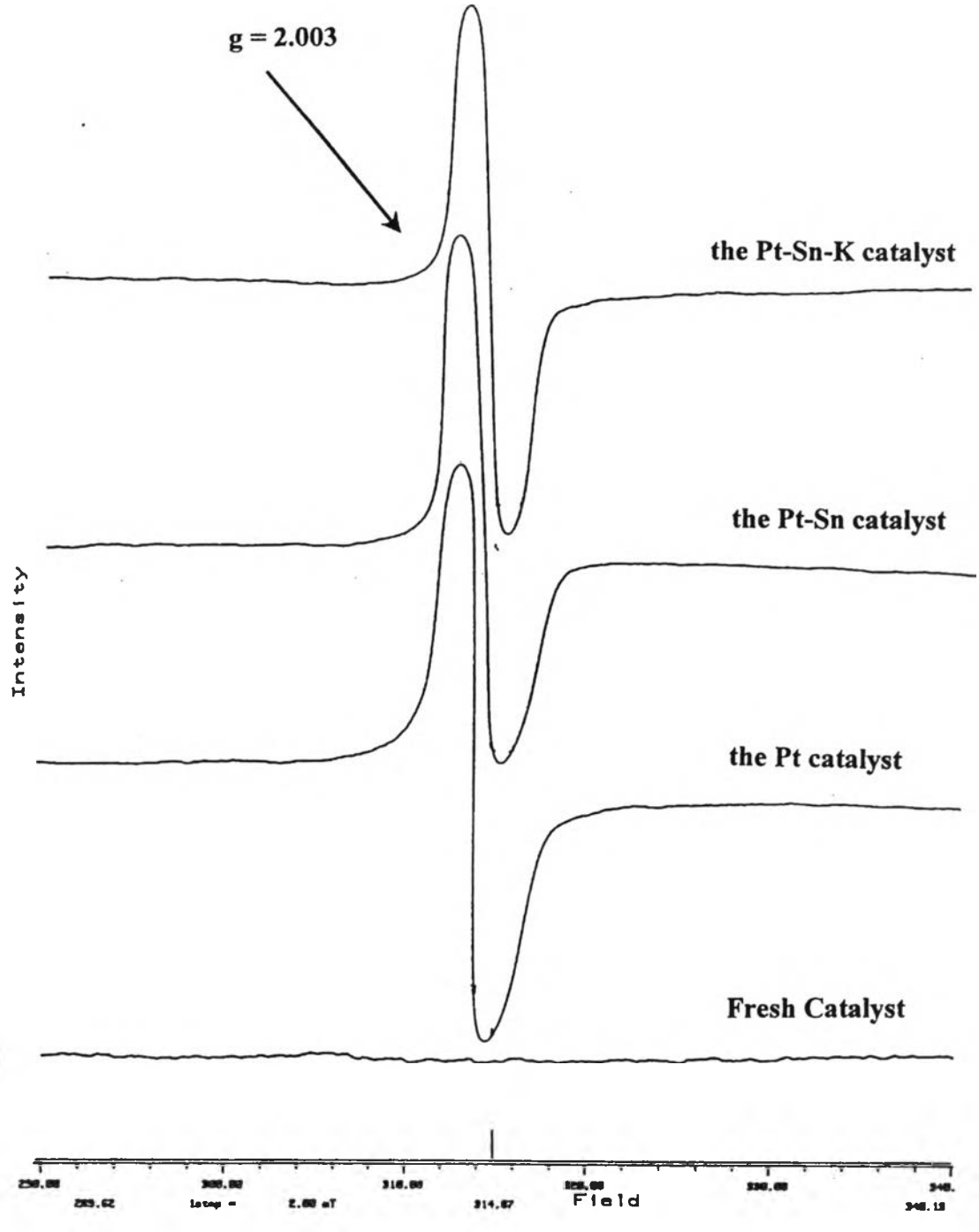

Figure 5.47 ESR spectra of coke on the support at 120 min and 475°C with different catalysts

Table 5.15 The density of carbon radicals of coke per gram catalyst with different catalysts

catalyst	The metal sites	The support sites
Pt catalyst	8.55×10^5	3.02×10^6
Pt-Sn catalyst	5.18×10^5	2.07×10^6
Pt-Sn-K catalyst	3.17×10^4	1.83×10^6

IR spectra of the coked Pt, Pt-Sn and Pt-Sn-K catalysts are illustrated in Figure 5.48. There was one band on the metal sites as shown in Figure 5.48 A whereas there are two main bands on the support (see Figure 5.48 B). The most intense band was at 1610 cm^{-1}, which appeared on the metal and support sites. This absorption region was assigned to the identification of aromatic ring bending vibration. Interestingly, the C=C stretching vibration around 1540 cm^{-1} occurred only on the support sites. The difference between IR spectra of coke on the metal and support sites reflected in the different rate formation and H/C ratio of coke. Moreover, it is seen that the order of intensity was Pt > Pt-Sn > Pt-Sn-K on both sites. Although the Sn and K addition did not affect on the overall patterns of these spectra in each site, the difference of intensity level was observed. The decrease of 1540 cm^{-1} band on the acidic sites was significantly obtained. Controversy, the catalyst modifications slightly reflected on the band at 1610 cm^{-1} on both sites [124].

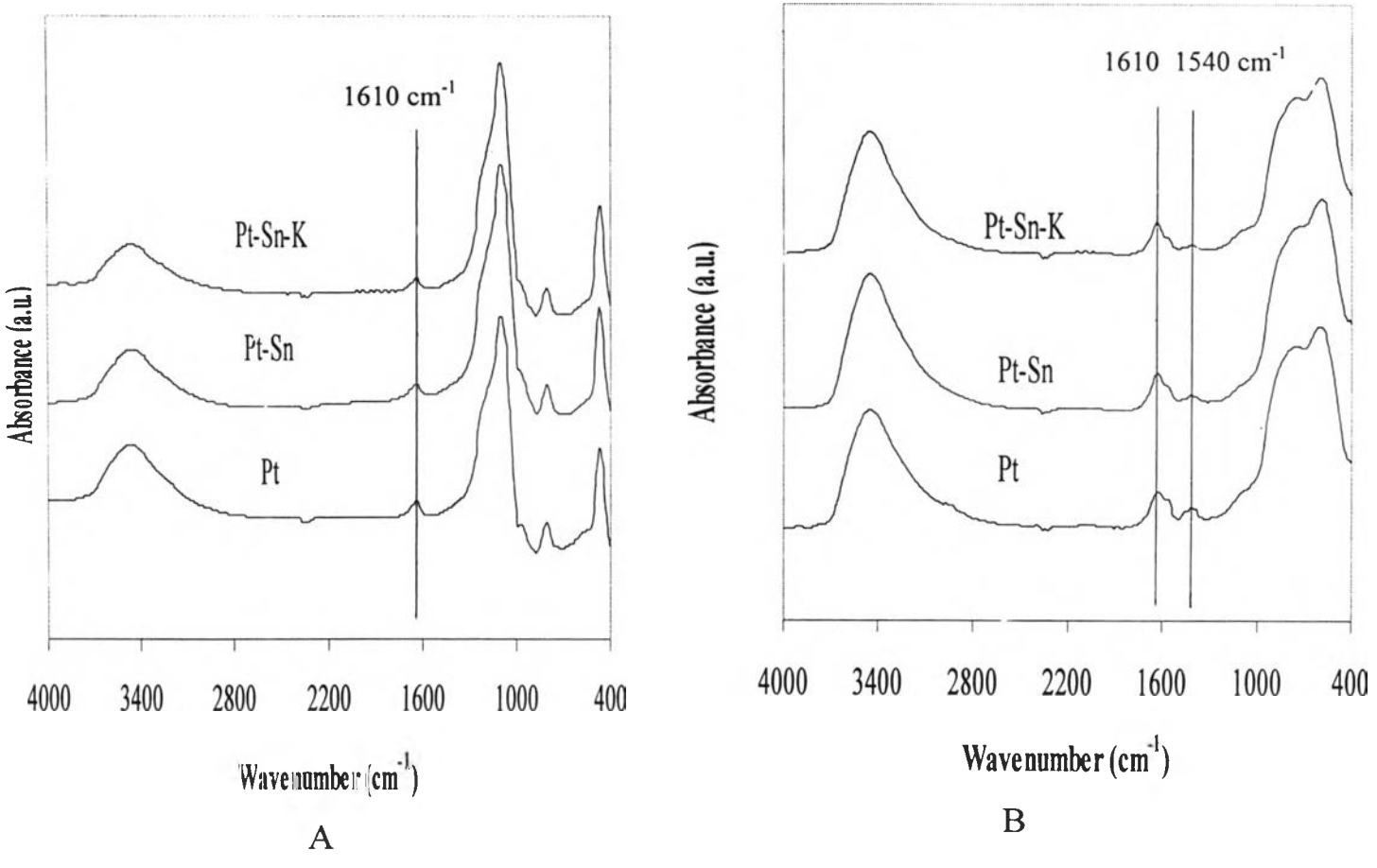

Figure 5.48 IR spectra obtained after coking with different catalysts over (A) the metal and (B) the support

3. The changes of textural properties and the dispersion factors of coke on the metal and acid of the Pt, Pt-Sn and Pt-Sn-K catalysts

Coking was claimed to be responsible for a decrease in the specific surface, pore surface and pore volume depending on a limitation of diffusion (dispersion) and nature of coke deposits. As the result, an investigation of textural changes in the surface area before and after coke deposition of Pt-based catalysts was carried out. Literature cited therein [131] introduced the dispersion factor to consider catalyst degradation of Pt/Al_2O_3 and $Pt\text{-}Re/Al_2O_3$ catalysts. Carbon deposited on $Pt\text{-}Re/Al_2O_3$ catalyst was better dispersed with the fine small grain structure. In our work, the dispersion factor of carbonaceous defined as the ratio of change of the surface area to the amount of coke deposits was investigated on Pt, Pt-Sn and Pt-Sn-K catalysts, respectively. Table 5.16 summarizes the textural properties of catalyst samples before and after coking and the dispersion factor, which was separated into the metal and alumina in each catalyst. The change of the surface area may be attributed to the blockage of catalysts by coke, through thermal sintering and the other factor except coking should not be ruled out. It is found that the modified catalyst lost their surface area after the reaction more than the unmodified catalyst containing only platinum. This might be due to the fine structure of coke readily occurred in case of Pt catalysts with the presence of Sn and/or K, which easily blocked the existing porous area of the catalyst. The obtained results were consistent with the report of fine small grain structure of coke deposits for the modification catalysts suggested in literature reviews [88, 105, 179, 180]. Moreover, noticeable higher values of dispersion factors are obtained from the Pt-Sn and particularly Pt-Sn-K catalysts as illustrated in Table 5.16. Comparing with the Pt catalyst, the dispersion factor of the Pt-Sn catalyst was about 1.7 times on the metal and about 1.8 times on the acid. In the case of K addition, the dispersion factors on the metal and support sites were about 2.4 times and 4.5 times compared with Pt catalyst, respectively.

Table 5.16 The textural properties of catalyst samples before and after testing and dispersion factor with different catalysts

Catalyst	The metal sites			The support sites		
	SA (m^2/g)		dispersion	SA (m^2/g)		dispersion
	Fresh	Used	factor	Fresh	Used	factor
Pt catalyst	447	386	171	390	343	19
Pt-Sn catalyst	417	325	291	390	330	35
Pt-Sn-K catalyst	380	283	462	390	283	85

4. Carbonaceous morphology

More detailed information of the structural characteristic of the various types of catalyst was revealed from TEM studies. As shown in Figures 5.49 and 5.50, it is noticed that the Pt/Sn and Pt/Sn/K catalysts differed from the Pt catalyst. They had a small particle since they may be formed in the alloy form in accordance with the literature reviews [7, 88, 94, 105]. It is clear that there was the difference of coke coverage on the various catalysts in each site. For the metal, the extent of coverage is often declined when added the additive of Sn and K. On the support, it is interesting to found that the coke coverage on various types of catalyst was quite similar. Indeed, these sites should be found the little coverage of coke. This account for the high dispersion factor on the modification catalysts as discussed above. Moreover, the different sizes of coke covered on each site were observed. This indicates that there were different types of coke. The coke on support had a small particle compared with that on metal sites. The TEM study showed that the coke deposited under the present coking condition was essentially amorphous.

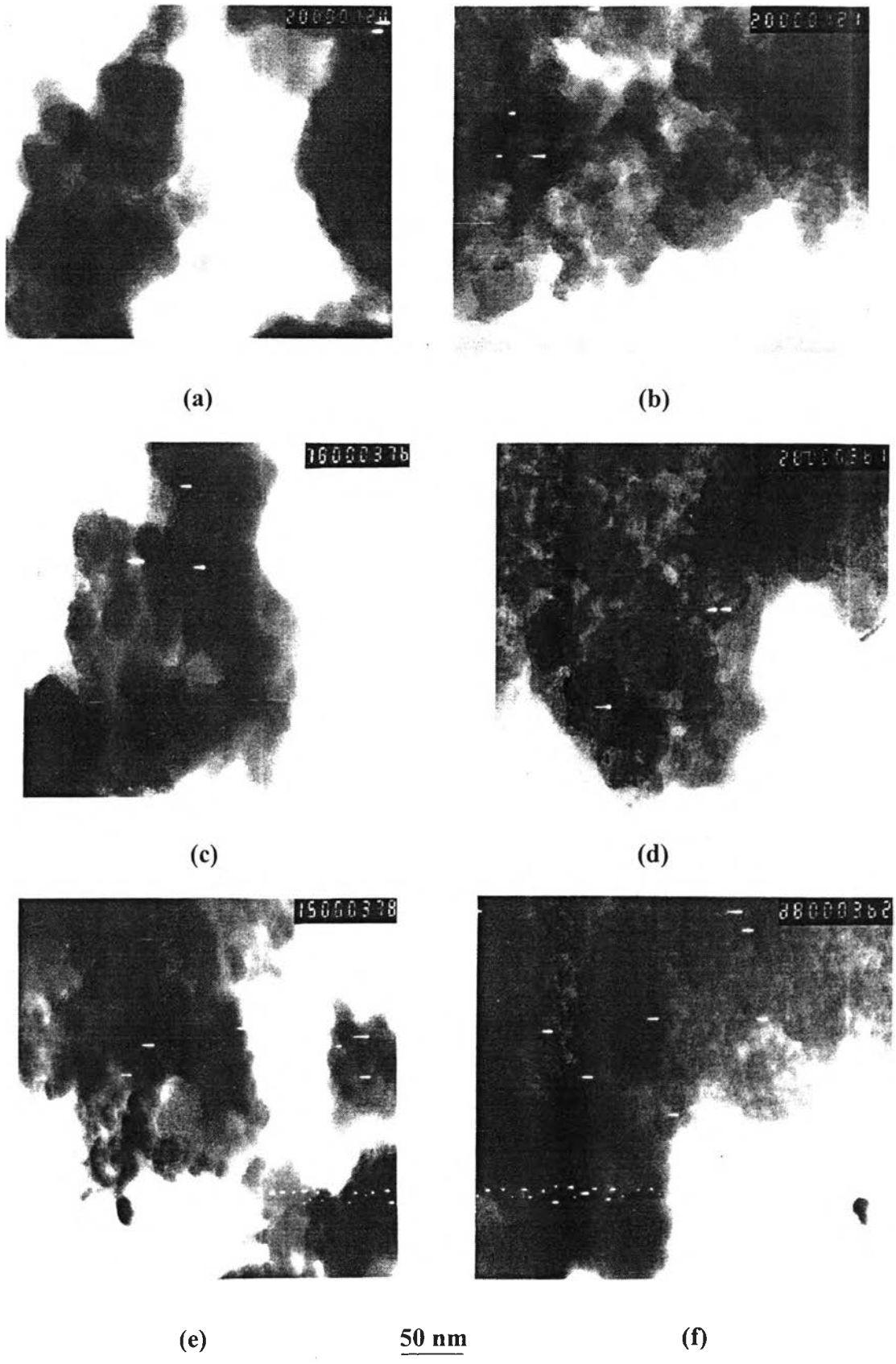

Figure 5.49 TEM photograph of coke on the metal with different catalysts: (a) fresh Pt catalst, (b) coked catalyst of Pt, (c) fresh Pt-Sn catalyst, (d) coked catayst of Pt-Sn, (e) fresh Pt-Sn-K catalyst and (f) coked catalyst of Pt-Sn-K

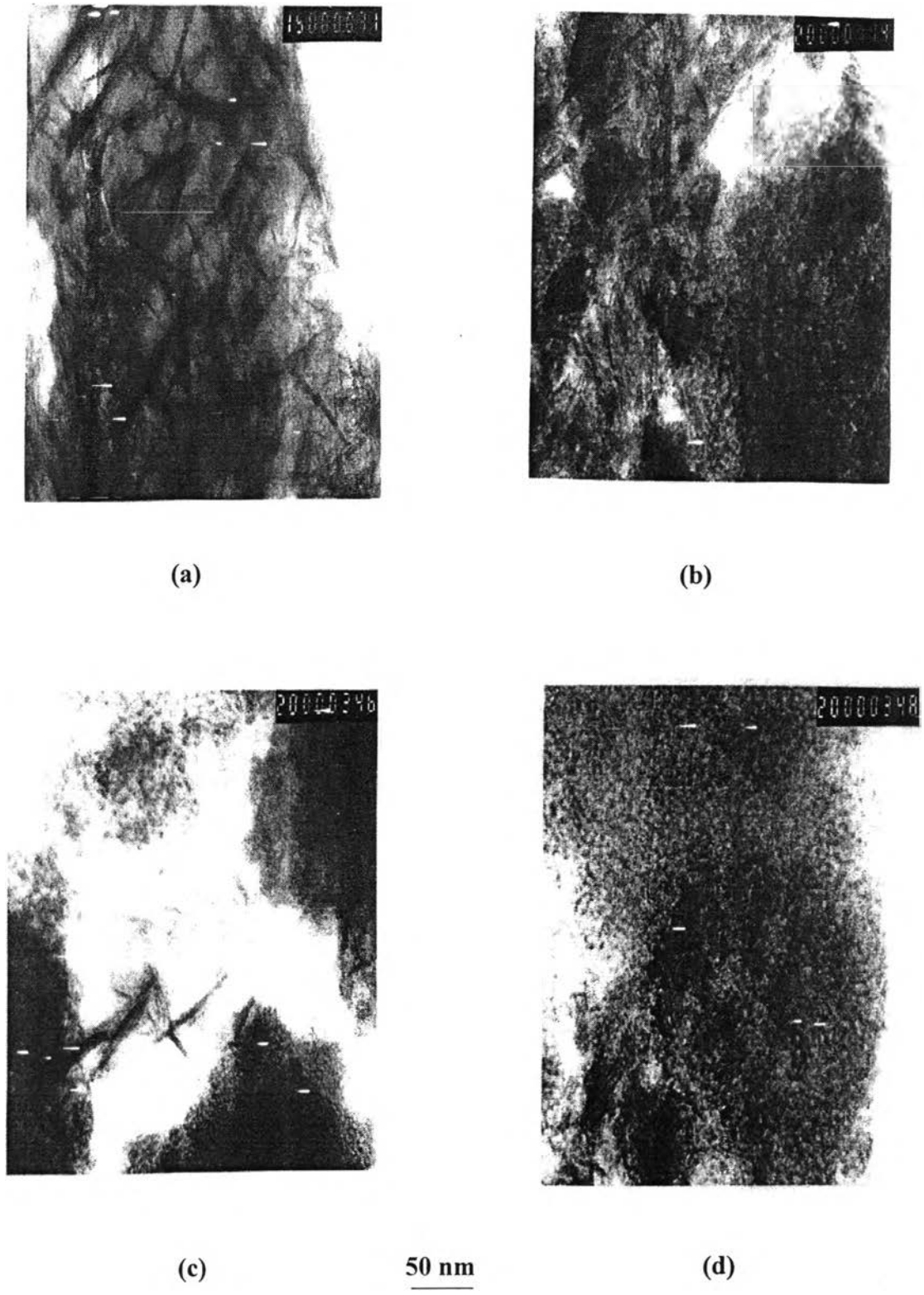

Figure 5.50 TEM photograph of coke on the support with different catalysts: (a) fresh Al_2O_3, (b) Pt catalyst, (c) Pt-Sn catalyst and (d) Pt-Sn-K catalyst

5. The influence of Sn and K addition on the coke formation

The main theories put forward to account for the improved properties of multi-metallic catalysts tend to involve either geometric or electronic effects [2, 7, 15, 24, 32, 89, 92, 98, 99, 109, 111, 135, 192]. Coke formation is known to require relatively large clusters or ensembles of adjacent metal atoms. For the Sn addition, the presence of Sn improved the diluting of the active metal surface into smaller ensembles (see Figure 5.49), which enhanced the catalysts' resistance to deactivation. The addition of Sn to Pt catalyst forms substitute surface alloys and it was shown that Sn interacts with platinum on silica to form a Pt/Sn alloy. Thus, carbon intermediates cannot readily form multiple carbon-metal bonds. Furthermore, it inhibits the formation of highly dehydrogenated surface species that are intermediates for coking. According to the earlier work [26, 91], one reason is that coke deposits bind more strongly to the Pt catalyst than to the Pt-Sn catalyst.

From TPO profiles and ESR spectra of the metallic sites, the adsorbed species attached less strongly to the metal surface would be explained by the significant minimization of coke on these sites and promotion of the migration of coke precursors to the support. The change in the peak height in the TPO profiles and ESR spectra evidenced for this idea.

The addition of K into bimetallic Pt-Sn catalyst decrease significantly the catalyst deactivation as shown in Figure 5.51 illustrating the conversion of hexane as a function of time. The decline in conversion was slower for catalysts containing tin and potassium than for catalysts containing platinum only because less amount of coke was formed on the modified catalysts. From Figure 5.51 and Table 5.14, it is obvious that Pt catalyst deactivated quickly and a considerable amount of coke was formed. It may be related to the incorporation of tin into the platinum surface through the formation of a substituted alloy, while potassium may be presented on the top of the platinum surface. As described elsewhere [29, 31, 111, 114, 132, 147, 193-195], it was found that K-doped catalyst significantly decreased the activation energy of HC dehydrogenation and the potassium diminished the interaction between Pt and Sn.

This modification in the interaction between both metallic components could be due to either a direct addition of K on the metallic phase or to an indirect effect of the alkali metal addition to support, which could change the metal-support and the metal-metal interactions, as suggested in the literatures [26, 132]. This resulted in a weakening of Pt-C bond strength to make the catalyst less susceptible to deactivation by deposition of carbonaceous species on both sites as illustrated in Figures 5.44-5.47, Table 5.14 and Table 5.15. This is known as an electronic effect [2, 7, 24].

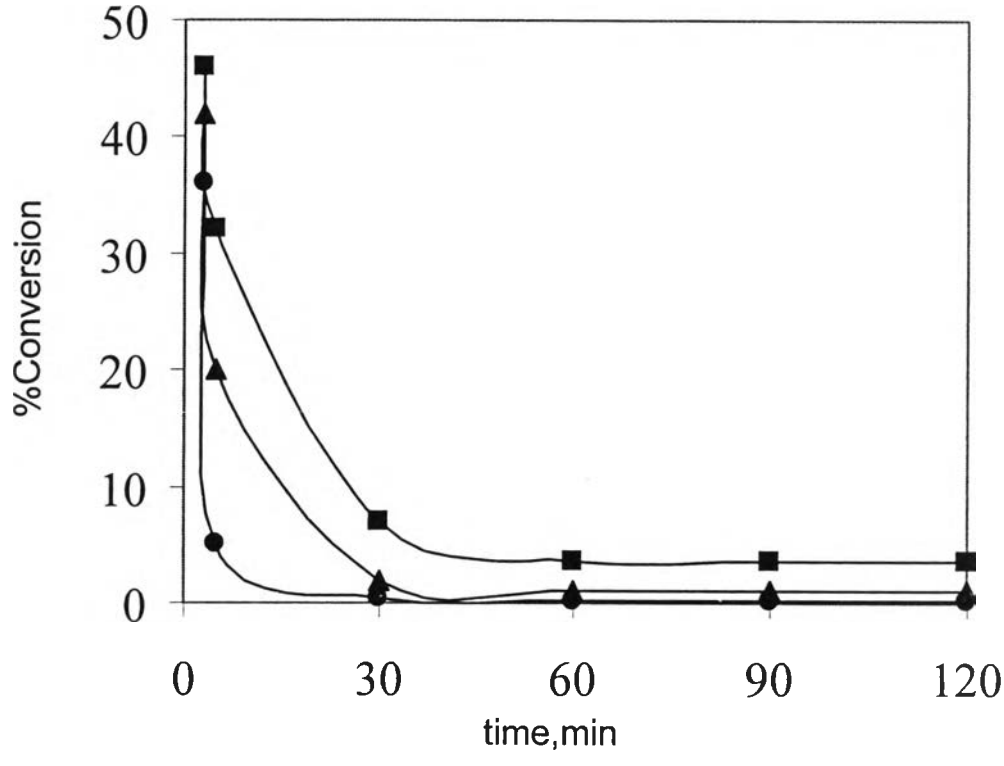

Figure 5.51 % Conversion of hexane dehydrogenation with the different catalysts as a function of time: ● the Pt Catalyst, ▲ the Pt-Sn Catalyst and ■ the Pt-Sn-K catalyst

Besides, the H_2-TPD profiles were used to estimate the capacity of H_2 spillover. Figure 5.52 shows TPD profiles obtained after hydrogen adsorption at 30°C. It appears that no desorption peak was detected in Al_2O_3 contrary to Pt- based catalysts. It can offer that hydrogen adsorption originally generated on the metal sites and then hydrogen migrated from these sites to the support sites. However, TPD profiles of hydrogen revealed striking differences for all catalysts. It is found that the

hydrogen uptake was increased as a consequence of the Sn and K addition due to spillover of hydrogen atoms to support surface. Specifically, the K-promoted sample exhibited a very large peak at higher desorption temperature. This result presented to a large capacity for spillover H_2 on the surface area. According to the early works [28-30], it is suggested that the adsorption bonds of metal active sites on the modification catalysts were also weaker causing an increased mobility of hydrogen. As the result, the interaction between the catalyst components via adsorbed hydrogen can be expected to accelerate coke gasification and reduce coke accumulation, which associated with our results. The order of the amount of hydrogen uptake was Pt < Pt-Sn < Pt-Sn-K.

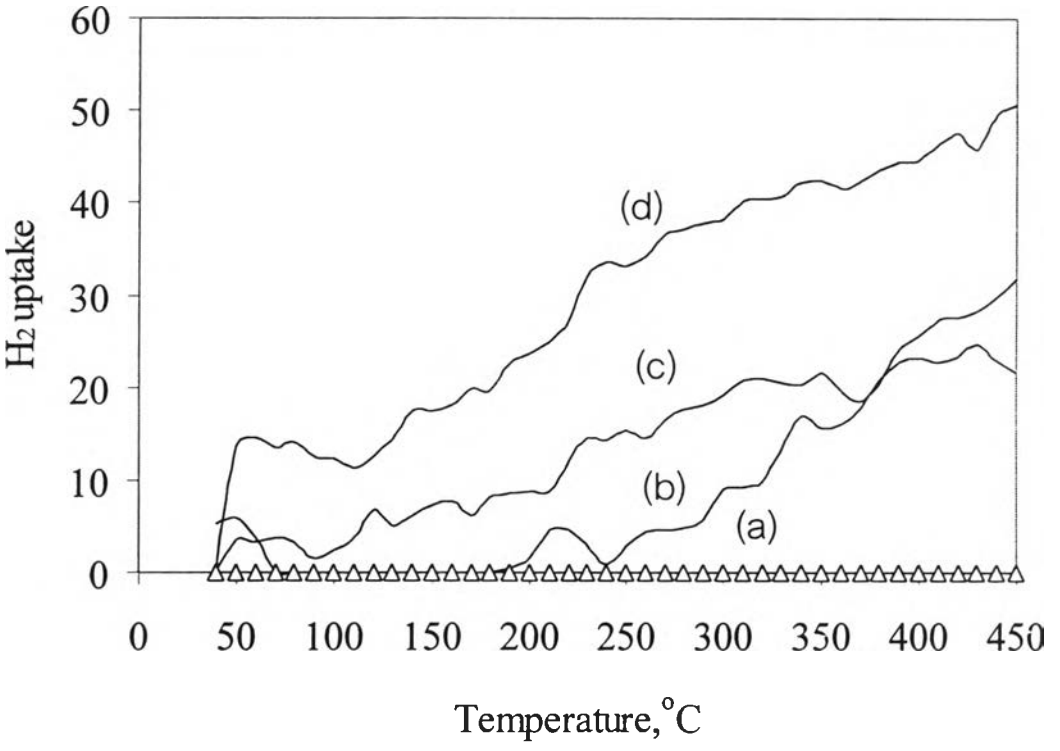

Figure 5.52 H_2-TPD of different catalysts: (a) Al_2O_3 , (b) the Pt catalyst, (c) the Pt-Sn catalyst and (d) the Pt-Sn-K catalyst

5. Characterization of coke extracted from coked catalyst

Runs analogues to those described in the previous sections, carried out at various types of catalysts were followed by the removal of coke with the Soxhlet extraction. Figures 5.53 and 5.54 exhibit the composition of soluble coke with various catalysts. The main components were C_8-C_{12} atom. On the metal (Figure 5.53), it is found that the C_{12} fragments of the Pt-Sn and Pt-Sn-K catalysts vanished. On the support sites, C_8 component was diminished in catalyst without modification and coke soluble was presented C_{12} composition. Moreover, the soluble coke of the Pt-Sn and Pt-Sn-K catalysts was more constituted of a lower C content (C_8-C_{10}). The modifier catalysts influenced on a lower coke formation resulted in a reduction density and mesoporosity on both sites. The decrease in acid site density hindered bi and polimolecular reactions involved in coking while the absence of a significant secondary mesoporous system limited the room available for voluminous coke precursors molecule. The latter characteristic resulted in a particularly significant reduction in insoluble coke content with decreasing mesoporosity

Analysis of the coked-soluble fractions by GC showed that their composition was not significantly affected by the different modification of catalysts, since the same families were identified over the three samples. Form the evaluation of TPO profile, a catalytic effect of Sn and K on promoting coke combustion could be suggested. It is generally accepted that coke formation was proportional to the rate of deactivation of the Brønsted acid sites and that strong centers deactivated more quickly than the weaker ones as introduced in the reviews [89, 100, 102, 196]. Consequently, the modification catalysts were less affected by coking than Pt catalyst. As stated by various authors, in n-C_6 reforming, methylcyclopentadiene (MCPde) was the key intermediate for producing coke via consecutive condensation reactions. The formation of coke precursors was inhibited over the Pt-Sn and Pt-Sn-K catalysts because they displayed a low activity for the transformation of MCPe to MCPde. The Pt-Sn catalyst was particularly resistant to coking resulted from enhanced gasification of coke precursors by tin. Moreover, tin inhibited coke formation by reforming ensembles with platinum that did not favor the production of carbonaceous deposits.

Several studies on coke formation over metal supported catalysts agree in that coke precursors were initially formed on the metal surface, and then through a slow diffusion mechanism. Thus, condensation and accumulation of coke were occurred on the support sites. Additionally, a monofunctional catalyst produced more C_5 and Bz, the important coke precursor, since the deactivation by coking was preferentially appeared. [197].

ASF plots used to calculate α values are exhibited in Figures 5.55 and 5.56. Figure 5.55 demonstrates the Schulz-Flory diagram for different catalysts on the metal. The modifications of catalysts influenced the probability of chain growth. It is found that a decrease of α value appeared on the modified catalysts. The α value on both sites in each case had a little change. This means that the chain was continued to grow with a constant on both sites. The order of increasing α value was Pt> Pt-Sn > Pt-Sn-K. It is implied that the addition of Sn and K affected on the change in structure of carbon intermediates. The reasons for the discrepancy in these results were not clear, but they may have to do largely with the relative adsorptivities of intermediates on these catalysts. As reviewed in [167], they reported the effect of stronger physisorption for larger olefins to predict the increase of the chain growth probability with chain length. Consequently, the intermediates obtained from the Pt were generally the heaviest in nature. Carbon intermediates formed much of low C fraction, which was strongly diffusivity, especially Pt-Sn-K catalyst. Thus, the deviation from Schulz-Flory did not occur, except for the Pt catalyst. The deviation of Schulz-Flory diagram was presented due to higher molecule formation of carbon. The reason is that Sn and K reduced the metal-carbon bond, leaving a larger metal surface, and promoted the migration of coke precursors to the carrier. It is attributed to the greater transformation of intermediates to carrier as associated with the literature reviews [100, 102].

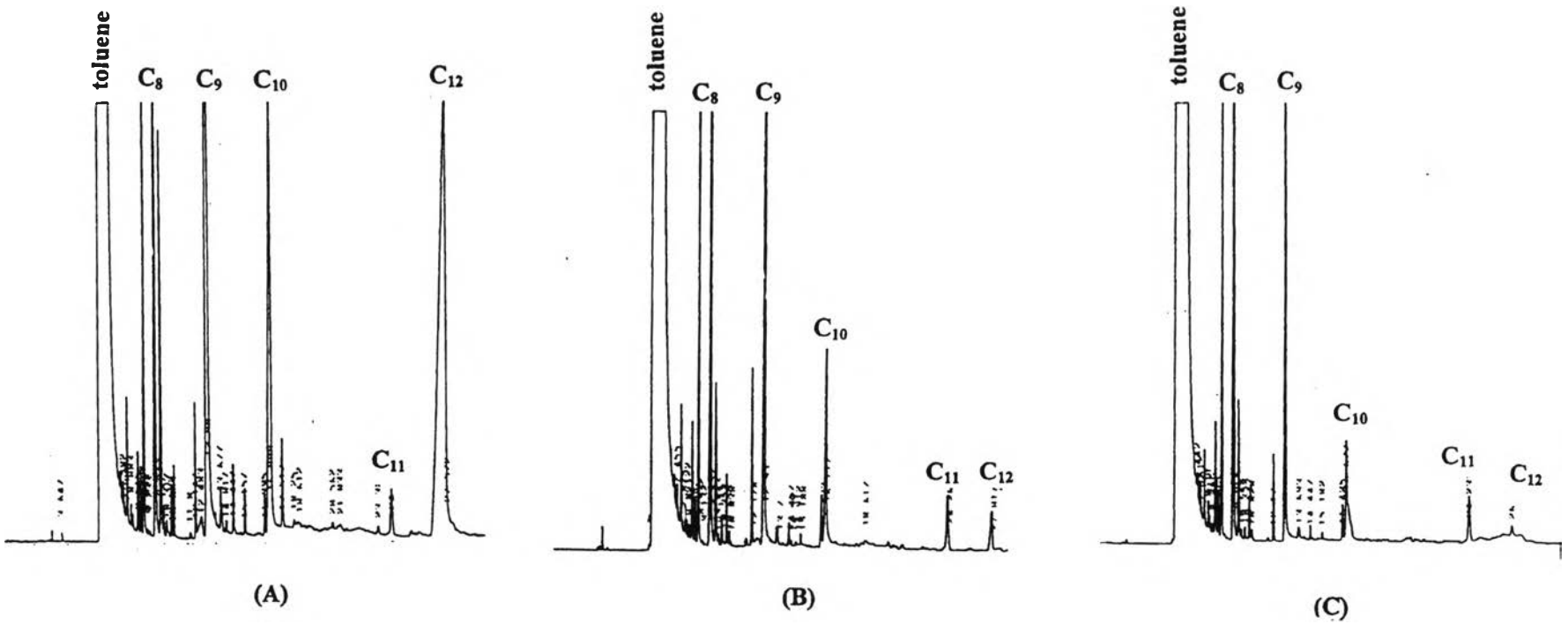

Figure 5.53 The component of the extracted coke on the metal with different catalysts: (A) the Pt catalyst, (B) the Pt-Sn catalyst and (C) the Pt-Sn-K catalyst

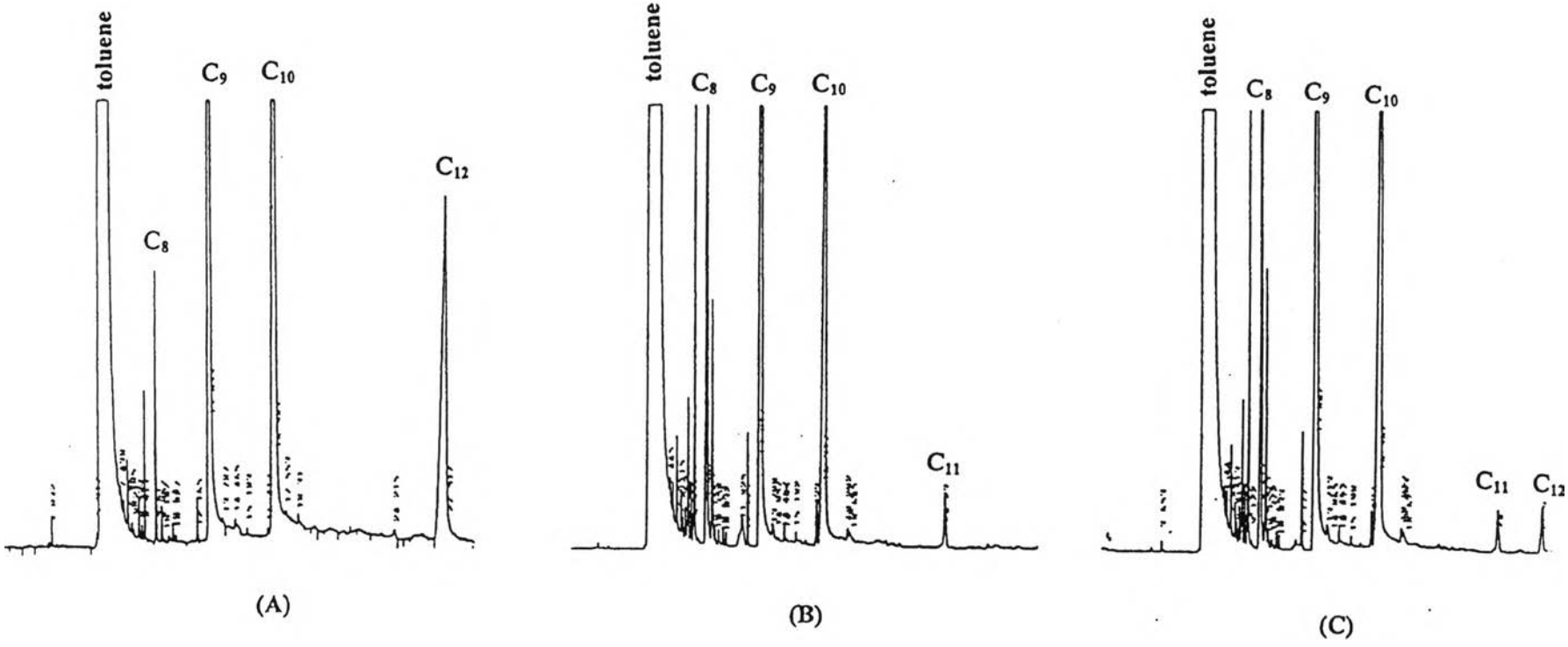

Figure 5. 54 The component of the extracted coke on the support with different catalysts: (A) the Pt catalyst, (B) the Pt-Sn catalyst and (C) the Pt-Sn-K catalyst

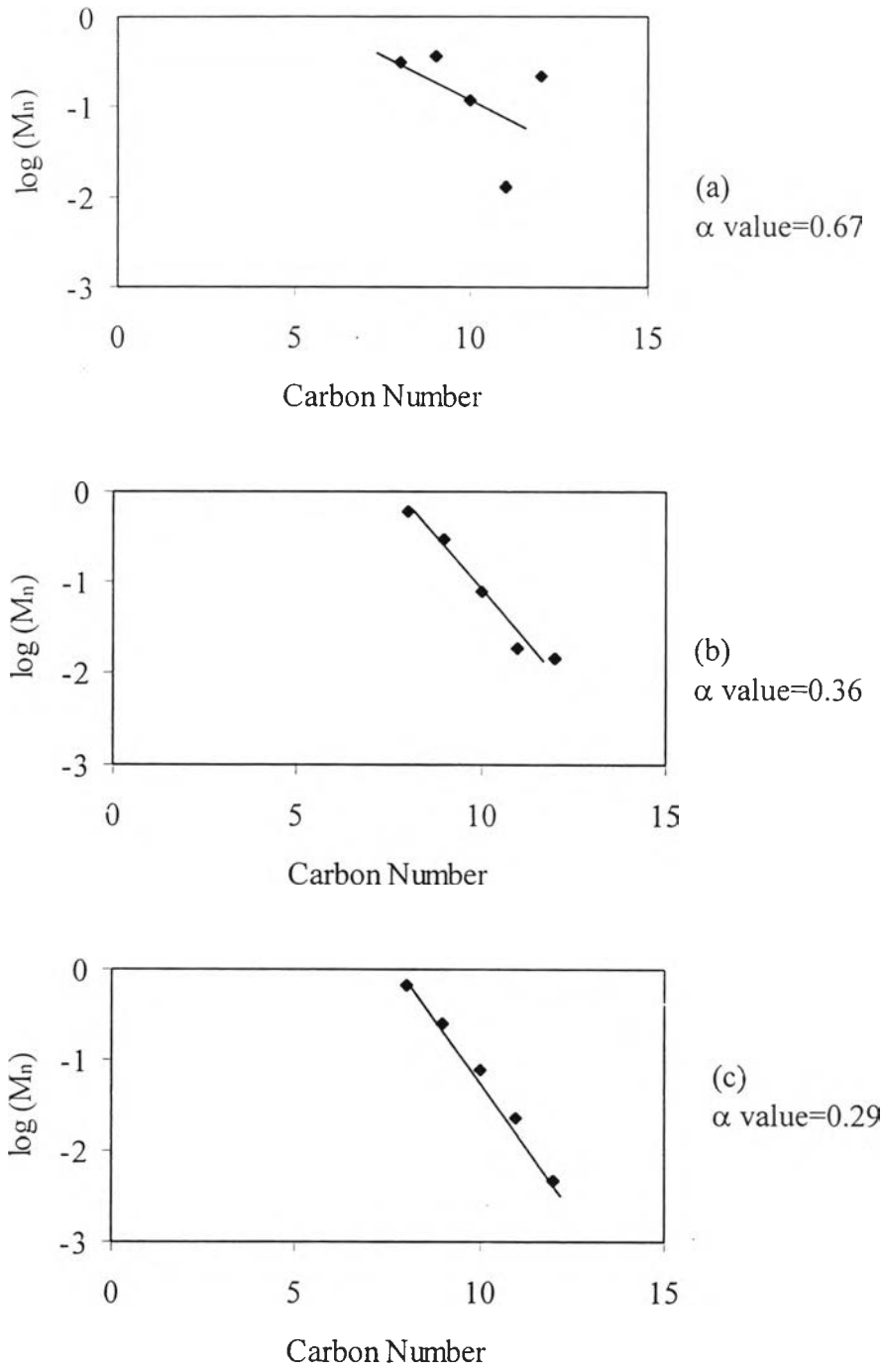

Figure 5.55 Schulz-Flory diagram of soluble coke from the metal with different catalysts: (a) Pt catalyst, (b) Pt-Sn catalyst and (c) Pt-Sn-K catalyst

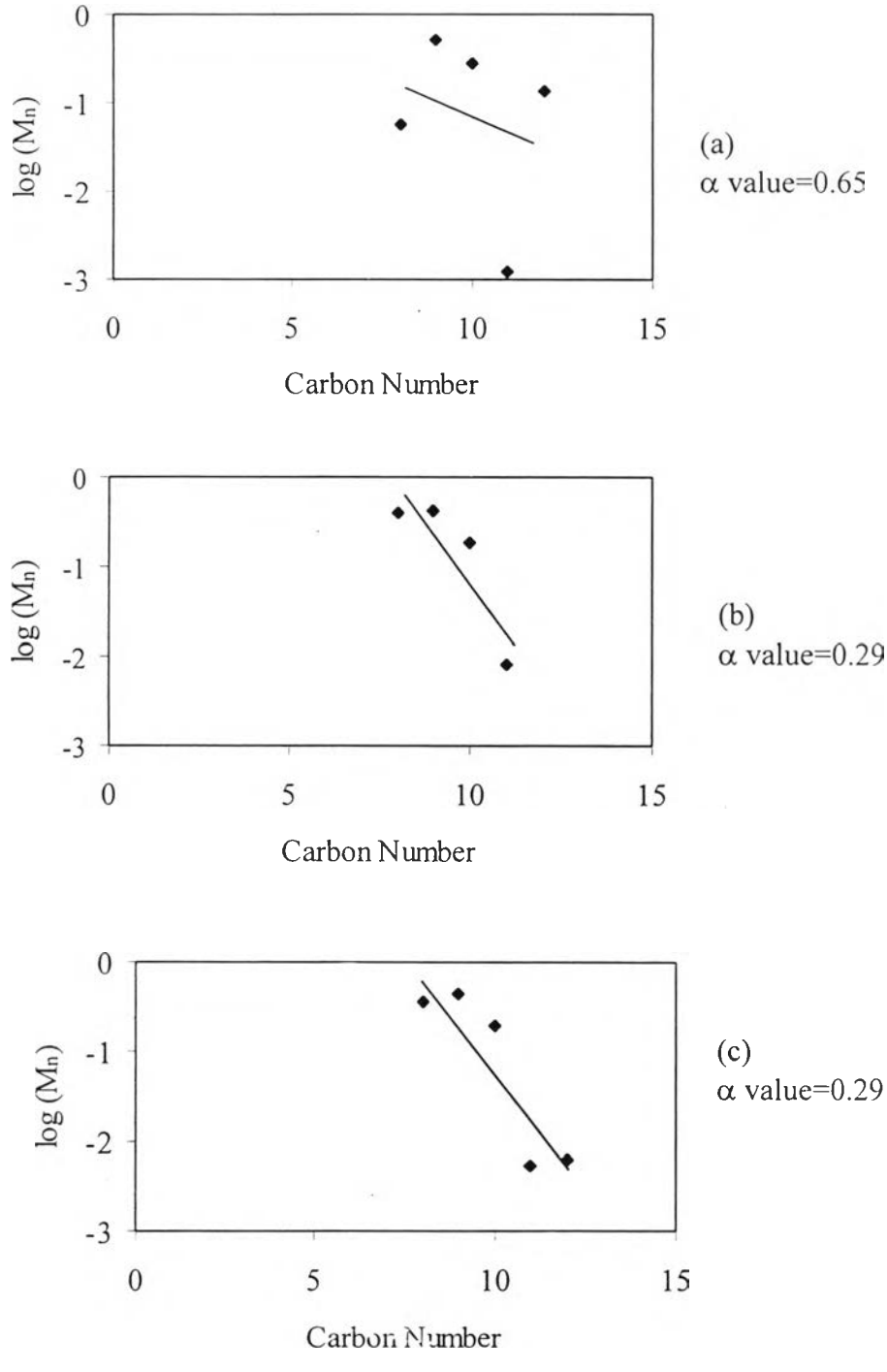

Figure 5.56 Schulz-Flory diagram of soluble coke from the support with different catalysts: (a) Pt catalyst, (b) Pt-Sn catalyst and (c) Pt-Sn-K catalyst

5.3 Mechanism of coke formation on the Pt supported catalyst

In the present study, it confirms that coke was built up on both the metal and support. Coke accumulation was extremely found to take place on the support. The coke morphology on the metal and support was amorphous structure, whereas the filament morphology was generally found on the metal. Moreover, it was found that coke was also polyaromatic structure, while the aliphatic structure was not found. The soluble coke was a main component of C_8-C_{12}. The soluble coke of the metal was constituted of much lower carbon atom that easily removed. However, the closely probability of chain growth on both sites was found. This reason was attributed to the original production of coke precursor or coke intermediates on the metal. It can be reasonably assumed that the soluble coke molecules were intermediates on the formation of complexly soluble coke, which was constituted of the higher polynuclear aromatics. Interestingly, the deviation form SF distribution occurred in the sever condition due to the dehydrogenation and the formation of higher molecular weight of coke. However, the decreasing of temperature and time, the addition of H_2 and the modification of catalyst reduced coke formation. The probability of chain growth on the metal and support was also diminished and followed by the SF distribution. Compared the effective of reduction of coke, the order from thigh effective to low effective is the effect of promoter > the effect of H_2 > the effect of temperature > the effect of time (see Table 5.17). From the combination study, it is found that the position and amount of coke on the support part for physical mixture were close to those for Pt/Al_2O_3. Thus, we may envisage that the transportation on gas phase of coke precursor from the metal to the support occurred.

As above discussed, a model of coking is proposed in Figure 5.57. Hydrocarbons first undergo dehydrogenating and cracking on the metal active surface to form precursors of coke deposits. In general, the unsaturated reaction intermediates such as monocyclic diolefins are formed and then reversibly adsorbed to form coke on the metal and in its direct vicinity. However, they can migrate to acid sites and become polymerized to the more graphite-like material. This implies a transportation

Table 5.17 The comparison of amount of coke, carbon radicals, coke species, dispersion factor and probability of chain growth in each condition

Conditions	The amount of coke	The carbon radicals	Dispersion factor	Coke species	The probability of chain growth
time	*	**	**	***	**
temperature	**	***	*	**	***
H_2/HC	****	*	***	****	**
promoter	***	****	****	**	****

**** > *** > ** > *

transport on the metal seems to be important. Coke is formed on it and in its direct vicinity, blocking also the further transport to the support and causing deactivation. This indicates that carbon depositions on these catalysts can be divided into two types: (i) coke deposited directly on metal and (ii) coke in the vicinity of metal centers, which correspond to the report somewhere else [15, 131]. Coke on the metal was burnt at low temperature whereas coke on the support was burnt at high temperature. The coke will be referred to as reversible and irreversible coke, respectively. In the earlier work, this terminology by showing the high and low H/C ratios for these coke types was confirmed. These results imply that coke deposits on the metal is less dehydrogenated and corresponds to species rich in hydrogen in accordance with the literature reviews [91, 177]. It displays the different nature of coke between the metal and alumina

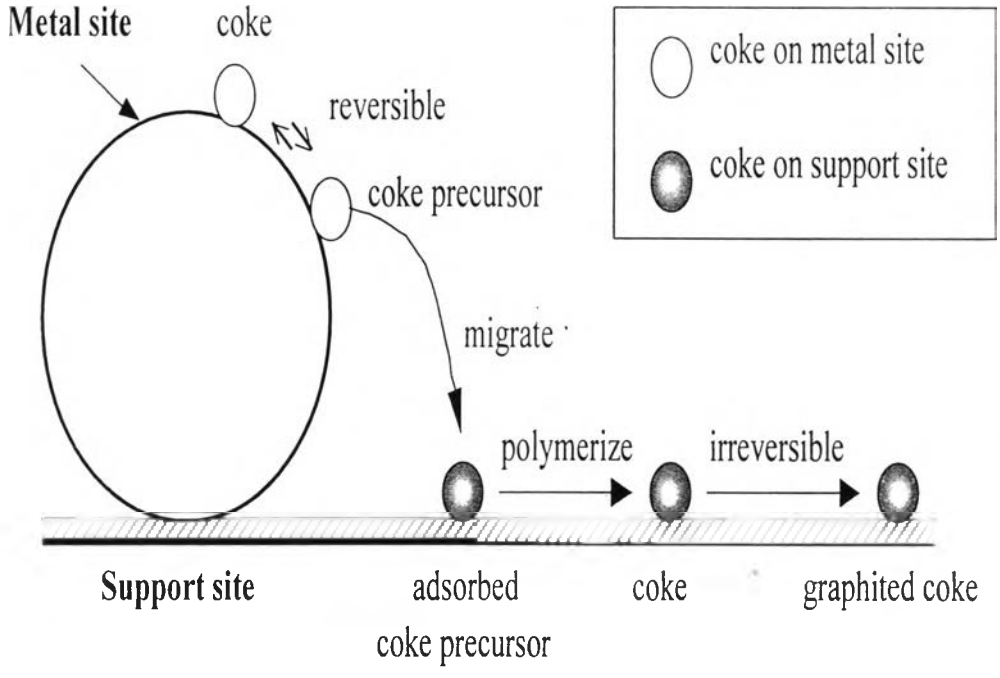

Figure 5.57 A model of coke formation